21806

NATIONAL LIBRARY
OTTAWA

BIBLIOTHÈQUE NATIONALE
OTTAWA

NAME OF AUTHOR..... C OGUGUA A EZE

TITLE OF THESIS..... A STUDY OF THE TEMPERATURE AND WALL HEAT FLUX DISTRIBUTIONS OF ENCLOSED TURBULENT FLAMES

UNIVERSITY..... UNIVERSITY OF ALBERTA

DEGREE FOR WHICH THESIS WAS PRESENTED..... MASTER OF SCIENCE

YEAR THIS DEGREE GRANTED..... 1974

Permission is hereby granted to THE NATIONAL LIBRARY OF CANADA to microfilm this thesis and to lend or sell copies of the film.

The author reserves other publication rights, and neither the thesis nor extensive extracts from it may be printed or otherwise reproduced without the author's written permission.

(Signed)..... C. O. Ezé

PERMANENT ADDRESS:

405 MICHENER PARK
EDMONTON. ALBERTA
T6H 4M5

DATED..10 MAY.....1974

NL-91 (10-68)

THE UNIVERSITY OF ALBERTA

A STUDY OF THE TEMPERATURE AND WALL HEAT FLUX DISTRIBUTIONS OF ENCLOSED TURBULENT FLAMES

by

© C. OGUGUA A. EZE

A THESIS

SUBMITTED TO THE FACULTY OF GRADUATE STUDIES AND RESEARCH IN PARTIAL FULFILMENT OF THE REQUIREMENTS FOR THE DEGREE OF MASTER OF SCIENCE

DEPARTMENT OF MECHANICAL ENGINEERING

EDMONTON, ALBERTA

SPRING, 1974

THE UNIVERSITY OF ALBERTA

FACULTY OF GRADUATE STUDIES AND RESEARCH

The undersigned certify that they have read, and recommend to the Faculty of Graduate Studies and Research, for acceptance, a thesis entitled "A STUDY OF THE TEMPERATURE AND WALL HEAT FLUX DISTRIBUTIONS OF ENCLOSED TURBULENT FLAMES" submitted by C. Ogugua A. Eze in partial fulfilment of the requirements for the degree of Master of Science.

.....
Supervisor

.....

.....

Date April 30, 1974.

ABSTRACT

The problem of computing the temperature and heat flux distribution within combustion chambers is introduced and briefly discussed, highlighting the Hottel-Cohen Zone Method. Sources of localised errors in using this method are indicated with reference to systems having little or no flow recirculation. A suggestion is advanced for minimising these errors by incorporating in the system model an equilibrium gas composition pattern that is explicitly linked with the jet-mixing process and the temperature pattern. The steps leading to the solution of the problem for the resulting complex model are outlined. Pursuant to this three computer programs are developed and shown to execute satisfactorily. The first program, EQUICALX, computes the equilibrium compositions of the combustion product gases of any fuel at any combination of temperature and pressure. The second, GRAYGAS, computes a mixed multiple-gray+1-clear gas idealisation of the radiative behaviour of the burned gases of any hydrocarbon fuel. The third, FTFIELDX, computes the temperature and heat flux distribution for an axi-symmetric system using the output of the previous two for two operating conditions with gaseous propane,

C_3H_8, fuel. A uniform gas composition pattern is provisionally adopted to facilitate the development of this program. The interfacing of these programs to facilitate the solution of the refined, complex model introduced is recommended for future research.

ACKNOWLEDGEMENTS

The author's sincere appreciation and indebtedness must be accorded:

- to Dr. J. Douglas Dale for invaluable supervision of and advice for this thesis.
- to the National Research Council for financial assistance through grants numbers NRC A-7510 and NRC C-0296.
- to my wife, Ifeoma, and children, Chinelo and Arinze, for their forbearance and moral support.
- to Mrs. J. Kerr for her diligence and typing expertise.

TABLE OF CONTENTS

LIST OF TABLES

LIST OF FIGURES

NOMENCLATURE

A	area.
$a_{G,i}$	weighting factor for the contribution of the ith gray gas to the radiative property of the real gas (see Chapter IV).
b_k^O	total moles of component k at the start of reaction.
b_{ij}, b'_{ij}	coefficients of T^j in the polynomial expressions for the $a_{G,i}$, $1/K'_R$ and $1/K'_S$ (see Chapter V and Appendix D).
C, $\overline{C}$	concentration; mass fraction.
C', $\overline{C}'$	hypothetical concentration, mass fraction (respectively) in a thorough pre-mixture of primary and secondary flows.
C''	$(C-C')/(C_O-C')$.
c''	$1/C''$.
c	a variable (see Appendix A).
$\overline{C}_p$	a mean constant-pressure specific heat (mass basis) - see Chapter V.
Ct	the Craya Curtet number.
D_M	diffusivity.
D	diameter ratio.
d	diameter.
E	emissive power $(=\sigma T^4)$.
$\underset{\sim}{E}$	a vector (equation (46)).

F	formula for chemical species.
f, f*	emissive power functions (see Chapter V and Appendix D).
G, G_i	Gibb's function; the partial molal Gibb's function: $\partial G/\partial n_i$.
$\bar{G}$, $\bar{G}_i$	G/RT, G_i/RT.
$\overline{gg}$, $\overline{gs}$	direct-exchange areas (gas-gas and gas-surface).
$\overline{GG}$, $\overline{GS}$	total-exchange areas (gas-gas and gas-surface).
$\overrightarrow{GG}$, $\overrightarrow{GS}$	directed-flux areas.
h	convective and bulk enthalpy flow heat transfer coefficients.
h', h"	radiative equivalents of h (see section 5.4).
H	enthalpy.
i_0, k_0	numbers of species and components, respectively.
K, K'	absorption coefficients, mean absorption coefficients.
L, $\bar{L}$	length, beam (path) length; $L/\frac{1}{2}d_B$.
$L'_{F,L}$	dimensionless quantity defined following equation (2).
m	total number of gray gases in an idealised multiple-gray-gas+1-clear-gas mixture. (Chapter IV).
$\dot{m}'$, $\dot{m}$	mass flux density, mass flow rate.

M	molecular weight.
$\underline{M}$, $\underline{M}^+$	matrices.
n	numbers of moles.
N, N'	total number of zones; number of surface zones (Chapter V).
P, p	total pressure; partial pressure.
$\dot{Q}$	energy flux.
$\dot{q}$	energy flux density.
r	radial distance of a point from burner axis.
R	universal gas constant.
$\underset{\sim}{R}$	a vector (equation (46)).
Re	Reynolds number.
$\overline{ss}$, $\overline{SS}$, $\overrightarrow{SS}$	surface-surface direct-exchange, total-exchange and directed-flux areas.
t^*	a characteristic reaction time (non-dimensional) for the fuel-air combination. (Chapter II).
T	absolute temperature.
U	velocity.
$\overline{U}$	velocity ratio ($U_{s,o}/U_{J,o}$).
U'	unit step function (Chapter IV).
V, $\dot{V}$	volume; volume flow rate.
X	see Appendix A.
x, $\overline{x}$	distance (axial) of a point from burner (jet) mouth, also a variable; $x/\frac{1}{2}d_B$.
Y	see Appendix A.

Z, z	symbol for a general zone (G,S and g,s).
α	absorptivity.
β_{tn}, β_{TN}	the 'original' and the modified Thring-Newby recirculation criteria, respectively.
δ_{ij}	the Kronecker delta.
δ'_{ij}	a neighbour selector operator - distinguishes between the neighbouring and the non-neighbouring zones for each zone, i.
ε, ε'	emissivity; change in value of specified variables from iteration to iteration, as defined following equation (23).
λ	wavelength.
λ'_1 (or 2)	empirical constants in equations.
λ''_1 (or 2)	(1) and (2).
λ'''	a step-size factor in equation (24c).
μ	chemical potential (see equation (12)); microns (10^{-6}m.).
$\bar{\mu}$	μ/RT.
ν, ν'	coefficients (Chapter III).
Φ, Φ'	air/fuel ratio; theoretical air expressed as the simple ratio of actual to stoichiometric air/fuel ratios. Alternatively, the inverse of the equivalence ratio.
ψ	an error parameter, defined in equation (28).

ρ	density.
σ	the Stefan-Boltzmann constant.
ξ, ξ'	defined following equation (23).
$\underline{\Omega}$, $\underline{\Omega}'$	mathematical functions (equations (5) and (6)).

Subscripts:

A	adiabatic.
a	ambient; air.
ax	axial.
B	burner.
b	bulk flow.
bp	breakpoint.
c	combustion.
cc	complete combustion.
D	chamber (duct, tunnel).
en	complete entrainment (of secondary flow).
F	flame.
f	fuel; fluid.
G	gray-gas; net generation (for the system).
g	gas-side; gas.
H	heat release (for the System).
i	numeral (including zero).
J	jet.
j	same as i.
jb	jet boundary at merger with confining walls.

k	numeral; also kinetic (as for U_k in Appendix A).
L	at beam length L; laminar; loss (by the system).
M	molecular (as for diffusivity, section 2.1).
max	maximum.
P	products (as for n_p in equation (3)).
R	Rosseland-mean; reactants (as for n_R in equation (3)).
r	at radial distance r; in the radial direction.
S	related to the Rosseland-mean (Chapter V and Appendix D).
s	surface; surrounding fluid; surface-ambient.
st	stoichiometric.
T	turbulent.
x	at axial distance x; in the axial direction.
λ	spectral (monochromatic) value.
O	at the zero value of the coordinate in question (e.g., x, r); specified values (as for T_O, P_O - equation (19)).
∞	at infinity.

CHAPTER I

INTRODUCTION

The design of combustion equipment often requires that attention be paid in some detail to the various aspects of the combustion process. These include the requisite size of the combustion chamber, the aerodynamics of the interior of the chamber as well as the transport of thermal energy between the hot burned gases and the cooler walls of the chamber. Considerations of the size of the combustion chamber, the combustion efficiency and thermal efficiency point to the necessity for a study of the aerodynamics of flow within the chamber. Certain flow conditions (for example, swirl) improve the supply of fresh oxygen to support combustion. This helps to reduce the size of the region occupied by the flame thereby affording some saving in combustion chamber size.

Most combustion equipment consist, in essence, of a coaxal circular jet system in which the fuel issues from the inner jet. The annular flow comprises the secondary air supply. For non-swirl flows the proportion of the chamber occupied by the flame depends upon the nature of the flow surrounding the flame jet. This may or may not be recirculatory. For non-combustion (i.e., cold) systems

some similarity criteria have been developed to enable the prediction of the existence or otherwise of recirculation eddies as well as their location. For combustion systems this task is much more difficult. The study of the flows in these systems has naturally taken the findings from those of cold systems as the starting point.

Heat transfer between the gases and the chamber walls depends upon the composition of the gases and on the temperatures of the gases and the walls. This sometimes necessitates some inquiry into the computation of the chemical equilibria of the combustion processes under various conditions of temperature and pressure. There is general agreement on the predominance of thermal radiation as the mechanism of heat transfer in combustion chambers. This follows from the fairly high temperatures usually encountered in such chambers and a realisation of the radiative behaviour of the burned gases, chiefly carbon dioxide (CO_2) and water vapour (H_2O). Convection plays but a minor role while conduction, through the gaseous medium, hardly deserves even a mention.

The passage of radiation through a volume of gas is essentially an exponential function of local temperature, pressure (the combined partial pressure of the 'radiatively active' gases) - via the absorption coefficient (K) - and

path (beam) length. This is stated concisely in the familiar Beer's Law. Consequently, the transport of radiation through the non-isothermal, non-homogeneous systems usually encountered in combustion practice is quite a complex subject. As of necessity, certain simplifying (often over-simplifying) assumptions have had to be made. The more immediate need has always been to have some estimates of the overall gas and wall temperatures and wall heat flux to enable questions relating to overall thermal efficiencies, economics and metallurgy to be dealt with.

The earlier analyses, therefore, have had to rely on some rather gross idealisations of the combustion systems. They also had to take account of the relatively primitive facilities available for carrying out the tedious calculations involved. Additionally, the dearth of thermal radiation data had to be put up with. Two of the most well-known of these simplified combustion system models are the Long Furnace and the Well-stirred Furnace [19,23]*.

The Long Furnace model was usually applied to cases in which the lateral dimension of the furnace could be considered small compared with the longitudinal dimension. In such cases the gas and surface temperatures and the

---

* Square brackets delineate numbered references detailed at end of dissertation.

wa heat flux could be considered as varying uni-dimensionally - i.e., in the longitudinal direction only. The combustion is idealised as essentially instantaneous and adiabatic. Use is made of the emissivity charts available for carbon dioxide (CO_2) and water vapour (H_2O) as well as the empirical relationships existing between the emissivity and absorptivity of these gases. The computation and the matching of the temperature and heat flux 'fields' proceeds along a trial and error route.

The Well-stirred Furnace model was designed to fit such systems as justified the assumption of a completely homogeneous and isothermal gas volume and a single wa (sink) temperature. The implication of this is that the turbulent mixing taking place within the chamber was very vigorous and isotropic. Energy balance and some physical realism were allowed for by introducing a more or less stepwise drop in gas temperature at the exit. The information available from this model was in the form of gross gas and wall temperatures, heat transfer and thermal efficiency.

With the advent of the fast digital computer came the ever-widening opportunity to obtain more detailed information, at the design stage, about a combustion system (be it a steam plant boiler, an oil refinery furnace, an oven, a laboratory-scale combustion test furnace etc.) than could

be furnished by the afore-mentioned models. More sophisticated models could then be constructed to better represent the real-life system than was formerly possible. One of the more successful developments in this connection has been the Hottel-Cohen Zone Method [19,29].

In this model the gas volume and the confining walls are represented as assemblages of simpler, smaller-sized units called zones. Each zone is assumed to possess more or less uniform attributes within itself in the form of temperature (and hence black emissive power) emissivity and absorptivity. For example, a circular cylindrical chamber may be divided up by a series of coaxal (with the chamber itself) circular cylinders and another series of planes perpendicular to the chamber axis. This produces gas zones that are either whole cylinders in themselves (i.e., those on the chamber axis) or annular cylinders (farther from the axis). The surface zones may be short cylinders (on the curved surface) or circular planes or yet annuli (on the end walls).

These zones are regarded as effecting the overall thermal energy transfer of the original system through simultaneous and successive interchange among themselves. The radiative component of such interchange is theorised as taking place through 'exchange areas' existing between all possible zone

pairs. These exchange areas involve, in the first instance, the relative geometrical locations of each zone-pair. There are, on the whole, three types of exchange areas used in the analysis of radiative transfer - direct-exchange, total-exchange and directed-flux areas.

The direct-exchange areas ($\overline{ss}$, $\overline{gs}$, $\overline{gg}$) are, in essence, a measure of the proportionality of the net direct radiative exchange between any zone-pair to the difference between their black emissive powers. The zone-pair is taken in isolation from the rest of the system. The value of this exchange area depends on the nature of the intervening medium, as well as the zones themselves if either or both of them are gas zones, the shapes of the zones and their relative geometrical locations. Tabulated values of these areas exist for cylindrical systems [19]. These tables use as a parameter the product of the mean absorption coefficient of the interval between the zone centres (K) and a typical zone dimension (B).

The total-exchange areas ($\overline{SS}$, $\overline{GS}$, $\overline{GG}$) additionally take into account the contribution, to the net radiative transfer occurring between any given zone-pair, of multiple reflections taking place throughout the chamber. They are calculated from the direct-exchange areas.

Each of the directed-flux areas ($\overrightarrow{SS}$, $\overrightarrow{GS}$, $\overrightarrow{GG}$) measure the proportionality which the one-way radiative flux passing from one zone to another bears to the black emissive power of the emitting zone. When the (real) gas in the inter-zone space is idealised as a mixture of gray gases, the directed-flux area becomes merely a weighted sum of the total-exchange areas corresponding to the different gray gas components.

All the exchange areas are then seen to depend on the composition and temperature of the intervening gas medium. This dependence would greatly complicate the application of the Zone Method if some simplifying assumptions were not possible. In combustion problems it is customary to ascribe a uniform composition (usually in the completely-burned state) to all the gas zones alike. This implies the uniformity of the gray gas absorption coefficients throughout the system.

Using the appropriate exchange areas, energy balance equations are written for each zone. These equations are non-linear inasmuch as they involve convective heat transfer between surface zones and their neighbouring gas zones, bulk flow terms for enthalpy transport between contiguous gas zones besides the radiation terms. The first two are linear functions of zone-temperatures while the radiation

terms are dependent on the zone emissive powers (i.e., the fourth power of the zone temperatures) and have temperature-dependent coefficients.

Linearisation is sometimes possible whereby one can make somewhat easier the task of solving the equations which solution must necessarily proceed along an iterative route. The results of such solutions are the zone black emissive powers (E) from which the zone temperatures are easily derived. The distribution of the (surface) zone heat fluxes is then only a step away.

Hottel and Sarofim [19] offer a partial example of the application of the method to a furnace in the shape of a rectangular parallelopiped with square end walls. Siddall [29] presents a step-by-step résumé of the method for a general furnace setting out a possible iterative procedure for solving the nonlinear energy balance equations. He does not give a specific numerical example of its successful application.

The shortcomings of the Zone Method are the assigning of the same composition to all the gas zones of the system and the assumption of complete combustion. The former, it will be recalled, is based upon the expectation that the turbulent recirculatory mixing occurring in the chamber is

vigorous enough. This expectation is not always satisfied, as in combustion chambers operating without swirl and under such flow conditions that flow recirculation is minimal. Under such flow conditions the role played by molecular and turbulent diffusion phenomena in effecting the mixing process is not insignificant. The very nature of these phenomena connote the existence of concentration (partial pressure) gradients in the chamber.

Hottel and Sarofim [19] comment on the applicability of the uniform concentration assumption to situations where the variations of the local concentrations of the radiatively active gases and/or their relative proportions are negligible. For other cases cited above the need arises for corrections to be made in the direct-exchange areas computed on the basis of uniform concentrations. Reference [19] suggests some apparently empirical corrections involving local absorption coefficients.

Pieri et al. [27] discuss in some detail some of the implications of the uniform-concentration assumption. These concern the zone temperature and heat flux distributions. The discussion centres around a furnace in the shape of a rectangular parallelopiped of square section. They illustrate some of the improvements to be expected under certain flow and operating conditions by allowing for the existence

of partial pressure gradients. These improvements vary in significance depending on the combustion chamber size.

The assumption of a uniform concentration leads to the over-estimation of the heat fluxes of the wall zones in the middle of the chamber as well as the corner wall zone temperatures. It also under-estimates the temperatures of most of the wall zones, the gas zones along the burner axis, the heat fluxes on the burner-end wall zones and on the exit-region wall zones. The errors in the temperatures can be as high as 600 F. The heat fluxes apparently exhibit a lower sensitivity than the zone temperatures to errors in the radiative properties of the system [22,27]. The discrepancy between the values computed with uniform and non-uniform concentrations can sometimes be as high as 110% of those calculated with the latter assumption [27].

The above-mentioned errors are attributable to the compromising effect introduced by the uniform-concentration assumption between the high-concentration (of the combustion products) and the lower-concentration zones. Examples of the former category of zones would include the exit-region zones, [illegible]e in the burner region typifying the latter category. This compromising effect also exists between the higher-temperature zones (e.g., those in the

middle of the furnace) and the cooler ones (e.g., those in the burner region). Where the concentrations are overestimated the (gas) zone emissivities will be too high. The zone temperatures are therefore more likely to be underestimated [27].

What may be considered an alternative and no less realistic assumption postulates the existence in each gas zone of chemical equilibrium appropriate to both the zone temperature and the mole fraction of fuel (or, alternatively, an air/fuel ratio) that would occur as a result of the jet-mixing process. This automatically introduces a pattern of concentration gradients coupled to the temperature field and the jet-mixing process. It would also account, implicitly, for any reducing effect that dissociation would have on the zone compositions, and hence on the gas zone radiative properties. For lower-temperature zones the radiative properties of the gas volumes would be well accounted for.

Consequently, it would seem ideal to integrate with the Zone Method a zone concentration pattern in accordance with this postulate. This would seem to connote the updating, during the iterative solution of the energy balance equations, of the zone concentration pattern. A refined, complex model of this nature should provide a more realistic

picture of the radiative interaction among the zones of the system, thereby improving the accuracy of the final computed distributions of temperature and heat flux. Hottel and Sarofim [19] suggest that the extra labour involved in such a refinement of the combustion system model may not always be worthwhile. However, the rather large discrepancies cited earlier as existing between the predicted temperature and heat flux distributions for the uniform-concentration model and those for the more refined variety suggest that such extra labour may sometimes prove fruitful.

The study reported herein is a preliminary step in that direction. Three computer programs are developed. The first of these, EQUICALX, is capable of computing the equilibrium states of reacting mixtures of fuel and air at various temperatures and fuel/air ratios. The possibility of varying the overall system pressure is also allowed for. The second program, GRAYGAS, can compute a mixed multiple-gray+1-clear-gas approximation for the combustion product gases of any hydrocarbon fuel-air mixture. The last program, FTFIELDX, predicts the temperature and heat flux distributions within an axi-symmetric test combustion chamber using gaseous fuel. Use is made of the Hottel-Cohen Zone Method. The preliminary nature of this study dictated the provisional adoption of the uniform-

concentration assumption with the expectation that analysis of the more sophisticated model will follow from a mating and extension of the procedures embodied in the computer programs and presented herein. Two operating conditions of the combustion system are considered and the associated flow conditions are characterised by the appropriate values of the Craya-Curtet Number (Ct). One of these is deliberately chosen to be identical with that for the (mildly recirculatory) flow surrounding a free-jet flame burning in a stagnant atmosphere [5]. The other is much smaller, representing a more strongly recirculatory flow situation.

The presentation covers the various aspects of the combustion phenomenon pertinent to the study. These are separated into a number of more or less self-contained chapters, with the Appendices serving as a repository for the requisite back-up information. The subject of combustion aerodynamics is broached in Chapter II, focussing on where it pertains to flame length and the use of flow recirculation parameters. Chapter III follows with an inexhaustive treatment of the theory of complex chemical equilibria in the gas phase. Next to be discussed, in Chapter IV, is the procedure for obtaining an idealised multiple-gray-plus-clear-gas representation of a real gas mass. Chapter V details the steps undertaken to set up and solve the

applicable system of simultaneous energy balance equations. Chapter VI offers some appraisal of the study undertaken and the results obtained, as well as some recommendations considered pertinent to the quest for improved accuracy in mathematical modelling of combustion systems. The Appendices, besides providing background and supporting information, also contain the listings of the three computer programs -- EQUICALX, GRAYGAS and FTFIELDX.

CHAPTER II

COMBUSTION AERODYNAMICS

2.1 Flame Length

The physical dimensions of a flame, whether pre-mixed or diffusion, is an important item in the design of combustion chambers. This is due, at least in part, to the undesirability of the soot deposition that would inevitably result from the impingement of a flame on the relatively cool walls of the enclosure - the wall quenching effect. Such contact between the flame and the chamber walls would, as can be imagined, have a deleterious effect on combustion efficiency. As noted in Chapter I, certain flow conditions, swirl, for example, help reduce the size (length and lateral spread) of the flame, thereby permitting some reduction in the overall size of the combustion chamber. The optimum size chosen for the chamber must necessarily, therefore, take into consideration the expected maximum flame length.

An early theoretical study of enclosed laminar diffusion flames was reported in 1928 by Burke and Schumann [7]. Numerous other theoretical and experimental studies have since been reported on free and enclosed laminar [3,4, 6,17,18,28,34] and turbulent [3,9,14,32,33,34,35] flames.

Naturally many different viewpoints have been represented, some more successful than others.

For laminar flames the outcome of these investigations is that the length of the flame is a function of the volume flow rate, $\dot{V}_{f,B}$, of the burner fluid and the primary air content of that fluid. The latter variable can be represented by the non-dimensionalised air/fuel ratio, Φ'_B (theoretical air; Φ_B/Φ_{st}, where Φ_{st} is the stoichiometric air/fuel ratio). The flame length is, to all intents and purposes, independent of burner diameter. Of the numerous expressions put forward relating the laminar flame length to the flow conditions and fuel properties, two stand out as the most widely successful.

One of these is a semi-empirical correlation due to Hottel and co-workers [17,18] which is expressible in the form:

$$\bar{L}_{F,L} = \lambda'_1 \log_{10}(\dot{V}_{f,B} t^*_f) + \lambda''_1 \qquad (1)$$

in which $\bar{L}_{F,L}$ is the dimensionless length of the laminar flame, i.e., $(L_{F,L}/\frac{1}{2}d_B)$, the symbols λ'_1 and λ''_1 representing empirical constants. The quantity t^*_f is a characteristic dimensionless reaction time for the fuel. It essentially measures the time taken, since issuance from the burner mouth, by the fluid on the burner axis to attain the

stoichiometric proportions deemed to exist everywhere on the flame envelope, including the flame tip [7,17.18]. This characteristic time measure is found to be $\{4 \ln [(1+\Phi_{st}^{-1})/(1+\Phi_B')]\}^{-1}$ which shows its dependence on Φ_B'. It is to be noted that t_f^* is a minimum when $\Phi_B'=0$. This implies that the longest laminar flames are the 'pure' diffusion flames.

The other important expression for the laminar flame length is a theoretical one proposed by Wohl et al. [34]. This can be put in the form:

$$\bar{L}_{F,L} = \lambda_2' L_{F,L}'/(1+\lambda_2'' L_{F,L}'^{1/2}) \qquad (2)$$

where λ_2' and λ_2'' are constants whose values depend on the fuel and the primary air content of the burner fluid supply. The quantity $L_{F,L}'$ represents the dimensionless group $(\dot{V}_{f,B} t_f^*/(d_B D_{M,B}))$. Equation (1) is said to work best for flames characterised by high values of $\dot{V}_{f,B}$ and whose lengths fall into the medium-large category. Equation (2) is supposed to be quite accurate in predicting the value of $\bar{L}_{F,L}$ over most of the range of variation of the latter.

Equations (1) and (2) indicate the dependence of the laminar flame length, $\bar{L}_{F,L}$, on $\dot{V}_{f,B}$ and Φ_B'. As $\dot{V}_{f,B}$ increases so does Re_B, the Reynolds Number of the (cold) burner-tube

flow. At a stage this enters the turbulent regime. The flame remains laminar, though, on account of the vastly increased gas viscosity to be found in the vicinity of the (hot) flame envelope. Beér and Chigier [6] report that increases of the order of 15 to 20 times the cold value are common.

Naturally such an increase in gas viscosity can only be expected to have a considerable 'laminarising' influence on the turbulent fluid flow issuing from the burner orifice. At some critical value of Re_B (turbulent), however, the flame itself breaks down into a turbulent, brushlike affair - the turbulent flame. This breakdown is initiated at the flame tip and progressively approaches the burner mouth as Re_B is increased. It is unable to reach the burner mouth, though, on account of the existence of a stable laminar stub at the base of the turbulent flame. This stub is referred to as the breakpoint length. Table I, from reference [6], lists the critical Re_B for a number of different fuels.

TABLE I. Critical Reynolds numbers, Re (cold), for various fuels [6].

Gaseous fuel	$Rex10^{-3}$
H_2	2
H_2*	5.5-8.5
City gas	3-4
City gas*	5.5-8.5
CO	5
Propane, C_3H_8	9-10
Acetylene, C_2H_2	9-10
Methane, CH_4	3

* with primary air

In the turbulent-flame regime the relationship between the flame length, $\bar{L}_{F,T}$ and the flow variables as well as the fuel properties is very different from that in the laminar regime. In fact, $\bar{L}_{F,T}$ is independent of $V_{f,B}$: for a given burner diameter it is essentially constant. This constant value may be lower or higher than the maximum laminar flame length, depending on the burner diameter. This is evidenced in the experimental results reported in reference [34]. For smaller d_B it is lower, in which case the flame passes through a maximum as Re_B varies from the laminar to

the turbulent regimes. For larger d_B the flame length increases monotonically even as the critical Re_B is traversed. All this is depicted in Figures 1a and 1b.

As is the case with laminar flames, turbulent flames have called forth quite a few different viewpoints to their analyses. These approaches have led to a number of mathematical expressions relating the flame length to the various fuel properties and flow variables. Wohl et al., [34] extended their analysis of the laminar flame to the turbulent. They emphasised the diffusion phenomenon involved, taking into account its necessarily turbulent nature, and obtained a somewhat reliable formula. The usefulness of this formula is hampered by the need for arbitrary correction factors to be used in order to account for the under-estimation of the effect of the eddy diffusivity.

Yagi and Saji [35] based their analysis upon an even more detailed knowledge of the theory of turbulence. Using a quasi-cylindrical flame model and enunciating a 'unit flame' concept, they obtained an expression for $\overline{L}_{F,T}$ which, though more complex than that of Wohl et al., is of more limited applicability.

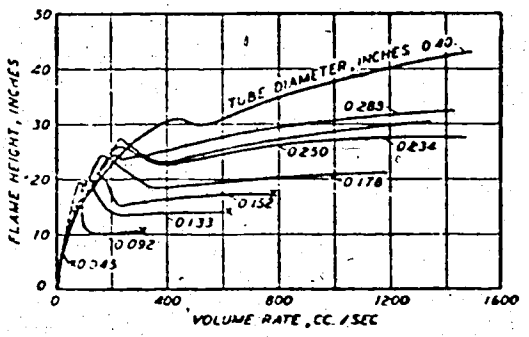

Figure 1 a.

Free-jet Flame Lengths vs. Fuel Volume Flow Rates for Various Burner Diameters. From Reference [17].

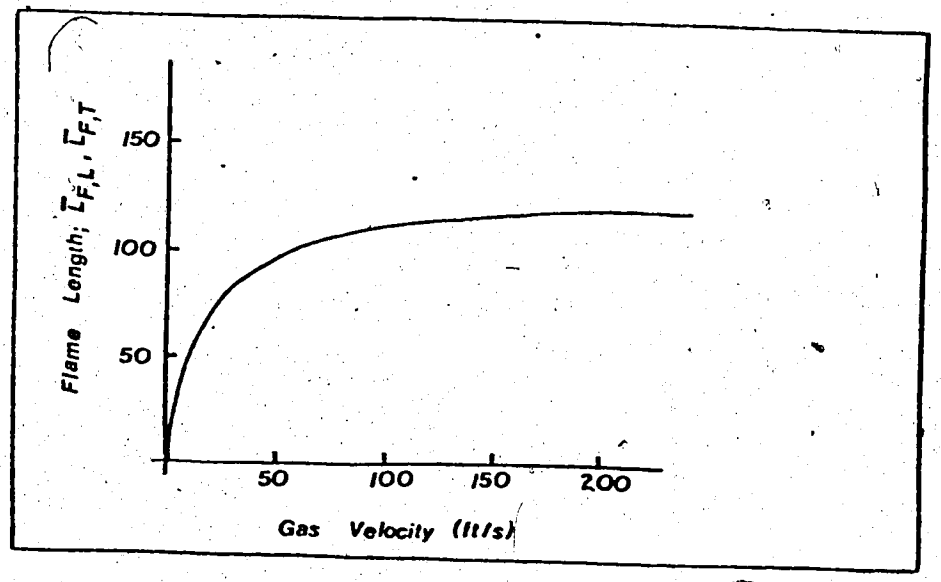

Figure 1 b.

Free-jet Flame Lengths vs. Gas Velocity at Burner Mouth. From Reference [34].

Hottel et al. [4,17], using the most general approach, and arguing from the point of view of the dynamic similarity of non-isothermal coaxial jets, vis à vis the relationship between the momentum change and buoyancy effects, have deduced, for situations characterised by low relative importance of buoyancy, a very general formula for $\bar{L}_{F,T}$. This formula has been shown to give satisfactory accuracy, averaging about 90% of the measured values. It can be put into the following form:

$$\bar{L}_{F,T} - \bar{x}_{bp} = 10.6 \left[c_F'' \frac{T_{F,A}/T_{J,O}}{(n_R/n_P)_{st,cc}} \left(1 + \frac{c_F'' - 1}{M_f/M_a}\right)\right]^{1/2} \qquad (3)$$

in which $c_F'' = 1/C_F''$, being evaluated at essentially stoichiometric conditions. The ratio n_R/n_P is determined for complete combustion. The quantity $\bar{x}_{bp}$ stands for the dimensionless breakpoint length. This quantity was shown to bear, in general, a maximum ratio of about 0.1 to the length of the turbulent portion of the turbulent flame, i.e., $(\bar{L}_{F,T} - \bar{x}_{bp})$. This is true for most fuels, the exception being CO for which the ratio has a maximum in the neighbourhood of 0.84 [17,18]. This ratio generally decreases with increasing Re_B. For most fuels the average value is about 0.05.

A comparison of the formulas proposed by Hottel et al., Yagi and Saji, and Wohl et al., is presented graphically in Figure 2 taken from reference [17]. The universality of equation (3) is evident, M_f/M_a being a parameter as would be expected on the grounds that gas diffusivities are strongly influenced by their molecular weights.

Beer and Chigier [6] quote a formula for $\bar{L}_{F,T}$ that is attributed to Guenther;

$$\bar{L}_{F,T} = 12.0\ (\Phi_{st} + 1)(\rho_{f,B}/\rho_F)^{1/2} \qquad (4)$$

the value of ρ_F being more or less the same for most gaseous fuels. This formula is alleged to be quite accurate (to within 10% of the measured values).

Enclosed flames in general behave differently from free flames. This is due to the effect of the confining walls on the flame aerodynamics. The confined flame is more prone than the free flame to instability resulting from recirculation. The confining walls set an upper limit to the amount of oxygen available to the combustion process. When the secondary air flow is too low, i.e., when the 'feed ground stream' [5] falls short of the 'entrainment capacity' of the flame jet, flow instability is the likely result. Such instability usually manifests itself in the

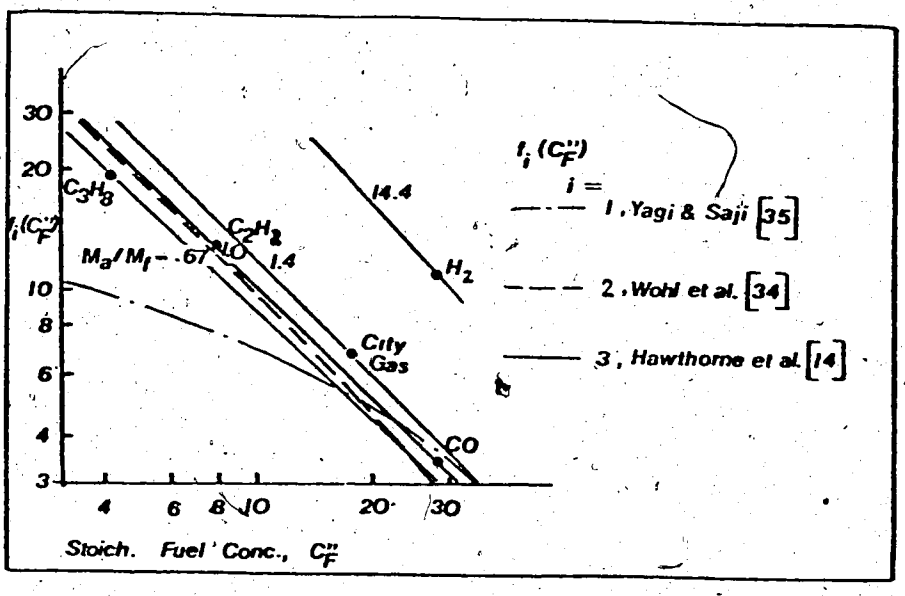

Figure 2. A Comparison of Various Expressions for Turbulent Flame Lengths. From Reference [17].

form of flow recirculation which can therefore be thought of as an attempt by the flame to entrain the necessary fresh oxygen to support its combustion processes [5,33].

The confining walls also effectively prescribe a physical limit to the lateral expansion of the flame. Confinement also increases the flame length besides tending to reduce the relative importance of buoyancy effects. Beér and Chigier [6] illustrate the increase in flame length due to confinement. The reduction of buoyancy effects is more significant for horizontal than for vertical flames.

2.2 Flow Recirculation

Burke and Schumann [7] applied the term 'over-ventilated' to flames whose secondary air supply is more than is necessary to ensure complete combustion. Such a flame was shown to possess a closed envelope whose shape can be a prohibitively complex mathematical expression even for the very simple cases treated in the quoted work. For a turbulent flame this envelope exhibits a random oscillation about a mean position, being penetrated intermittently and randomly (in space and time) by turbulent eddies.

When the secondary air flow is too low the flame is said to be 'under-ventilated' and its envelope was shown by Burke and Schumann to fan outwards radially until it merged with the confining walls. This would indicate the complete entrainment, by the flame jet, of the secondary flow. This situation usually precedes the establishment, within the enclosure, of recirculatory flow. Figure 3 illustrates the point.

Recirculatory flow is a complex mathematical problem even for the simplest isothermal, iso-density, free-jet systems. It has been possible to establish some applicable similarity criteria [5,6,32,33]. This is based upon the established fact of the reasonable constancy of the free-jet-spread angles.

The treatment of the recirculation phenomenon for enclosed and free non-isothermal, non-isodensity, (combustion) systems has usually taken the form of an extrapolation of the results for the simpler isothermal, isodensity, free-jet variety. Sunavala et al. [32] point out the close similarity between the behaviour of the early stages of the flame jet with that of a free jet. The confinement of a flame jet necessitates the inclusion into the appropriate similarity criterion of the ratio of the typical lateral dimensions of the combustion chamber and burner, for

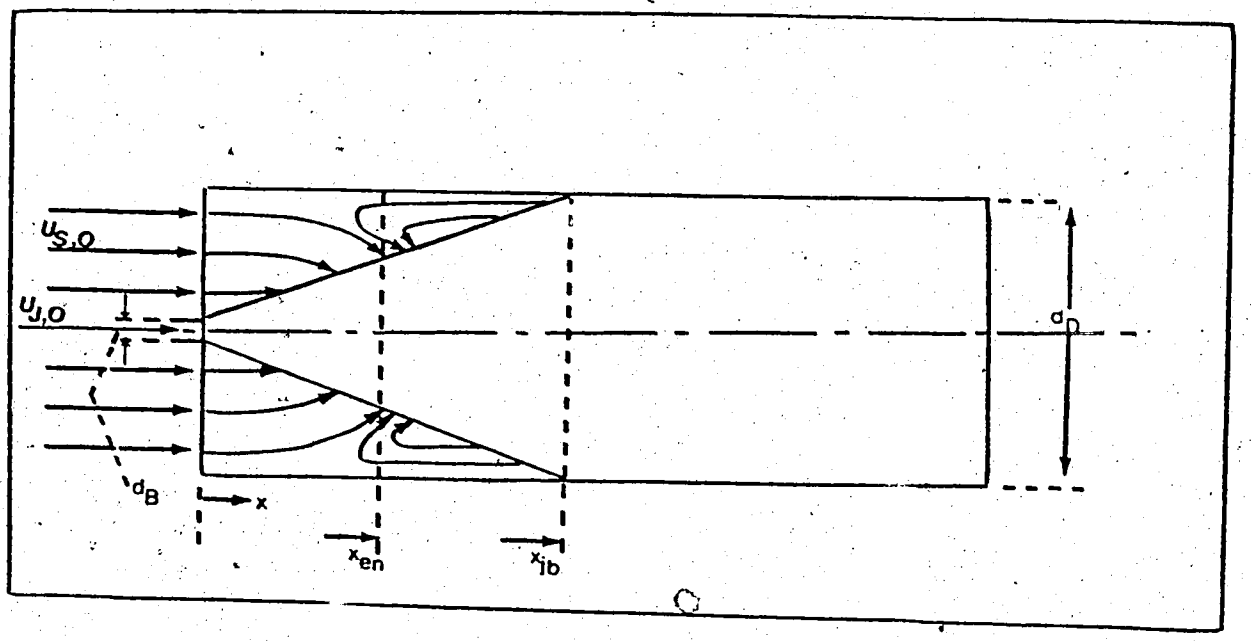

FIGURE 3. An Enclosed Jet with Recirculatory Flow.

example, the diameter ratio, D, for a cylindrical system [33].

Arguing from a physical point of view, Thring and Newby [33] have shown recirculation to depend on the relative 'strengths' of the primary (jet) and secondary (ground-stream) flows. This relativity is expressed in the ratio $\bar{x}_{en}/\bar{x}_{jb}$ which exists between the axial distance, from the plane of the burner mouth, of the plane at which complete entrainment of the secondary air flow would occur ($\bar{x}_{en}$) and that of the plane at which the steadily expanding jet would hit the walls of the enclosing chamber. This ratio can be shown to be proportional to the quantity $\bar{C}_f'D$, the first member of which stands for the (hypothetical) mass fraction of the fuel in a thorough pre-mixture of the primary and secondary flows. This product is essential for the definitions of the similarity parameters known as the Thring-Newby recirculation criterion (β_{tn}) and the Modified Thring-Newby criterion (β_{TN}) [6,32] (see Appendix A). Either parameter can be used to predict the occurrence or otherwise and the location of recirculation eddies. The 'raw material' for all this includes simply the mass flow rates of the primary and secondary flows and the dimensions of the jet (burner) and confining chamber [6]. For combustion systems β_{TN} has been found to be quite a reliable similarity parameter. This is depicted in Figure 4. This

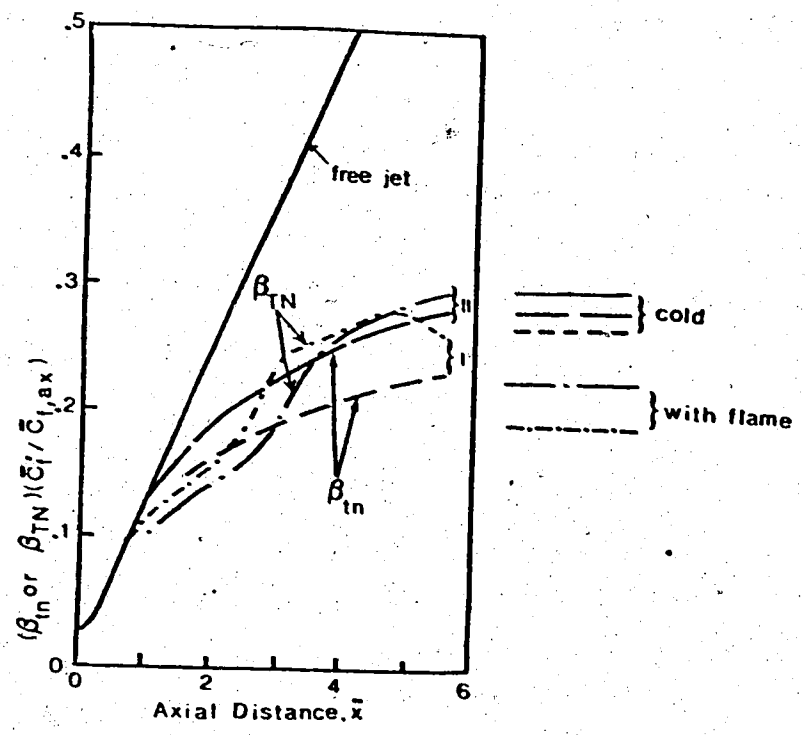

FIGURE 4. Use of β_{tn} and β_{TN} as Similarity Parameters for enclosed Jet Systems. From Reference [33].

figure also illustrates that for isothermal systems β_{tn} is the more appropriate flow parameter.

An analogous parameter to β_{tn} is the Craya-Curtet Number, Ct, which is derived from the fluid-dynamic equations of motion. It has been shown to be more or less identical with β_{tn} within the range of values from zero to unity [6]. Being derived from the fundamental equations of motion, it is the more rigorous and accurate indicator of flow similarity [5,6]. Becker et al. [5] have indicated the use of Ct in enclosed isothermal, isodensity jet systems and have described it as a unique criterion, for a given diameter ratio, D, of dynamic similarity. It usually varies in value, for jet-type flows, from $(D^2-0.5)^{-0.5}$ to infinity for given D. For recirculatory flows they have shown that the Ct can be used, contrary to the suggestion of Beér and Chigier [6], to statistically correlate the different attributes of the recirculation eddy - its eye, upstream edge, downstream edge, and the associated volumetric flux of fluid.

Becker et al. also discussed the significance of the Ct value of 0.75. It represents the borderline between flows that are recirculatory (with Ct smaller than 0.75) and those that are not (with Ct larger than 0.75). Flows whose Ct fall between the values of 0.5 and 0.75 possess very

little recirculation. Smaller values of Ct represent flows having progressively stronger recirculation. For such flows the assumption of a uniform concentration is tenable. On the other hand, for flows that have little or no recirculation (i.e., with Ct greater than about 0.5) the validity is increasingly questionable. Becker et al. also demonstrated quite conclusively the possibility of reproducing in an enclosure flow conditions that are, to all intents and purposes, dynamically similar to those associated with a free jet issuing into a stagnant free stream. Such flow conditions are characterised by a Ct of 0.673.

For any given system (with a given D and fluid supply conditions) there exists a 1:1 correspondence between β_{tn} (or β_{TN}) and Φ' (the theoretical air) as well as between Ct and Φ' (see Appendix A). For the system studied, D had a value of 72 which gave values of Ct of 0.673 and 0.230 when Φ' was 3.0 and 1.0 respectively.

CHAPTER III

CALCULATION OF EQUILIBRIUM COMPOSITIONS

3.1 Introduction

The radiatively active gases of principal interest in combustion studies are carbon dioxide (CO_2) and water vapour (H_2O). The emissivity as well as the absorptivity of any given volume of combustion product gases depends upon the partial pressures of these two gases, among other things [19]. The uniform-concentration assumption, throughout the combustion chamber, discussed earlier in connection with the Zone Method (Chapter I) has been portrayed as leading to localised errors in the calculation of temperature and heat flux distributions. These errors are more serious in the former than the latter [22,27].

Gas zones can attain temperatures that are high enough for the effects of dissociation to become significant. In that case the zone concentrations should be computed to take account of the phenomenon. Thus the radiative interactions of the zones of the system will be more truly assessed. An analogous situation could arise during the iterative solution of the energy balance equations mentioned earlier.

The analogy would become clear upon considering the iterative solution to be something of a non-steady-state operation of the system, the iterations representing some hypothetical time scale. Thus the validity of the final results of the computation would be enhanced.

An additional motivation for the investigation of the computation of the equilibrium compositions of reacting systems was the need to have on hand a documented facility of that nature. Its inclusion herein also lends completeness to this study.

Combustion and chemical literature abound in studies of the equilibria of reacting systems [12,13,26,36]. . Zeleznik and Gordon [36] provide an extensive list of references. Their paper deals in some detail with the chemical, thermodynamic and mathematical aspects of the subject, and it is their methodology that was adopted and will be briefly outlined.

In general, there are two schools of thought on the problem of equilibrium computations: the 'equilibrium constant formulators' and the 'free energy minimisers' [36]. By establishing the relationship between equilibrium constants and free energy, Zeleznik and Gordon have shown the two parties to have much in common. Differences between them

seem to lie chiefly in the detailed manipulation of the equations describing the reacting systems.

In essence, the computation of chemical equilibrium can be visualized as the solution of a set of non-linear equations of the form;

$$\underline{\Omega}'(\underline{x}) = 0 \qquad (5)$$

where $\underline{x}$ is vector representing the state variables of the reacting system. In the equilibrium constant approach these equations are essentially equilibrium constant expressions for elementary reactions involving the species present in the system. In the free energy minimisation approach the determination of the extremum of the free energy function, $\underline{\Omega}(\underline{x})$ say, becomes the solution of the equation;

$$(d/d\underline{x})\ \underline{\Omega}\ (\underline{x}) = 0 \qquad (6)$$

A comparison of equations (5) and (6) indicates two possible relationships between $\underline{\Omega}'(\underline{x})$ and $\underline{\Omega}(x)$:

$$\underline{\Omega}'(\underline{x}) = (d/dx)\ \underline{\Omega}\ (\underline{x}) \qquad (7)$$

or $$\underline{\Omega}\ (\underline{x}) = (1/2)\ \underline{\Omega}'^{(t)}\ M^{+}\ \underline{\Omega}' \qquad (8)$$

$\underline{M}^{+}$ being any PD matrix, the unit matrix, for instance, and $\underline{\Omega}'^{(t)}$ the transpose of $\underline{\Omega}'$ [36].

Naturally the solution of the equilibrium problem would be greatly facilitated if the equations (5) are kept as simple as possible. This is achieved through the use of the formation reactions of the chemical species present in the system.

3.2 An Overview of the Theory

For any system operating at a constant temperature and pressure, the equilibrium state is marked by the fact that the Gibb's free energy of the system is at a minimum. This consideration would apply to a large number of combustion systems. This free energy function is a function of the system temperature, pressure and composition. In other words, for a chemical system containing i^o species the Gibb's function can be stated as

$$G = G(T,P,n_1,n_2, \ldots n_{io}) \qquad (9)$$

It is an extensive property and as such must satisfy the equation

$$G = \sum_{i=1}^{i^o} n_i \mu_i \qquad (10)$$

The equilibrium condition can therefore be stated as,

$$\sum_{i=1}^{i^o} n_i d\mu_i = 0 \qquad (11)$$

For gases, to which the theory presented here is intentionally limited, the chemical potentials (μ_i) are defined as

$$\mu_i = \mu_i^*(T) + RT \ln (n_i/n) P \qquad (12)$$

where the $\mu_i^*(T)$ are the zero-pressure chemical potentials at the temperature T and n is related to the n_i by

$$\sum_{i=1}^{i^o} n_i = n \qquad (13)$$

In writing the formation reaction equations mentioned earlier the reacting system is considered to be no more than an assembly of i^o species of which k^o essentially constitute the 'building blocks' for the remainder. These k^o species are referred to as the 'components' of the system.

In a 'C-H-O-N' (Carbon-Hydrogen-Oxygen-Nitrogen) combustion system the appropriate species could include $C, H_2, O_2, N_2, CO, CO_2, CN, H, HCO, HO_2, H_2O, O, OH, N, NO$ ($i^o = 15$) of which the first four constitute the components ($k^o = 4$). These are the

chosen sets of species and components for the combustion system considered in this study.

The formation reaction equations for the remaining $i^o - k^o$ species are then of the form;

$$\sum_{i=1}^{i^o} \nu_{ij} F_j = 0 \qquad k^o < j \leq i^o \tag{14}$$

where the ν_{ij} are stoichiometric coefficients and the F_j are the chemical formulae of the species. These formulae can be mathematically symbolized in terms of the components as,

$$F_i = \prod_{k=1}^{k^o} (F_k)_{\nu'_{ki}} \quad , \quad 1 \leq i \leq i^o \tag{15}$$

in which ν'_{ki} is the number of molecules of the k^{th} component contained in one molecule of the i^{th} species. The coefficients ν_{ij} and ν'_{ki} must then satisfy the relation,

$$\sum_{i=1}^{i^o} \nu'_{ki} \nu_{ij} = 0 \tag{16}$$

$$1 \leq k \leq k^o \quad , \quad k^o < j \leq i^o$$

The chemical law of conservation of the atoms (molecules) of the components has to be satisfied at all times during the chemical reaction.

A conservation equation can therefore be written for the molecules of each component giving,

$$\sum_{i=1}^{i^o} (\nu'_{ki} n_i) - b_k^o = 0 \qquad (17)$$

$$1 \leq k \leq k^o$$

where b_k^o is the number of molecules of component k at the start of the reaction. The use of equations (16) and (17) transforms the equilibrium condition (equation (11)) into the form;

$$\bar{\mu}_i - \sum_{k=1}^{k^o} \nu'_{ki} \bar{\mu}_k = 0 \qquad (18)$$

$$k^o < i \leq i^o$$

the dimensionless form being preferred.

To complete the thermodynamic description of the system it is requisite to specify any two state variables chosen from among T,P,S,H and V. In combustion problems the choice

might be,

$$P = P_0$$

and

$$T = T_0 \qquad (19)$$

where P_0 and T_0 are constants.

Equations (13), (17), (18) and (19) constitute a system of i^o+3 equations in as many variables (n being one of them). In theory a solution is possible. The system is non-linear on account of equations (18) so the solution must proceed iteratively. This is considered in the next section.

3.3 Method of Computation

A suitable procedure is the so-called Newton-Raphson iteration [36]. In this method some initial estimates of the variables $\underline{x}$ are made, and at each subsequent iteration I the current values of $\underline{x}$ are used to recalculate the variables for the next -- (I+1)th -- iteration in a functional manner, i.e.,

$$\underline{x}_{I+1} = \underline{x}_I - \underline{J}^{-1}(\underline{x}_I)\ \underline{\Omega}'\ (\underline{x}_I) \qquad (20)$$

or

$$\underline{J}(\underline{x}_I).\Delta\underline{x}_{I+1} = -\ \underline{\Omega}'(\underline{x}_I) \qquad (21)$$

where $\underline{J}$ is the Jacobian matrix and $\Delta\underline{x}_{I+1}=\underline{x}_{I+1}-\underline{x}_I$

This kind of functional iteration can in theory be carried out on the system of equations (13), (17), (18) and (19), thereby progressively approximating the equilibrium composition of the reacting system. However, one important observation needs to be made. In theory, as the equations stand, there is nothing to prevent the mole numbers becoming negative at any stage in the iterative process. But physical realism and the very nature of equation (12) (which should be always satisfied by the variables in equation (18)) demand that the mole numbers be always positive. An effective artifice that eliminates this prospectively awkward situation is to use the logarithms of these quantities as the variables rather than the quantities themselves.

Using this approach and performing one or two convenient variable transformations (see Appendix B), one would obtain the following set of equations:

$$\sum_{k'=1}^{k^o} (\xi'_{kk'} u_{k'}) + \xi_k \Delta \ln n = \varepsilon'_{b,k} + \sum_{i=1}^{i^o} \nu'_{ki} \bar{G}_i \qquad (22)$$

$$1 \leq k \leq k^o$$

$$\sum_{k'=1}^{k^o} (\xi_k u_{k'}) + (-\varepsilon_n)\ \Delta \ln n = \varepsilon_n + \bar{G} \qquad (23)$$

$$1 \leq k' \leq k^o$$

where $\xi'_{kk'} = \sum_{i=1}^{i^o} (\nu'_{ki} \nu'_{k'i}\ n_i)$

$u_{k'} = \Delta \ln n_{k'} + \bar{\mu}_{k'} - \Delta \ln n$

$\xi_k = \sum_{i=1}^{i^o} \nu'_{ki} n_i$

$\varepsilon'_{b,k} = b_k^o - \sum_{i=1}^{i^o} (\nu'_{ki} n_i)$

and $\varepsilon_n = n - \sum_{i=1}^{i^o} n_i$

In an expanded form these equations look like this:

$$\begin{bmatrix} \xi'_{11} & \xi'_{12} & \cdots & \xi'_{1k^o} & \xi_1 \\ \xi'_{21} & \xi'_{22} & \cdots & \xi'_{2k^o} & \xi_2 \\ \vdots & \vdots & & \vdots & \vdots \\ \xi'_{k^o 1} & \xi'_{k^o 2} & \cdots & \xi'_{k^o k^o} & 0 \\ \xi_1 & \xi_2 & \cdots & \xi_{k^o} & (-\varepsilon_n) \end{bmatrix} \begin{bmatrix} u_1 \\ u_2 \\ \vdots \\ u_{k^o} \\ \Delta \ln n \end{bmatrix} = \begin{bmatrix} \varepsilon'_{b,1} + \sum_i \nu'_{1i} \bar{G}_i \\ \varepsilon'_{b,2} + \sum_i \nu'_{2i} \bar{G}_i \\ \vdots \\ \varepsilon'_{b,k^o} + \sum_i \nu'_{k^o i} \bar{G}_i \\ \varepsilon_n + \bar{G} \end{bmatrix}$$

$$1 \leq i \leq i^o$$

At each iteration (I) this matrix equation is easily solved. The mole numbers and the total number of moles are updated using the u_i and the approximate relation:

$$\Delta x_I \approx (x_{I+1} - x_I)/x_I \qquad (24a)$$

from which

$$x_{I+1} \approx x_I + x_I \Delta \ln x_I \qquad (24b)$$

The risk of over-correction, which would be run should equation (24b) be used as it stands, is considerably reduced by

using a modified version of the same equation;

$$x_{I+1} \simeq x_I + \lambda''' x_I \Delta \ln x_I \qquad (24c)$$

in which λ''' is an empirical step-size factor. Reference [36] recommends that λ''' be determined such that,

$$|\Delta \ln n| \leq 2 \qquad (25)$$

$$\Delta \ln (n_i/n) \leq 2; \quad \text{for } (n_i/n) \leq 10^{-8} \qquad (26)$$

$$\Delta \ln (n_i/n) \leq -9.212 - \ln (n_i/n); \quad \text{for } (n_i/n) < 10^{-8} \qquad (27a)$$

Equation (27a) may be written more informatively in the form;

$$\Delta \ln (n_i/n) \leq \ln(10^{-4}) - \ln (n_i/n); \quad \text{for } (n_i/n) < 10^{-8} \qquad (27b)$$

Evidently the value of λ''' varies from iteration to iteration. Its use, subject to the conditions listed in equations (25), (26) and (27a) or (27b), would limit the growth of all currently significant species (with $n_i/n \geq 10^{-8}$) to a maximum of e^2 (equation (26)). The currently insignificant species (with $n_i/n < 10^{-8}$) are also prevented from suddenly rising to mole fractions in excess of 10^{-4} (equation (27a) or (27b)).

The iterative process is carried on until acceptable limits of error are attained. The approach to those limits is monitored by an error parameter (ψ) given by,

$$\psi = \frac{1}{2}\left[\sum_{k=1}^{k^o}(\varepsilon'^{2}_{b,k}) + \varepsilon_n^{\,2} + \sum_{i=1}^{i^o}\varepsilon'^{2}_{\bar{\mu},i}\right]^{1/2} \qquad (28)$$

where $\varepsilon'_{\bar{\mu},i} = \bar{\mu}_i - \sum_{k=1}^{k^o}\nu'_{k,i}\bar{\mu}_k$. It can be seen from equation (28) that ψ is essentially something of a 'root mean square error', following each iteration, in the computed species mole numbers, total number of moles and the chemical potentials. When this quantity is small enough, depending on the desired accuracy, the problem of computing the equilibrium composition of the reaction products will have been expended with.

3.4 Computed Results

Appendix B contains a listing of EQUICALX, a computer program written in FORTRAN IV to carry out the computation procedure described above. Sample results of that program are reproduced in Table II for heptane (C_7H_{16}) at 2700 R for three values of Φ'. Similar results for the same fuel are taken from reference [8] and included in that table for comparison.

TABLE II. Mole fractions computed by EQUICALX for the products of the combustion of Heptane (C_7H_{16}) in air at 2700 R (1500 K) for $\Phi' = 0.5$, 1.0 and 2.0 compared with similar results given in reference [8].

Species	Computed by EQUICALX			from Reference [8]		
	Φ'=0.5	1.0	2.0	0.5	1.0	2.0
C	0.0	0.0	0.0	--	--	--
H_2	0.14427	0.00001	0.00000	0.14559	0.00004	0.00000
O_2	0.00000	0.00085	0.10112	0.00000	0.00005	0.10046
N_2	0.57961	0.73318	0.76006	0.57354	0.72576	0.75200
CO	0.16121	0.00002	0.00000	0.16211	0.00009	0.00000
CO_2	0.03498	0.12408	0.06436	0.03371	0.12381	0.06422
CN	0.0	0.0	0.0	--	--	--
H	0.00001	0.00000	0.00000	0.00001	0.00000	0.00000
HCO	0.00000	0.0	0.0	--	--	--
HO_2	0.0	0.0	0.00000	--	--	--
H_2O	0.07995	0.14181	0.07352	0.07819	0.14155	0.07337
O	0.00000	0.00000	0.00000	--	--	--
OH	0.00000	0.00002	0.00006	0.00000	0.00001	0.00006
N	0.0	0.0	0.0	--	--	--
NO	0.00000	0.00008	0.00089	0.00000	0.00002	0.00089
Ar	--	--	--	0.00686	0.00868	0.00900

The effectiveness and accuracy of the above procedure are now evident. Discrepancies between the concentrations of N_2 in corresponding columns of that table almost exactly accounted for by the difference between pure and atmospheric N_2.

TABLE III. Mole fractions of CO, CO_2 and H_2O present in the products of the combustion of C_3H_8 with air in the temperature range 1000 - 4500 R ($\Phi' = 1.0$)

	1000 R	1500	2000	2500	3000	3500	4000	4500
CO	0.0	0.0000	0.0000	0.0000	0.0004	0.0020	0.0104	0.0279
CO_2	0.1163	0.1163	0.1163	0.1163	0.1159	0.1136	0.1050	0 0856
H_2O	0.1550	0.1550	0.1550	0.1550	0.1548	0.1539	0.1498	0.1385

TABLE IV. Mole fractions of CO, CO_2 and H_2O present in the products of the combustion of C_3H_8 with air in the temperature range from 1000 R to 4500 R ($\Phi' = 3.0$)

	1000 R	1500	2000	2500	3000	3500	4000	4500
CO	0.0	0.0	0.0000	0.0000	0.0000	0.0001	0.0008	0.0038
CO_2	0.0409	0.0409	0.0409	0.0409	0.0409	0.0408	0.0400	0.0368
H_2O	0.0545	0.0545	0.0545	0.0545	0.0544	0.0539	0.0524	0.0484

It is possible to tabulate, using EQUICALX, the gas composition following the combustion of any fuel at any temperature and theoretical air (Φ'). This is done for gaseous propane (C_3H_8) in the temperature range 1000 R to 4500 R and at two values of Φ' (1.0 and 3.0), as depicted in Tables III and IV. Only the mole fractions of CO, CO_2 and H_2O are listed since the latter two are of the most interest in the study reported. CO is included merely for comparison with the other two gases.

The integration of the equilibrium computation scheme into the calculation of the distributions of temperature and wall heat flux is a fairly straightforward matter, as will be discussed in Chapters V and VI.

CHAPTER IV

THE RADIATIVE PROPERTIES OF COMBUSTION PRODUCT GASES

4.1 Introduction

Thermal radiation is a form of energy transport whose emission or absorption by matter is a consequence of the possession or results in the increased possession, by matter, of temperature. It collectively refers to the infra-red, the visible and the ultra-violet forms of radiation. Thermal radiation represents, therefore, a small portion of the much wider family of electromagnetic wave phenomena whose members range in wave length, λ, from the very-short-wavelength γ-rays through the X-rays, thermal radiation, to the long-wavelength Hertzian (radio and electric) waves. These wave phenomena have at least one thing in common: they all travel at the same characteristic speed, the speed of light. Consequently their frequencies vary in a reverse manner to their wavelengths as the spectrum is traversed.

Electromagnetic waves result from or give rise to energy-level transitions within the atomic/molecular structure of matter. The atom is theorised as consisting of a central core, the nucleus, surrounded by a number of electrons all statistically distributed in discrete energy levels, the

number of electrons per nucleus depending on the species of matter (atomic number) and its state of ionisation. The nucleus itself is composed of even smaller units than itself, including the so-called 'nucleons' (protons and neutrons) and other more esoteric particles. These nucleons are also arranged in nuclear energy levels. Atoms bond together to form molecules which may be symmetric, e.g., H_2,O_2 and N_2, or asymmetric, e.g., CO_2, H_2, SO_2 and CO. These molecules are perpetually in vibratory and, in fluids, rotatory as well as translatory motion. The vibratory and rotatory motion of the molecules take place only in a number of discrete associated energy levels.

It is the transitions that occur among the energy levels enumerated above that are responsible for, or that do result from, the interplay between radiation and matter. These transitions occur only with the emission or absorption of radiation possessing energy exactly equal in magnitude to the energy differentials among the energy levels in question.

The Quantum Theory postulates electromagnetic wave phenomena to be lumps or particles (quanta) of energy. Each quantum is associated with a particular wave (frequency) and with a particular energy-level transition within matter. The γ-rays are associated with nuclear energy-level

transitions, X-rays with those of the lower electronic energy levels, whereas the ultra-violet and the visible parts of the electromagnetic spectrum are involved in the transitions occurring among the higher electronic energy levels. The vibrational and rotational energy-level transitions occur sequel to the emission or absorption of infra-red radiation. The longer-wavelength members of the spectrum, e.g., the Hertzian waves, have to do with the excitation of (i.e., energy level transitions among) the valence electrons of matter. Such excitation is the result of the application to matter of an electric potential.

Thermal radiation is emitted and absorbed by all bodies at all temperatures above absolute zero. The amount emitted and absorbed by matter increases with the absolute temperature of the source (emitter). Generally, in most computations of engineering heat transfer, thermal radiation becomes important only when the absolute temperature of the emitter is t nds of degrees. Thermal radiation, as hinted to abo is dispersed through the spectrum of wavelengths. This is due to the statistical nature of all atomic movements. The general level of such movements determines the general 'level' of wavelengths of the significant emitted radiation, as depicted in the spectral-distribution (spectro-radiometric) curves sketched in

Figure 5 for an ideal (black body) radiator. The black-body radiator emits (and absorbs) the maximum possible radiation at any given temperature. The shapes of these curves are given by the so-called Planck's Law [19,24];

$$E_\lambda = (C_1/\lambda^5)/(e^{C_2/\lambda T} - 1) \qquad (29a)$$

where C_1 and C_2 are the Planck's constants (first and second, respectively) and E_λ the monochromatic emissive power of the emitter.

It is evident from Figure 5 that, in general, the hotter a body, the shorter the wavelength range for the major part of the emitted radiation and the more peaky the spectroradiometric curve. The converse is true for cooler bodies. For example, the sun, at a temperature of about 10 500 R emits over 90% of its thermal radiation between 0.1 and 3μ whereas a body at about 2 500 R emits between 1 and 20μ [24]. The total thermal radiation emitted by a body is the area under its spectroradiometric curve. This has been found to be related to its temperature as follows;

$$E = \sigma T^4 \qquad (29b)$$

which is the Stefan-Boltzmann Law, σ being the Stefan-Boltzmann constant.

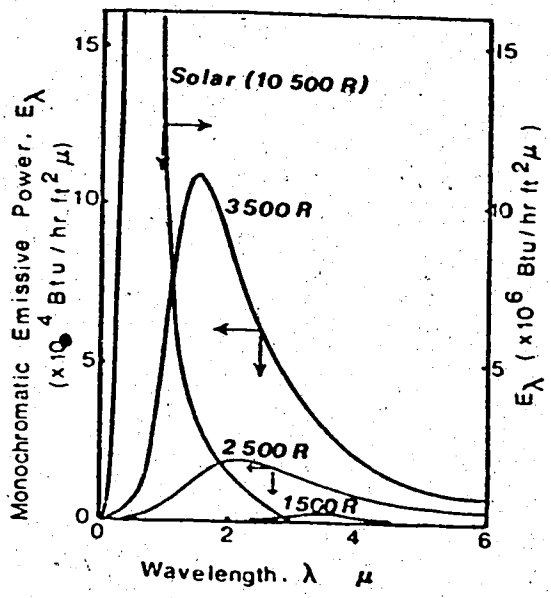

Figure 5. Spectroradiometric Curves for a Black Body at Various Temperatures.

For solids, the vast majority of which are opaque to thermal radiation, this phenomenon is essentially an af r of the solid surface. Most solid surfaces do not em chermal radiation in conformity with the spectroradiometric curve of the ideal radiator. The monochromatic emissive power of conductors at a given temperature decreases with increasing wavelengths whereas it increases irregularly for non-conductors. The monochromatic emissivities of the (real) surfaces vary in a similar fashion with wavelength. It is usually possible, however, to adequately approximate a real surface with a 'gray' surface - one with an emissivity that is constant throughout the spectrum [19,24]. The spectroradiometric curves of gray surfaces then duplicate that of the black-body surface on reduced emissive-power scales.

All the statements made above as well as those to follow will still hold if for 'emissivity' one read 'absorptivity', bearing in mind that the temperature of interest is, and will be, that of the emitter. Use of the emitter temperature ensures the satisfaction of Kirchhoff's Law which requires that for a body in thermal equilibrium $\alpha_\lambda = \varepsilon_\lambda$. For a gray body this requirement becomes $\alpha = \varepsilon$ (involving, in effect, 'total' hemispherical values).

Unlike what happens in solids, thermal radiation in fluids is a volume phenomenon. In combustion studies, gases are of much greater interest than liquids, from the point of view of radiation heat transfer. The emission of thermal radiation in gases (as well as its absorption) is a 'function' of the nature and the composition of the gases as well as the temperatures of the emitter and the absorber. The emission from the gas proper is non-luminous, but the presence of solid particles like soot adds a luminous component to the radiated energy besides introducing the phenomenon of radiation scatter.

The Bouguer-Lambert Law states that the attenuation of a collimated beam of radiation passing through a volume of gas is an exponential decay function. This leads to the following expression for the monochromatic emissivity of the gas

$$\varepsilon_{\lambda,L} = 1 - e^{-K_\lambda L} \qquad (30a)$$

where the K_λ is the monochromatic extinction coefficient for absorption. The assumption is tacitly made that the gas is homogeneous, in which case K_λ is constant along the beam length. This beam length, L, is usually defined as the radius of a hemisphere containing the gas whose radiation is perceived at the centre of the flat face. In

general, K_λ varies throughout the spectrum. An idealisation is usually conceived in the form of the 'gray' gas - one whose absorption coefficient, by analogy with the emissivity of a gray surface, is constant throughout the spectrum. It is a very useful concept as will be seen shortly.

A real gas has neither a spectrum-wise constant absorption coefficient, nor one that is a continuous function of wavelength. In combustion the term 'real gas' usually denotes either CO_2 or H_2O or some mixture of the two. These gases have radiative properties that are complex functions of the partial pressures of the gases, the total pressure and temperature. They are subject to several 'broadening' phenomena including pressure-, collision-, self- and line-broadening. They also overlap in several wavebands, resulting in their radiative properties not being strictly additive. In addition they selectively emit and absorb in some wavebands whilst being transparent to the rest of the spectrum. This selectiveness has origins in the resonance of the molecular rotations and vibrations that have been referred to earlier. A consequence of this behaviour is that a plot of K_λ versus $1/\lambda$ usually is a series of isolated roughly triangular shapes dispersed through the spectrum, as sketched in Figure 6. The values of K_λ are more or less symmetrical about the mean values of $1/\lambda$ (corresponding to the apices of the

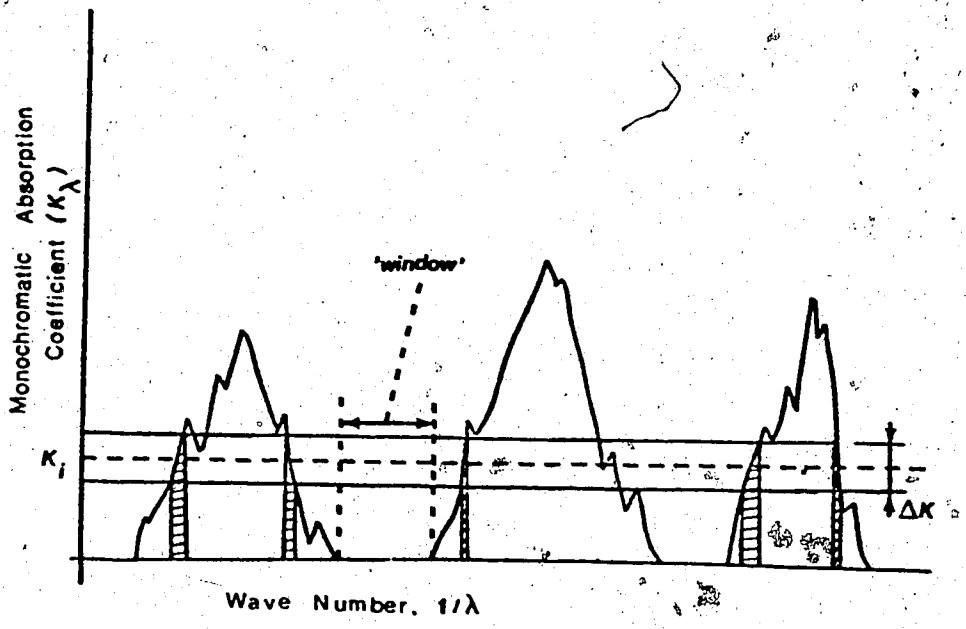

Figure 6. Monochromatic Absorption Coefficient (K_λ) of a Real Gas.

triangles). The gaps between successive 'triangles' are referred to as the 'windows' and they collectively represent the 'clear' gas (radiatively transparent) component of the real gas. Charts have been compiled and published for the emissivities of CO_2, H_2O and other gases. Hottel and Sarofim discuss these at some length in their book. Some complex correction factors and schemes have been developed to reduce the errors introduced by the various phenomena cited herein.

It is evident then that some simplifications are mandatory if the emissivity charts of the gases CO_2 and H_2O are to be usable for the purpose of solving the energy balance equations cited in Chapter I. Fortunately this is possible in the form of an idealised multiple gray gas and clear gas mixture that approximates the radiative behaviour of the real gas.

4.2 Gray Gas Approximations

The basis for this artifice can be established quite simply by taking the definition of the total hemispherical emissivity of any volume of gas. This is,

$$\varepsilon_{g,L} = \int_0^\infty \varepsilon_{\lambda,L}\, E_\lambda\, d\lambda \;/\; \int_0^\infty E_\lambda\, d\lambda$$

which can easily be transformed into

$$\varepsilon_{g,L} = \int_0^1 (1 - e^{-K\lambda L})\, df \qquad (30b)$$

where $f = \int_0^{\lambda} (E_\lambda/E)\, d\lambda$. This quantity is the fraction of the total emissive power occurring within the wavelength interval from zero to λ. It becomes unity, naturally, when the upper limit of integration is taken to infinity.

By invoking the congruence between an integral and the summation of discrete strips of area under a curve,

it is possible to re-express the integral in equation (30b) as the summation:

$$\varepsilon_{g,L} = \sum_{i=1}^{m} \Delta f_i\, (1 - e^{-K_i L}) \qquad (30c)$$

in which the K_i are constant, the Δf_i being the fraction of the total emissive power falling within the range(s) of λ to which the mean of $K_i \pm \Delta K/2$ would apply (see Figure 6). The number (m) of the discrete items under the summation sign can conceivably be very large. It is evident from Figure 6 that the ranges of λ to which $K_i \pm \Delta K/2$ apply are not necessarily contiguous. However, this is really immaterial as long as the proper values of

Δf_i are used. Using the definition of a gray gas, equation (30c) can be looked upon as the weighted sum of the emissivities of a number (m) of gray gases. The weighting factors, Δf_i can be alternatively symbolised as $a_{G,i}$ so that equation (30c) becomes,

$$\varepsilon_{g,L} = \sum_{i=1}^{m} a_{G,i} \, (1-e^{-K_i L}) \qquad (30d)$$

It has been found in practice that m rarely exceeds 3 [19, 20,22,27]. For this study m = 2 was found to yield satisfactory accuracy. The temperature variation of $\varepsilon_{g,L}$ demands that the $a_{G,i}$ and the K_i be functions of temperature also. The potential difficulty resulting from this is obviated by keeping the K_i constant at some mean values while the $a_{G,i}$ are forced to account for the temperature variation of $\varepsilon_{g,L}$. The procedure for computing the $a_{G,i}$ and the K_i have been outlined by Hottel and Sarofim [19] and will be briefly reviewed.

4.3 Method of Computation

The emissivity of an irregular gas volume, as perceived at a point within the volume, is a function of beam length, L. This varies with direction. It is customary, therefore, to define a mean value, L_m. This is recommended to be

$$L_m = 3.5\ (V/A)_D \tag{31}$$

Using this mean value, a table is prepared of $\varepsilon_{g,L}$ versus L while the latter varies from the minimum value to be encountered in the system to something more than twice the mean beam length [19,29]. This is done at the temperature in the middle of the expected temperature range. Equation (30d) is then recast in the more general form;

$$(\varepsilon_{g,\infty} - \varepsilon_{g,L}) - U'(i-1) \sum_{j=1}^{i-1} a_{G,i}\, e^{-K_j L} = \sum_{i'=i}^{m} a_{G,i'}\, e^{-K_{i'} L} \tag{32}$$

where U' (i-1) is a unit-step function having a value of zero for $i \leq 1$ and unity for all $i > 1$. In other words, it is zero during the computation of $a_{G,1}$ and K_1. The quantity $\varepsilon_{g,\infty}$ (the gas emissivity at infinite beam length) is given by,

$$\varepsilon_{g,\infty} = \sum_{i=1}^{m} a_{G,i} = 1 - a_{G,O} \tag{33a}$$

where $a_{G,O}$ is the weighting factor for the clear gas component.

If the RHS of equation (32) is assumed to be arranged such that

$$K_{i'} >> K_{i'-1} \quad \text{for all } i' \tag{33b}$$

then one finds that at 'large' values of L the RHS of that equation will be dominated by its first member, i.e., by $a_{G,i}\, e^{-K_i L}$. Consequently if a judicious choice is made of $\varepsilon_{g,\infty}$ then a semi-log plot, using common logarithms, of the LHS of equation (32) versus L would, at large enough values of L, be a straight line of slope $-K_i$ with an intercept on the vertical axis of log $a_{G,i}$.

A repeated application of this procedure will yield all the pairs of $a_{G,i}$ and K_i deemed necessary to satisfactorily approximate the emissivity of the real gas at the given temperature. As indicated above the number of gray gases required is generally less than 3. The weighting factor, $a_{G,0}$, for the 'clear gas' component is calculated residually from equation (33a). At other temperatures in the expected range the $a_{G,i}$ are re-calculated (keeping the K_i unchanged) by matching the computed with the actual values of emissivity at conveniently chosen values of L. For m=2 the suggested values of L are L_m and $2L_m$.

Having calculated the $a_{G,i}$ at the selected temperatures covering the expected range, the next step is to obtain the best polynomial (ordinary) in T to fit the temperature variation of each $a_{G,i}$. A good way of doing this is first

to obtain the best Chebyshev polynomial (with the minimax property of such polynomials) to fit each $a_{G,i}$ over the temperature range. These Chebyshev polynomials are then easily converted into their equivalent ordinary polynomials thereby retaining the accuracy of the former. Standard subroutines for these polynomial operations are available in the IBM SSP (Scientific Subroutine Package).

The ordinary polynomials representing the $a_{G,i}$ can be generally written thus;

$$a_{G,i} = \sum_{j=0}^{j_{max}} b_{ij} T^j \qquad (34a)$$

where the b_{ij} are the temperature coefficients, j_{max} being the degree of the polynomial. Siddall [29] suggests that in general a quadratic ($j_{max}=2$) would be adequate. However, for the cases studied (propane gas-air combustion at $\Phi' = 1.0$ and 3.0) it was found necessary to use polynomials with $j_{max}=5$ to obtain an acceptable accuracy. This was particularly true of the very last gray gas component to be computed which would suggest significant round-off errors accruing from the computation of the 'earlier' gray gas components. The dotted portions of the curves for $a_{G,3}$ in Figure 7b and $a_{G,2}$ in Figure 8 illustrate this last point. Equation (34a) can now be used to express the emissivity

(or absorptivity of the real gas mass, at any beam length (L) and temperature (T) as,

$$\varepsilon_{g,L} = \sum_{i=1}^{m} \left(\sum_{j=0}^{j_{max}} b_{ij} T^j \right) (1-e^{-K_i L}) \qquad (34b)$$

A computer program named GRAYGAS was written to carry out the above procedure and is listed in Appendix C. It incorporates calls to the SSP subroutines mentioned above.

4.4 Results

Figures 7a (curve 1) and 7b present the output of this program for a test case. They show a mixed 3-gray+1-clear idealisation of an equi-molal mixture of CO_2 and H_2O at 2500 R. The total pressure of the gas mixture is one atmosphere and the mean beam length of the enclosure is 3.4 feet. The range of beam lengths used was as in Figure 6-26 of reference [19], the full (i.e., the non-dotted) curve of which is reproduced in curve 3 of Figure 7a. Curve 2 shows the $\varepsilon_{g,L}$ vs. L as computed by GRAYGAS interpolating within the H_2O and CO_2 emissivity tables. The latter were constructed using the emissivity charts in the same reference. The discrepancies observed among these curves can be attributed to a number of factors. These

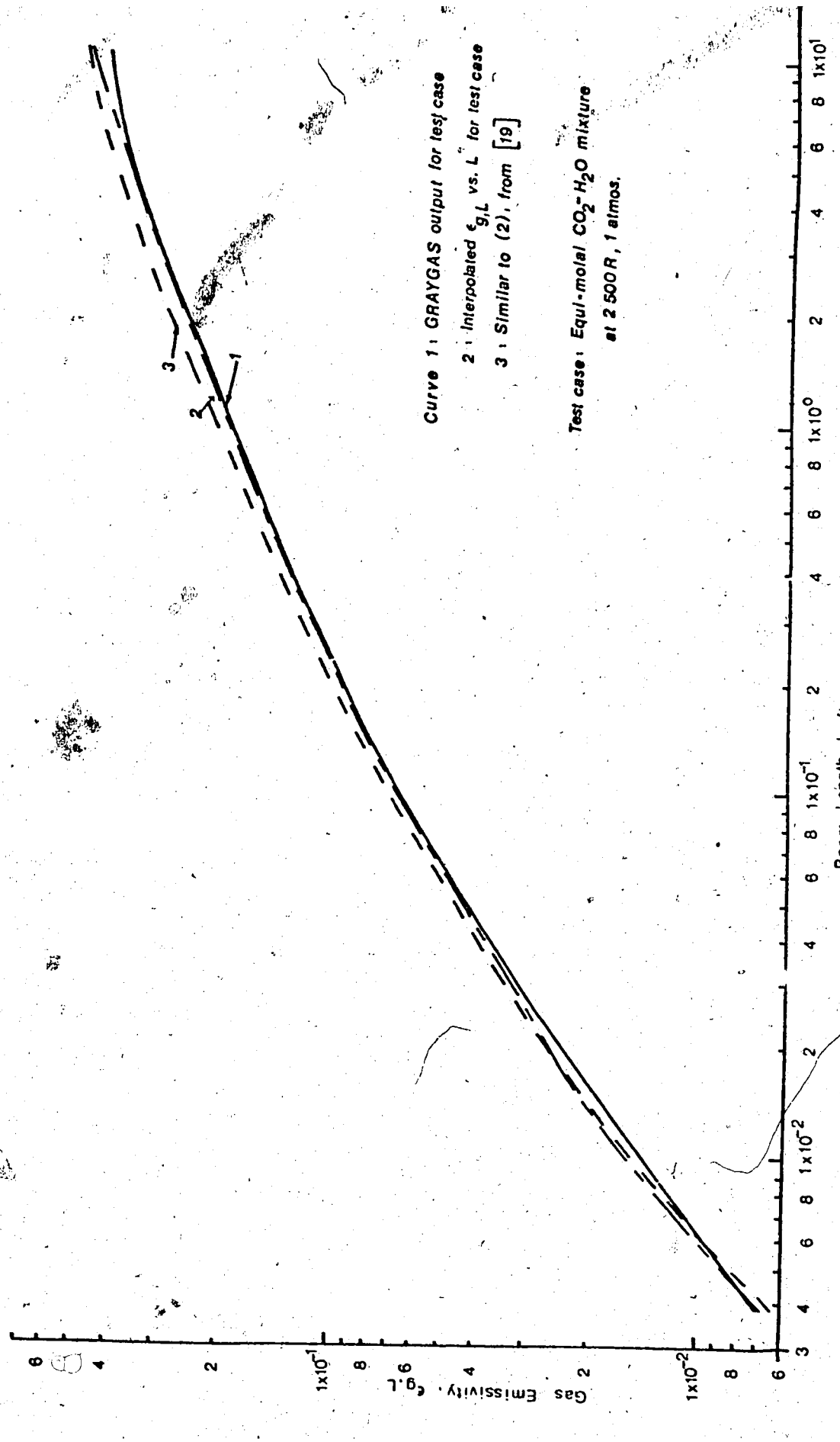

Figure 7a. $\epsilon_{g,L}$ vs. L for an Equi-molal Mixture of CO_2 and H_2O at 2500 R, 1 atmos. Pressure

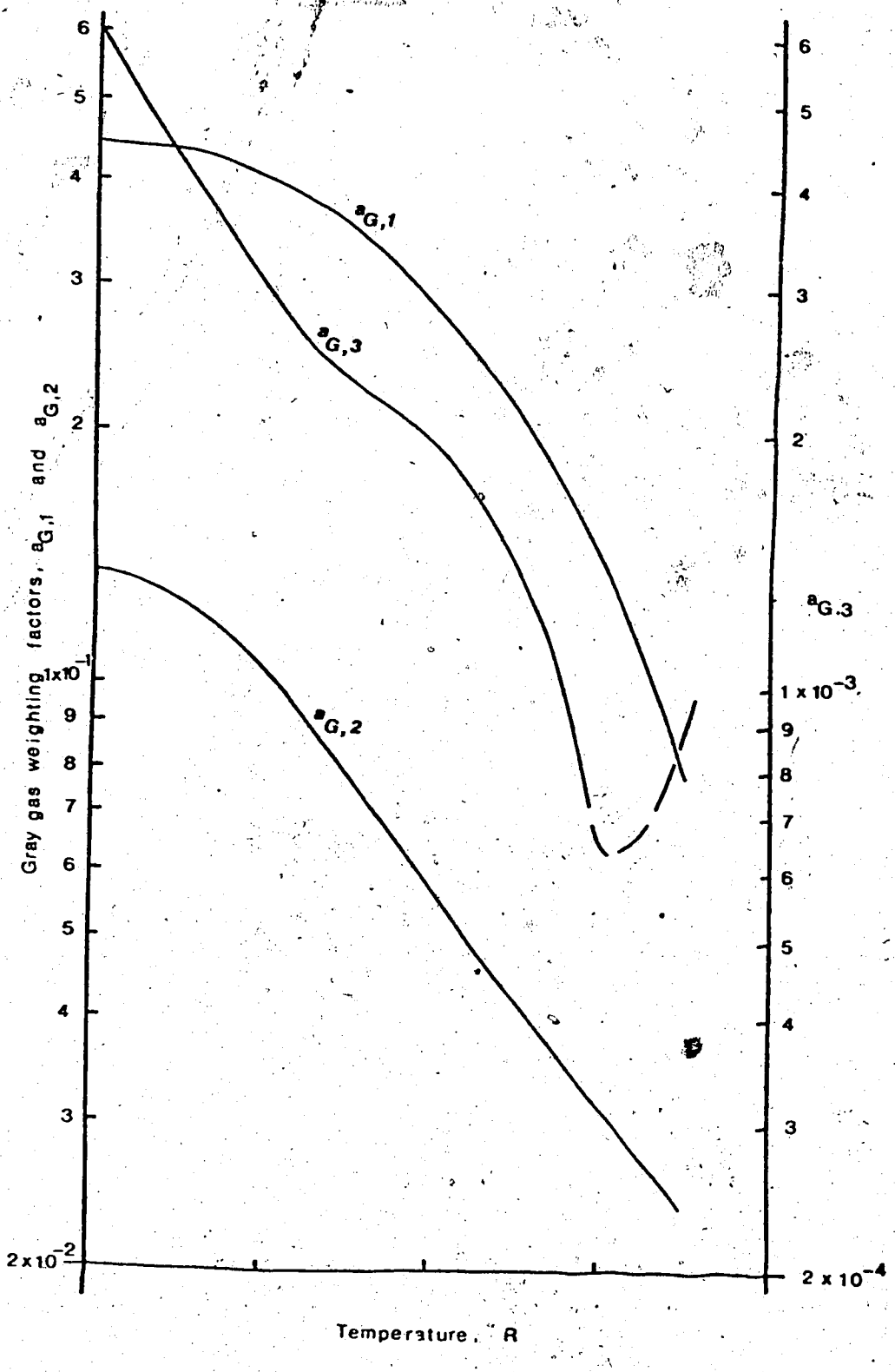

Figure 7b. Temperature Variation of the Component Gray Gas Weighting factors ($a_{G,i}$) for an Equi-molal Mixture of CO_2 and H_2O at 1 atmos. Pressure

include the extrapolation of the (semi-log) charts to higher temperatures; the interpolation within the small-scale charts, especially at the very long and the very short beam lengths; the uncertainties inherent in the corrections for the pressure-broadening and spectral overlap phenomena as well as the round-off errors inevitable in single-precision arithmetic.

It may be noted at this point that the procedure as set out by Hottel and Sarofim [19] requires m to be specified at the start of the computation, to be changed if the accuracy obtained is not acceptable. This need not be the case if it is borne in mind the assumption of equation (33b) indicates at least an order of magnitude difference between successive gray gas absorption coefficients. This connotes an order of magnitude difference between the weighting factors. Furthermore, the maximum contribution of a gray gas to the emissivity of the mixture is its corresponding weighting factor. Consequently, the need to calculate the ith (say) gray gas would not exist if its maximum contribution, $a_{G,i}$, estimated at about $\frac{1}{10}\, a_{G,i-1}$, is negligible. This ensures that no more gray gases are calculated than are necessary to approximate the real gas system to an acceptable degree of accuracy (See Appendix C).

The program, GRAYGAS, was used to approximate the products of propane-gas-air combustion at $\Phi' = 1.0$ and 3.0. The results are shown in Figure 8 and Table V. The former illustrates the variation with temperature of the $a_{G,i}$ while the latter lists the b_{ij} and the K_i.

TABLE V. Gray gas extinction coefficients, (K_i) and the temperature coefficients for polynomial (in T) approximations to the gray gas emissivity weighting factors within the temperature range 1000 to 4500 R ($\Phi' = 1.0$ and 3.0)

	$\Phi' = 1.0$		$\Phi' = 3.0$	
i =	1	2	1	2
K_i	1.214989	12.747631	0.863911	26.484680
	b_{ij}			
j = 0	0.53724 (10^0)	-0.50682 (10^0)	-0.68503 (10^0)	0.21875 (10^0)
1	-0.57285 (10^{-3})	0.10828 (10^{-2})	0.18238 (10^{-2})	-0.44917 (10^{-3})
2	0.49245 (10^{-6})	-0.85458 (10^{-6})	-0.14268 (10^{-5})	0.36157 (10^{-6})
3	-0.23079 (10^{-9})	0.32558 (10^{-9})	0.52167 (10^{-9})	-0.14131 (10^{-9})
4	0.50079 (10^{-13})	-0.60475 (10^{-13})	-0.92702 (10^{-13})	0.26810 (10^{-13})
5	-0.40724 (10^{-17})	0.43945 (10^{-17})	0.64613 (10^{-17})	-0.19797 (10^{-17})

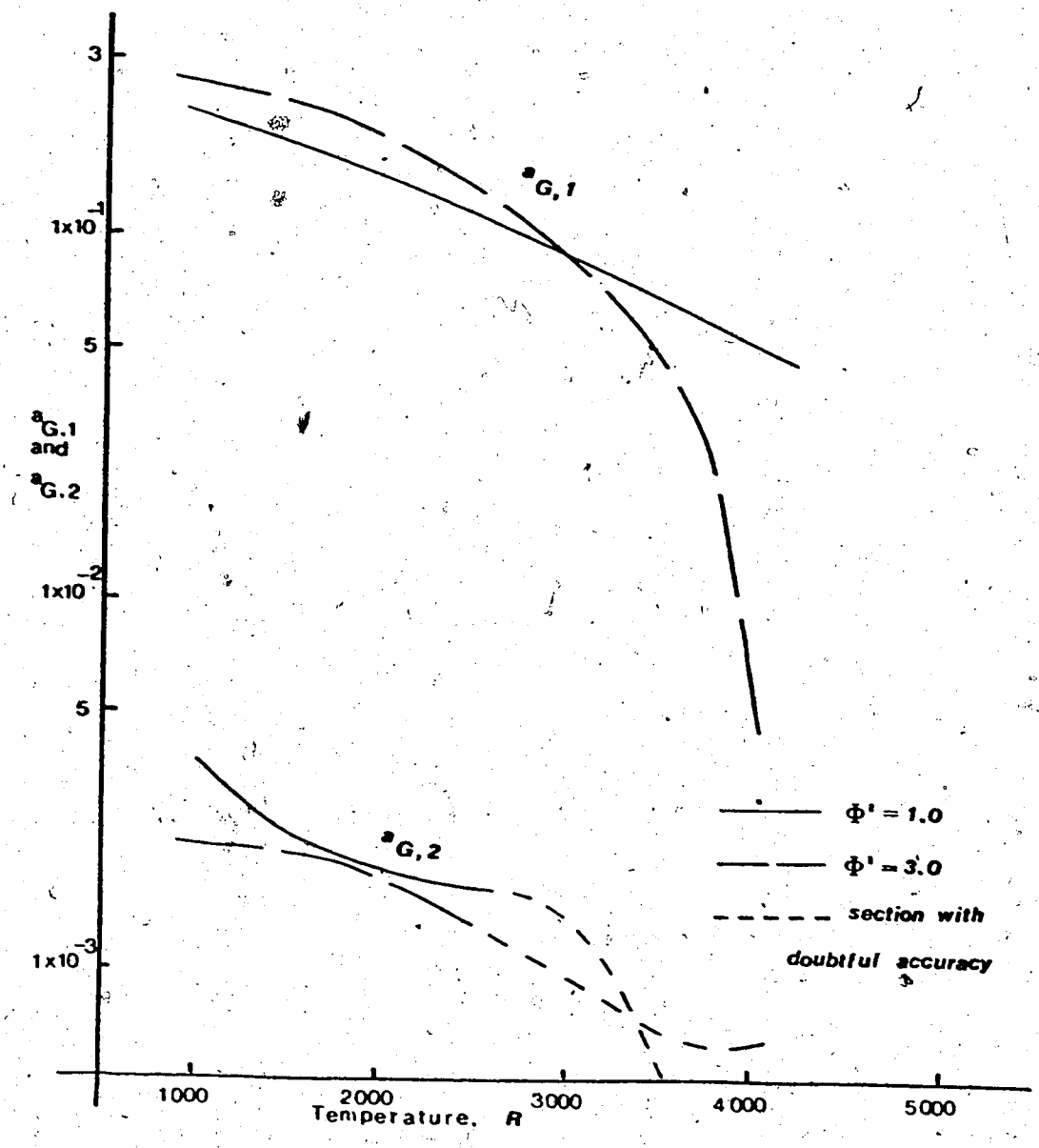

Figure 8. Temperature Variation of the $a_{G,i}$ for the Combustion Products of Gaseous Propane (C_3H_8) and Air (Φ' = 1.0, 3.0; 1 atmos. Total Pressure

CHAPTER V

TEMPERATURE AND HEAT FLUX DISTRIBUTIONS - THE ZONE METHOD

5.1 The Combustion System Model

The system under study is now briefly described. A horizontal cylindrical test combustion chamber 6 feet long and 1.5 feet in diameter encloses an axially positioned turbulent flame. The flame is maintained by a constant supply of gaseous propane (C_3H_8) through a 1/4-inch diameter fuel jet surrounded by a uniform annular secondary air flow. The mass flow rate of the fuel was fixed at 9.75 lb_m/hr. and two different air supply rates were specified so that $\Phi' = 1.0$ and 3.0. The ambient and fluid supply temperatures were taken to be 537°R.

This system is modelled as a closed cylindrical chamber with a plug flow directed towards the 'exit' end and exhausting through an exit hole 6 inches in diameter located on the axis. It is reduced to a collection of zones, gas and surface, in accordance with the Hottel-Cohen Zone Method. The gas volume is divided into 4 contiguous cylindrical zones coaxial with the chamber. The curved surface of the chamber is similarly divided into 4 shorter cylinders. The inlet end is taken as the fifth surface zone while the exit end, excluding the exit hole, makes up the sixth.

This simple coarse-zone configuration, sketched in Figure 9, was adopted in order to facilitate the development of the computer program required for the exercise discussed in this chapter. Naturally, a finer zoning could be used and would be required for more realistic and accurate results. Further comment is reserved for later this section. For each zone an energy balance equation is written. This equation can, assuming steady-state conditions, be summarily stated in the general form;

rate of energy gain - rate of energy loss = 0 (35)

The search for the solution of the simultaneous equations of this kind constitutes the mainstay of the Zone Method.

For a typical gas zone, the first member of equation (35) would involve the rate of energy generation within the zone. Thus the combustion (heat generation) pattern needs be known if the problem is to be solved. For the axi-symmetric system under study, the chamber-fuel-jet diameter ratio is 72. It seems reasonable, then, to presume the combustion process to occur along the chamber axis. In other words, if the system possessed more than one gas zone in the radial direction, then the energy generation term in equation (35) would not exist for all gas zones except those situated on the [illegible] the chamber and

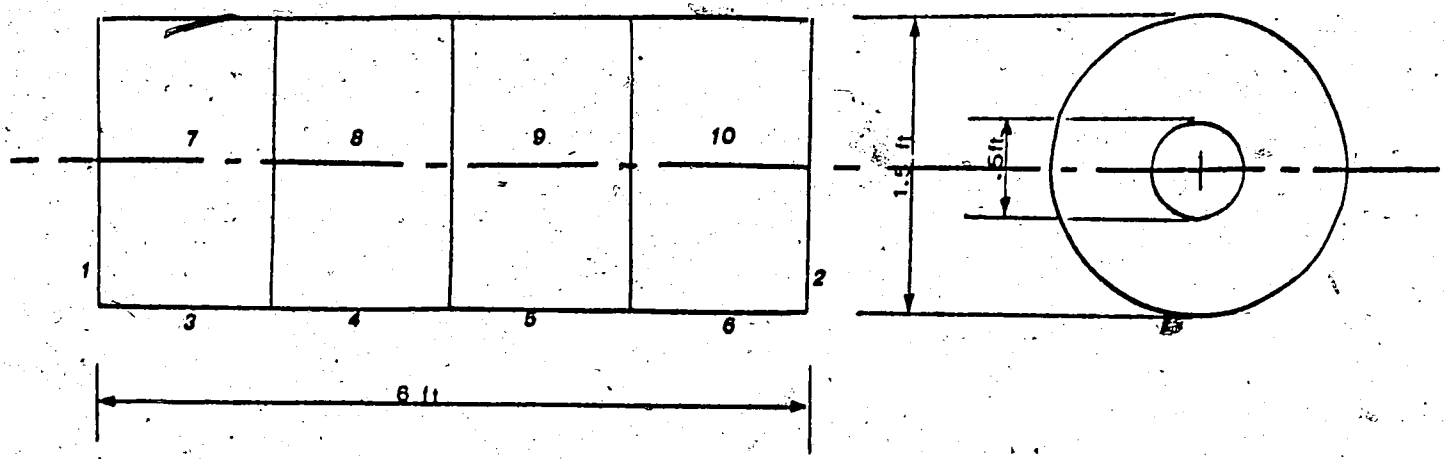

Figure 9. Zone Configuration for the Confined Turbulent Flame Jet System Studied.

within the length of the same occupied by the flame.

The length of the flame is thus also required. It may be computed using one of the two relationships presented in Chapter II. For this study equation (3) was used on account of its established universality and reliability [4,17]. It predicted a flame length of 4.7 feet. Equation (4) was employed to check that computed flame length with which it was found to agree within 5%.

The computation of the radiative exchanges among the zones requires information on the gas zone compositions. In Chapter I it was stated that in the application of the Zone Method a uniform, constant gas composition was usually assumed to be in effect [19,27,29]. This usually leads to localised errors in the computed distributions of temperature and heat flux and these errors are sometimes sizeable [27]. Some improvements would naturally result if allowance is made for the partial pressure gradients occurring in the chamber [27].

It was suggested earlier that a zone-temperature and mixing-process-dependent equilibrium composition may exist in each of the gas zones. This supposition would strengthen somewhat the coupling among the gas zone radiative properties, the zone temperatures and the mixing process. During

an iterative procedure the zone temperatures would vary from iteration to iteration. The assumption of a zone-temperature-and-mixing-process-dependent equilibrium composition would, therefore, add both to the rigour of, and the computational effort required by, the combustion system model.

It is often rewarding to imbue a theoretical model such as this with all available conceptual and mathematical rigour. In the light of this, Hottel and Sarofim [19] have suggested the initiation of a theoretical modelling exercise with the most rigorous approach as a possible means of abstracting the value of the model, presumably through the subsequent, progressive and selective shedding of various aspects of that model. One cannot cavil at this proposition. However, it sometimes happens that other considerations make the opposite approach more attractive and feasible. Such is the case with the work reported herein.

The setting up and successful operation of the subordinate, constituent aspects of the complex theoretical model was regarded as a necessary initial step towards their eventual merger into the composite system. Consequently the uniform, constant composition assumption was provisionally adopted with the expectation that the outcome of this work

will be of value in the eventual inclusion, into the Zone Method of analysis, of variable, non-uniform gas compositions.

The program GRAYGAS (Chapter IV) is used to obtain an idealised multiple-gray+1-clear-gas mixture for the burned gases. This program also fits a polynomial in T to each $a_{G,i}$ within the temperature range 1 000 R - 4 500 R as outlined. The output of this program serves as data for the solution of the energy balance equations to be discussed later in this Chapter.

5.2 Exchange Areas

The real significance of the gas zone compositions lies in their effect on the radiative properties of the gas zones and, through the latter, on the exchange areas construed to exist between all the zone-pairs of the system [27]. In the non-isothermal systems usually encountered in combustion, the directed-flux areas are of predominant interest (see Chapter I). They are calculable from the total-exchange areas as follows,

$$\overrightarrow{Z_i Z_j} = \sum_{i'=i_1}^{m} a_{G,i'} (\overline{Z_i Z_j})_{i'} \qquad (36)$$

where Z represents the symbol for a general zone, gas (G) or surface (S), i_1 being unity for all gas-surface, surface-gas and gas-gas interchange but zero (to include the clear gas contribution) for surface-surface interchange. The weighting factors $a_{G,i}$, are computed as in Chapter IV. The numerals i and j refer to the zones. The total-exchange areas ($\overline{ZZ}$) are computed from the direct-exchange areas ($\overline{zz}$) [19]. The latter have been computed for a number of combustion system configurations for which formulas and charts have been developed.

For cylindrical chambers Hottel and Sarofim [19] furnish a set of tables attributed to H. Erkku. These tables are directly applicable to chambers whose lengths and diameters are such that a common typical zone dimension, B say, is easily stated. The tables then provide the inter-zone direct-exchange areas for various values of KB, where K is a gray gas absorption coefficient applicable to the system. There are as many direct-exchange areas, for any zone-pair, as there are gray gases in the medium between the zone centres. The tables are applicable to systems with up to 12 axial and 5 radial gas zones. They therefore enable the directed-flux areas to be computed.

One drawback on the use of these tables is that (cylindrical) combustion chambers are not always of dimensions that

are integral multiples of a common dimension, B. Furthermore, systems are often encountered with a larger number of axial gas zones than are covered by the tables. This usually results from attempts to keep KB within the range of the tables (0 to 1.25). Hottel and Sarofim [19] suggest some approximate, but not so simple-to-use, formulas for such systems. Another apparent defect in the tables is the need to apply to the tabulated exchange areas correction factors whose values are often unknown or difficult to determine. Additionally, Hottel and Sarofim advise the avoidance of KB values in the range 0.4 to 3.0 which practically includes the range of KB used in the tables. For KB in excess of 3.0 (i.e., for 'optically thick' gases) they recommend the diffusion approximation for radiative transport [1,10,19,21,29]. The values of KB encountered in this work ranged from 1.3 to 39.8 (see Table VI for the values of K_i at the different Φ').

This concept of diffusion is attributed to S. Rosseland. It considers the transport of radiation through an optically thick medium as being akin to the diffusion process or to thermal conduction. The diffusing or conducted material is the thermal radiation quantum, the photon. Using this concept, formulae are obtained for the directed-flux areas. It is usual to assume that the zones are only influenced by their neighbours except in surface-surface

exchange in which the clear gas contribution is undiminished.

The use of the diffusion approximation is facilitated by the definition of a certain absorption coefficient, the Rosseland-mean absorption coefficient, K'_R, which is given by,

$$(1/K'_R) = \int_o^\infty \frac{1}{K_\lambda} (\partial E_\lambda / \partial E)_\lambda d\lambda \qquad (37a)$$

which can be put in the form

$$(1/K'_R) = \int_o^1 (1/K_\lambda)\ df^* \qquad (37b)$$

where K_λ is the monochromatic absorption coefficient at wavelength λ, f^* being defined by

$$f^* = \int_o^\lambda (\partial E_\lambda / \partial E)_\lambda\ d\lambda \qquad (37c)$$

The quantity f^* is easily shown to be related to f defined in Chapter IV (see Appendix D). With the tacit assumption of a step-wise relationship between K and λ [19] and hence between K and f^*, equation (37b, is then transformed into

$$(1/K'_R) = \sum_{i=1}^{m} (a_{G,i} + \frac{1}{4} T \frac{da_{G,i}}{dT})/K_i \qquad (37d)$$

which shows that K'_R can be calculated from the $a_{G,i}$ and K_i and as such is as much a function of temperature as they are.

For two adjacent zones i and j whose interface area is A_{ij}, the directed-flux area is

$$\overrightarrow{Z_i Z_j} = A_{ij}/\frac{3}{4}(K'_R B)_{T_i} \qquad (38)$$

where T_i is the temperature of the emitting zone and B is the zone centre-centre distance. This formula is directly applicable to homogeneous gas-gas exchange. For gas-surface, surface-gas and dissimilar gas-gas situations [21] it gives erroneous results because of the exclusion, from its derivation, of the phenomenon variously known as 'energy jump' [10], 'temperature jump' [1,19] and 'radiation slip' [21]. This phenomenon manifests itself in a temperature discontinuity at the interface. The original concept of the diffusion approximation, which works so well in the interior of a homogeneous gas mass, is unable to detect or account for this discontinuity.

Deissler [10] discusses this phenomenon in some detail. He cites some earlier works that use a 'first order energy jump' giving insufficiently accurate estimates of the temperature jump. He also proposes formulae for his 'second order energy jump' which yield what appear to be a remarkable improvement in the accuracy of the predicted temperature discontinuity in the region around the interface, a solid wall, for example. For an emitting-absorbing gas flowing uniformly through a tube of diameter, d_D, he puts forward the following formula for the directed-flux area (per unit interface area) between the gas and the wall:

$$(\overrightarrow{GS}/A)^{-1} = \left(\frac{-q_{r,w}}{E_g - E_s}\right)^{-1} = \frac{1}{2}\frac{3}{4}\left(K'_R \frac{1}{2}d_D\right) + \left(\frac{1}{\epsilon_s} - \frac{1}{2}\right) + \frac{27}{32}\frac{(K'^2_R/K'_S)}{\frac{3}{4}\left(K'_R \frac{1}{2}d_D\right)} \tag{39}$$

where E_g and E_s are the emissive powers at the tube centre and at the wall surface, respectively, K'_S is related to the K'_R and is defined as

$$(1/K'_S) = \int_0^\infty (1/K_\lambda^2)(\partial E_\lambda/\partial E)\, d\lambda \tag{37e}$$

which leads to

$$(1/K'_S) = \sum_{i=1}^{m} (a_{G,i} + \frac{1}{4} T \frac{da}{dT}_{G,i})/K_i^2 \qquad (37f)$$

The development of this relationship is outlined in Appendix D.

It is notable that K'_R and K'_S are computed at the temperature of the emitter to account for the dependence of $\overrightarrow{GS}$ on the emitter temperature. This requirement also ensures that Kirchhoff's law is satisfied should the emitting and the absorbing zones both attain the same temperature. Equation (39) can be applied in the Zone Method if d_D is replaced with Δr, the radial width of the gas zone adjacent to the wall, E_g and E_s becoming the gas and wall zone black emissive powers.

The radiative exchange between a flowing gas and the end walls of a cylindrical chamber, taking account of the energy jump, has received no treatment in the available literature. As a first approximation, however, the formula developed by Deissler [10] for a stationary gas mass between parallel walls may be cautiously adopted, viz.;

$$(\overrightarrow{GS}/A)^{-1} = (\frac{-q_{x,0}}{E_{g,0}}) \frac{1}{2} \frac{3}{4}(K'_R \frac{1}{2}\Delta x) + (\frac{1}{\epsilon_s} - \frac{1}{2}) \qquad (40)$$

where Δx is the axial width of the gas zone adjacent to the end zone, E_g and E_s being the gas and end-wall zone emissive powers.

For optically thick systems, the surface-surface interchange may be approximated by that which takes place through the 'windows' of the radiation spectrum, i.e., the clear gas contribution. From equation (26) this would be

$$\overline{S_i S_j} = a_{G,O} \, (\overline{S_i S_j})_{K=O} \qquad (41)$$

5.3 The Energy Balance Equations

For a surface zone, the first composite term of equation (35) is made up of

(1) the direct one-way flux from all zones, including self-irradiation and

(2) the internal convective heat transfer from the neighbouring gas zone, whereas the second term includes

(1) the radiation emitted by the surface, of the general form $\epsilon_s A$, and

(2) convective thermal losses from the exterior of the system to the surroundings, in the general form

$hA(T_i-T_o)$, which contains the applicable heat transfer coefficient (h), zone surface area (A) and temperature (T_i) and the ambient temperature (T_o).

If the zones of the system are so numbered that the first N' zones are surface zones, the rest being gas zones, then the energy balance equation for a surface zone may be symbolized in the form

$$\sum_{j=1}^{N'} \overrightarrow{S_j S_i} E_j + \sum_{j=N'+1}^{N} \overrightarrow{G_j S_i} E_j + \sum_{j=N'+1}^{N} \delta'_{ij} h_{cg} A_{ij} (T_j - T_i)$$

$$- \varepsilon_s A_i - h_{cs} A_i (T_i - T_o) = 0 \qquad (42)$$

for $1 \leq i \leq N'$, where N' and N are the number of surface zones and the total number of zones, respectively; δ'_{ij} is a neighbour-selector operator, being unity for gas zones adjacent to the surface zone but zero for all others, h_g and h_s are the gas-side and ambient convective heat transfer coefficients, A_{ij} the interfacial area between zones i and j, and A_i the area of zone i.

For a gas zone the rate of energy gain, neglecting conduction through the gas, will include

(1) direct one-way flux from all zones, self-absorption inclusive,

(2) energy generation rate on account of combustion processes taking place within the zone, and

(3) the bulk enthalpy inflow from the neighbouring gas zones.

The rate of energy loss will be made up of

(1) all radiation emitted by the gas zone, of the general form 4KV, where V is the volume of the zone,

(2) convective heat loss to the neighbouring surface zones, and

(3) bulk enthalpy outflow to the neighbouring gas zones.

The plug flow assumption stated earlier has the effect of forcing each gas zone to receive bulk inflow only from the gas zone immediately upstream of itself. Similar considerations would hold for the bulk outflow.

If the gas zone numbering is carried in such a manner that the zone numbers increase downstream and outwards radially, then the energy balance equation for a typical gas zone takes the mathematical form:

$$\sum_{j=1}^{N} \overrightarrow{S_j G_i} E_j + \sum_{j=N'+1}^{N} \overrightarrow{G_j G_i} E_j + \dot{m}' \bar{C}_p A_{i,i-1} (T_{i-1} - T_o) + \dot{Q}_{c,i}$$

$$- \left(\sum_{i'=1}^{m} 4a_{G,i',K_{i'}} \right) V_i E_i - \sum_{j=1}^{N'} \delta'_{ij} h_{c,g} A_{ij} (T_i - T_j)$$

$$- \dot{m}' \bar{C}_p A_{i,i+1} (T_i - T_o) = 0 \qquad (43)$$

for $N'+1 \leq i \leq N$, where $\dot{m}'$ is the mass flow rate per unit area, $\bar{C}_p$ the appropriate mean specific heat at constant pressure for the temperature range encountered and $\dot{Q}_{c,i}$ the rate of combustion-generated energy release within the gas volume. For this study $\dot{Q}_{c,i}$ was zero for all zones except those residing on the chamber axis and containing at least some part of the flame. It was assumed to be directly proportional to the proportion of the flame contained in the particular zone. Equations (42) and (43) then constitute a set of N simultaneous equations in as many unknowns, vis., the zone emissive powers.

5.4 The Solution of the Equations

These equations are nonlinear, containing terms in E with

temperature-dependent coefficients as well as terms in T. Their solution must therefore be obtained iteratively. Some simplification may be attempted to facilitate the solution. This may be in the form of a linearisation of the equations - by converting the terms in T to their rough equivalents in terms of E [19]. When this is done, one obtains the following set of equations;

$$\sum_{j=1}^{N'} \{\overrightarrow{S_j S_i} - \delta_{ij}[(\varepsilon_s + h'_{s,j})A_j + (\sum_{j'=N'+1}^{N} \delta'_{jj'} h''_{g,j'j} A_{j'j})]\} E_j$$

$$+ \sum_{j=N'+1}^{N} [\overrightarrow{G_j S_i} + \delta_{ij} h''_{g,ji} A_{ji}] E_j = -h_s A_i T_o \qquad (44)$$

for $1 \leq i \leq N'$ and

$$\sum_{j=1}^{N'} (\overrightarrow{S_j G_i} + \delta'_{ij} h_{g,ji} A_{ji}) Ej$$

$$+ \sum_{j=N'+1}^{N} [\overrightarrow{G_j G_i} + \delta_{j,i-1} h''_{b,ji} A_{ji} - \delta_{ij} (\sum_{i'=1}^{m} 4a_{G,i} K_{i'}) V_j$$

$$+ (\sum_{j'=1}^{N'} \delta'_{jj'} h''_{g,j'j} A_{j'j}) - \delta'_{j,i+1} h''_{b,ji} A_{ji}] E_j = -\dot{Q}_{c,i} \qquad (45)$$

for $N' + 1 \leq i \leq N$

where $h'_{s,j} = h_s T_j / E_j$, $h''_{g,ji} = h_g (T_j - T_i)/(E_j - E_i)$

and $h''_{b,ji} = \dot{m}' \bar{C}_p (T_j - T_i)/(E_j - E_i)$ all of them computed at the current temperatures and emissive powers. A_{ji} is the interface area between neighbouring zones j and i, while A_i is the area of the ith surface zone.

The set of equations can be summarised in matrix form thus

$$\underline{M}\ \underline{E} = \underline{R} \qquad (46)$$

where $\underline{M}$ is the matrix of the coefficients of the E_j, $\underline{E}$ a vector comprising the E_j, and $\underline{R}$ the vector of the RHS of the set of equations.

Siddall [29] suggests a procedure for solving these equations. The essence of that procedure is adopted, with slight modifications, and will be briefly outlined as follows:

(1) fill in the vector $\underline{R}$ using the specified ambient temperature, convective heat transfer coefficient (h_s), and combustion pattern,

(2) guess the distribution of temperature among the zones of unspecified temperature with which to

(3) calculate the directed-flux areas ($\overrightarrow{ZZ}$) in accordance with equations (38), (39), (40) and (41). Using these and the specified gas-side convective heat transfer coefficient,

(4) compute the elements of $\underline{M}$ and

(5) solve for $\underset{\sim}{E}$, the new temperature distribution. This is done either directly by Gaussian elimination or by the Gauss-Seidel procedure depen ing on the conditioning of $\underline{M}$ which in turn depends on the ordering of the system of equations as well as the current temperature distribution. Having computed the vector $\underset{\sim}{E}$, then

(6) test its members for agreement or otherwise with the previously computed values of the same. If there is considerable error, go back to step 3 above and repeat. If not, then one would have obtained the required temperature distribution. For this study an agreement within 10° R was considered adequate.

(7) Calculate the net heat fluxes through the surface zones — the heat flux distribution. As a check on the calculations,

(8) compute the total rate of heat loss to the surroundings as,

$$\dot{Q}_L = \sum_{i=1}^{N'} h_s A_i (T_i - T_o) \qquad (47)$$

and the net heat generation rate ($\dot{Q}_G$) as

$$\dot{Q}_G = \dot{Q}_H^* - \dot{m}'\bar{C}_p A_D (T_{exit} - T_{inlet}) \qquad (48)$$

Where $\dot{Q}_H^*$ is the overall heat release rate, A_D the cross-sectional area of the chamber, the subscripts to the temperatures being self-explanatory. The quantities $\dot{Q}_G$ and $\dot{Q}_L$ should agree within acceptable limits. For this study an agreement of 80% or better was considered adequate for the coarse-zone configuration used on account of the approximations pertaining to the composition, flow and combustion patterns and the energy balance equations themselves.

A computer program, FTFIELDX, was written to apply the procedure reviewed above. This program is listed in Appendix D. It uses, as part of its input, the output of GRAYGAS (see Chapter IV) to facilitate the execution of step 3 of the procedure.

5.5 Computed Results

The output of the program, for the assemblage of 4 gas and 6 surface zones, is listed in Table VI and is diagrammatically displayed in Figure 10 for $\Phi' = 1.0$ and 3.0.

The curves in Figu[illegible] exhib[illegible] trends in general agreement with those repo[illegible] from experi[illegible]nts [33] with, and theoretical predictions [7] for, some enclosed combustion systems. Figures 11[illegible] illustrate these results.

TABLE VI. The temperature and heat flux distributions, the $\dot{Q}_G$ and the $\dot{Q}_L$ of the combustion system (Φ' = 1.0 and 3.0)

		Temp. (° R)		Heat Flux (Btu/hr. ft.^{2} °R)	
		Φ'=1.0	3.0	1.0	3.0
end zones	1	1446.7	927.5	5458.0	2343.0
	2	1076.9	1046.1	3239.1	3054.6
wall zones	3	1389.6	878.4	5115.9	2048.3
	4	1528.3	1093.8	5947.7	3340.7
	5	1494.9	1221.7	5747.4	4107.9
	6	931.0	980.9	2364.2	2663.2
gas zones	7	1563.4	1000.1		
	8	1843.7	1301.2		
	9	1868.1	1494.7		
	10	1099.1	1148.0		
$\dot{Q}_G$	(x10^3 Btu/hr.)			170.3	117.5
$\dot{Q}_L$	"			150.3	94.9
$\dot{Q}_L/\dot{Q}_G$	(per cent.)			88.3	80.8

It is clear that the iterative procedure set out above and employed in the computer program, FTFIELDX, yields results in qualitative agreement with the expected system behaviour in practice. The maximum temperatures compare with the adiabatic flame temperatures. From a detailed quantitative viewpoint the temperatures and heat fluxes may not be in very good agreement with measured values. This is partly due to the assumption of a uniform, constant concentration and partly to the apparent contradiction between the plug flow assumption and the pheonomenon of flow recirculation. The former source of error would be more significant for the low recirculation case (Ct = 0.673, Φ' = 3.0) while the latter would affect the higher recirculation case (Ct = 0.230, Φ' = 1.0) to a greater degree.

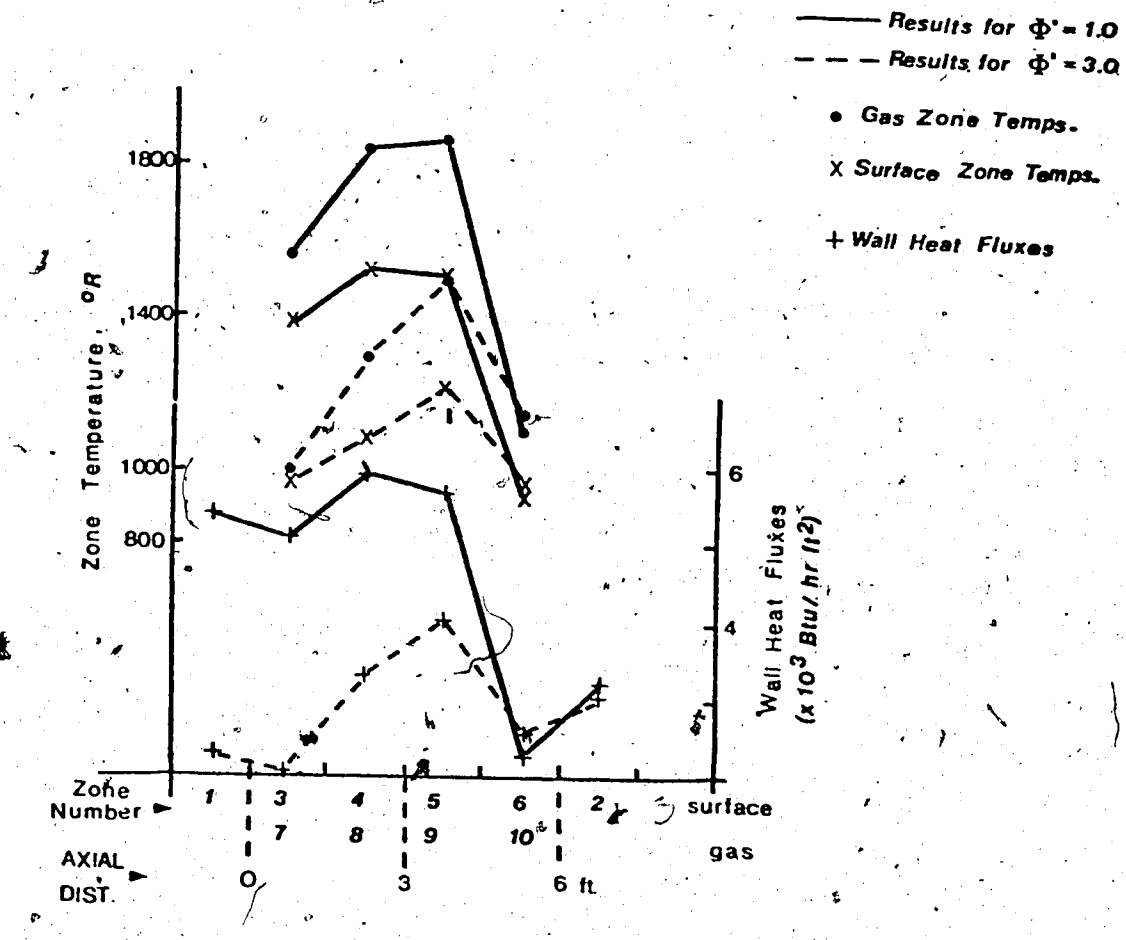

Figure 10. Temperature and Heat Flux Distribution Computed by FTFIELDX for the Confined Turbulent Flame Jet System Studied (Φ' = 1.0 and 3.0)

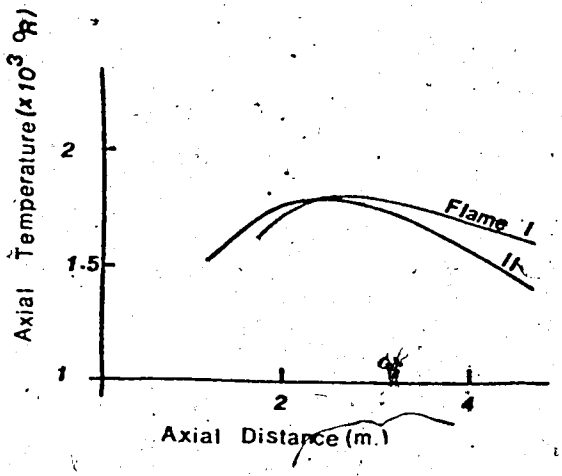

Figure 11a.

Measured Axial Temperatures for Two Enclosed Turbulent Jet Flames. Reference [33]

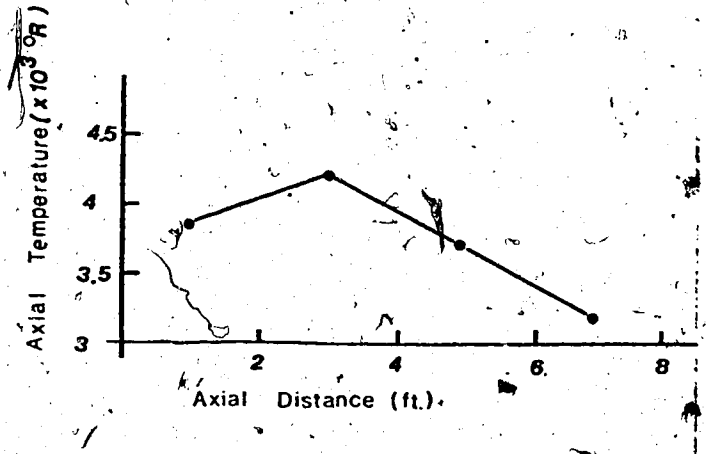

Figure 11b.

Computed Axial Gas Temperature Distribution for an Enclosed Turbulent Jet Flame (Uniform Concentration). Reference [27], Run 7.

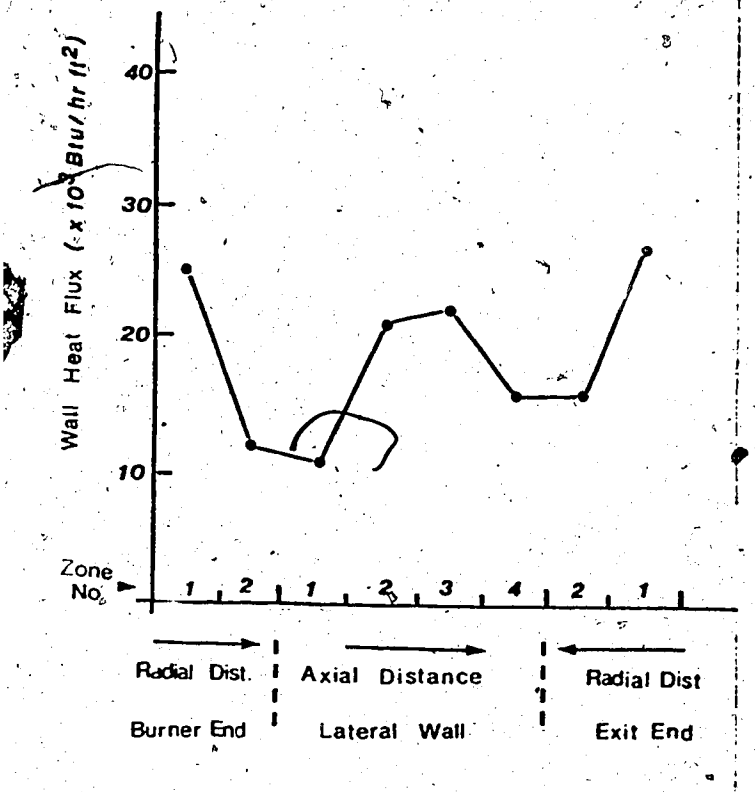

Figure 11c.

Computed Wall Heat Flux Distribution for an Enclosed Turbulent Jet Flame (Uniform Concentration). Reference [27], Run 7.

CHAPTER VI

CONCLUSIONS AND RECOMMENDATIONS

The coaxal jet system, which typifies most combustion systems, can be succinctly represented by similarity parameters of the Thring-Newby or the Craya-Curtet variety. These parameters encapsulate information about the aerodynamics of the combustion system interior, vis à vis flow recirculation and jet mixing. The presence of strong recirculation within the combustion chamber (i.e., at low values of these parameters) would validate the assumption of a uniform composition throughout the chamber. For other systems without a strong recirculatory flow some allowance needs be made for the existence of concentration gradients in the interests of accurate predictions of the temperature and wall heat flux distributions within the chamber.

A suggestion has been put forward of a means of making such an allowance, namely, the existence of equilibrium gas compositions, in the gas zones, that is linked to the zone temperatures and the jet-mixing process. Pursuant to this a computer program, EQUICALX, has been developed to carry out the computation of equilibrium compositions. This program has been shown to yield quite accurate results.

The computation of the temperature and heat flux distributions extant in the combustion chamber is greatly facilitated if the 'real' gas contained therein is idealized as a mixture of a relatively small number of gray gases and a 'clear' component. To this end a computer program named GRAYGAS was developed and, as indicated by the discussion in Chapter IV, gives results that are satisfactorily accurate. This program provides a vital link between the emissivity charts and the computation of the temperature and the heat flux distributions.

The execution of this latter step was carried out, for the system studied, with the aid of a third computer program, FTFIELDX, whose output was shown to agree qualitatively with published measured values. As was indicated, improvements in the accuracy of these results are to be expected if the theoretical model is further refined. This is due to the coupling existing among the temperature and heat flux distributions, the concentration gradients and the jet-mixing process.

Hottel and Sarofim [19] have suggested that when the variations in the local concentrations of the radiatively active gases and/or their relative proportions are significant, the theoretical model should allow for the non-uniformity of the gas concentrations. The assumption of an

equilibrium gas composition pattern linked to the zone temperatures and mixing process is one way of doing this. The output of EQUICALX shown in Tables II, III and IV indicate that although the equilibrium composition, for a given Φ', does not change very much with temperature as long as the latter is not too high (i.e., less than about 3000 R for $\Phi' = 1.0$ and about 3500 R for $\Phi' = 3.0$), the relative proportions of CO_2 and H_2O change significantly with Φ'. The connection between this fact and the equilibrium gas composition postulate mentioned earlier should now be obvious.

The procedures outlined in Chapters III, IV and V which are embodied in EQUICALX, GRAYGAS and FTFIELDX should prove useful in setting up and analysing the more sophisticated model that would account for this interconnection among the temperature distribution, the heat flux distribution, the gas composition pattern and the jet-mixing process. This may take form of first computing the value of Φ' for each gas zone in the absence of combustion and as determined by the jet-mixing process. The one-to-one correspondence existing between Φ' and the equilibrium gas composition of each zone at any given temperature should determine the radiative behaviour of each gas zone. By using the procedures described in Chapters IV and V, the analysis of the model can be carried through to obtain the temperature and heat flux distributions.

REFERENCES

1. Abu-Romia, M. M., and C. L. Tien: 'Appropriate Mean Absorption Coefficients for Infra-red Radiation in Gases', J. Heat Transfer, 89C:321 (1967).
2. Alpert, N. L., W. E. Keiser and H. A. Szymanski: 'Theory and Practice of Spectroscopy', Plenum Press, New York, 1970.
3. Barnett, H. C. et al., 'Basic Considerations in the Combustion of Hydrocarbon Fuels with Air', NACA Report 1300 (1959).
4. Barr, J.: 'Length of Cylindrical Laminar Diffusion Flames', Fuel, Vol. 33, pp. 51-59, 1954.
5. Becker, H. A., H. C. Hottel and G. C. Williams: 'Mixing and Flow in Ducted Turbulent Jets', Ninth Symposium (International) on Combustion, p. 7, Academic Press, New York, 1963.
6. Beér, J. M., and N. A. Chigier: 'Combustion Aerodynamics', Applied Science Publishers, Essex, England, 1972.
7. Burke, S. P., and T. E. W. Schumann: 'Diffusion Flames', Industrial and Engineering Chemistry, Vol. 20 No. 10, p. 998 (1928).
8. Caretto, L. S., and R. F. Sawyer: 'Combustion Thermodynamics', 'Combustion-generated Air Pollution', E. S. Starkman (ed.), Plenum Press, New York, 1971.

9. Codegone, C.: 'A Law of Similarity for Temperature in Enclosed Turbulent Flames', Combustion and Flame, 1:194 (1957).

10. Deissler, R. G.: 'Diffusion Approximation for Thermal Radiation in Gases with Jump Boundary Condition', Trans. ASME, 86C:240 (1964).

11. Exley, J. T., and J. A. Brighton: 'Flow Separation and Reattachment in Confined Jet Mixing', Trans. ASME, 93D:192 (1971).

12. Harker, J. H.: 'The Calculation of Equilibrium Flame Gas Compositions', J. Inst. Fuel, Vol. 40, No. 316, May 1967, pp. 206-213.

13. Harker, J. H. and D. A. Allen: 'The Calculation of the Temperature and Composition of Flame Gases', J. Inst. Fuel, Vol. 42 No. 340, May 1969, pp. 183-187.

14. Hawthorne, W. R., D. S. Weddell and H. C. Hottel: 'Mixing and Combustion in Turbulent Gas Jets', Third Symposium on Combustion, Flame and Explosion Phenomena, p. 266, Williams and Wilkins, Baltimore, 1949.

15. Hayes, J. G. et al.: 'Numerical Approximation to Functions and Data', Athlone Press, London, 1970.

16. Herzberg, G.: 'Molecular Spectra and Molecular Structure: I - Spectra of Diatomic Molecules'. Trans. J. W. T. Spinks, D. Van Nostrand Co., New York, 1950.

17. Hottel, H. C.: 'Burning in Laminar and Turbulent Fuel Jets', Fourth Symposium (International) on Combustion, p. 97, Williams and Wilkins, Baltimore, 1957.

18. Hottel, H. C., and Hawthorne, W. R.: 'Diffusion in Laminar Flame Jets', Third Symposium on Combustion, Flame and Explosion Phenomena, p. 254, Williams and Wilkins, Baltimore, 1949.

19. Hottel, H. C., and A. F. Sarofim: 'Radiative Transfer', McGraw-Hill Book Co., New York, 1967.

20. _____: 'The Status of Calculations of Radiation from Non-luminous Flames', J. Inst. Fuel, Vol. 46 No. 378, Aug./Sept. 1973, p. 295.

21. Howell, J. R.: 'On the Radiation Slip Between Absorbing-Emitting Regions with Heat Sources', Int. J. Heat Mass Transfer, 10:401 (1967).

22. Johnson, T. R. and J. M. Beér: 'Radiative Heat Transfer in Furnaces: Further Development of the Zone Method of Analysis', Fourteenth Symposium (International) on Combustion, p. 639, The Combustion Institute, Pittsburgh, 1973.

23. Kern, D. Q.: 'Process Heat Transfer', McGraw-Hill Book Co., New York, 1950.

24. Kreith, F.: 'Principles of Heat Transfer', 3rd ed., Intext Educational Publishers, New York, 1973.

25. Lewis, B., and G. von Elbe: 'Combustion, Flames and Explosions of Gases', 2nd ed., Academic Press, New York, 1961.

26. Miller, P. A., and S. G. McConnell: 'A Computerised Method for Assessing the Temperatures of Stoichiometric and Lean Natural Gas-Air Mixtures', J. Inst. Fuel, Jan. 1972.

27. Pieri, G., A. F. Sarofim and H. C. Hottel: 'Radiant Heat Transfer in Enclosures: Extension of Hottel-Cohen Zone Method to Method to allow for Concentration Gradients', J. Inst. Fuel, Vol. 46 No. 378, Aug./Sept. 1973, p. 321.

28. Savage, L. D.: 'The Enclosed Laminar Diffusion Flame', Combustion and Flame, Vol. 6 No. 2, p. 77 (1962).

29. Siddall, R. G.: 'The Calculation of Radiative Heat Transfer in Gas-Filled Enclosures', ...from 'Thermal Radiation in Industrial Flames', Von Karman Institute for Fluid Dynamics, Lecture Series 41, Rhode-Saint-Genese, Belgium, December 1971.

30. Steward, F. R., S. Osuwan and J. J. C. Picot: 'Heat Transfer in a Cylindrical Test Furnace', Fourteenth Symposium (International) on Combustion, p. 651, The Combustion Institute, Pittsburgh, 1973.

31. Stull, D. R. et al.: 'JANAF Thermochemical Tables', Clearinghouse, U. S. Dept. Comm., Springfield, Va., August 1965.

32. Sunavala, P. D., C. Hulse and M. W. Thring: 'Mixing and Combustion in Free and Enclosed Turbulent Jet Diffusion Flames', Combustion and Flame, 1:179 (1957).

33. Thring, M. W. and M. P. Newby: 'Combustion Length in Turbulent Jet Flames', Fourth Symposium (International) on Combustion, p. 789, Williams and Wilkins, Baltimore, 1952.

34. Wohl, K., C. Gazley and N. Kapp: 'Diffusion Flames', Third Symposium on Combustion, Flame and Explosion Phenomena, p. 288, Academic Press, New York, 1949.

35. Yagi, S. and K. Saji: 'Problems of Turbulent Diffusion and Flame Jet', Fourth Symposium (International) on Combustion, p. 771, Williams and Wilkins, Baltimore, 1952.

36. Zeleznik, F. J. and S. Gordon: 'The Calculation of Complex Chemical Equilibria', Industrial and Engineering Chemistry, Vol. 60 No. 6, pp. 27-57, June 1968.

APPENDIX A

THEORETICAL AIR AND RECIRCULATION CRITERIA

A.1 Relationship between Φ' and Ct

Becker et al. [5] give the following expression for Ct,

$$Ct = U_k / [(U_{J,O}^2 - U_{s,O}^2)\ \frac{1}{D^2} + \frac{1}{2}\ (U_{s,O}^2 - U_k^2)\ ]^{1/2} \qquad (A.1)$$

where $U_k = (U_{J,O} - U_{s,O})\ \frac{1}{D^2} + U_{s,O}$ and D is the diameter ratio d_D/d_B. By making the substitutions $c = 1 + \frac{2}{Ct^2}$; $B = 1 - 1/D^2$ and $\bar{U} = U_{s,O}/U_{J,O}$, one obtains

$$c = [2(B\bar{U}^2 + \frac{1}{D^2}) - \bar{U}^2] \ /\ (B\bar{U} + \frac{1}{D^2})^2 \qquad (A.2)$$

This directly relates Ct and $\bar{U}$ for any given D. Beér and Chigier [6] give an expression for the ratio of the secondary and primary mass flow rates that can be put in the form:

$$\dot{M}_s/\dot{M}_f = (D^2 - 1)\ \frac{\rho_{s,O}}{\rho_{J,O}}\ \bar{U} \qquad (A.3)$$

For a hydrocarbon fuel C_XH_Y,

$$\dot{M}_s/\dot{M}_f = 4.76 \frac{M_a}{M_f} (X + \frac{Y}{4}) \Phi' \qquad (A.4)$$

Consequently, equations (A.2), (A.3) and (A.4) furnish a relationship between Ct and Φ'. This is graphically depicted in Figure A.1 for two temperature ratios ($T_{s,O}/T_{J,O}$ = 1.0 and 1.4) of the secondary air to the fuel jet, D serving as a parameter.

From this chart Ct and Φ' can be easily correlated. For example, if D=72 and $T_{s,O}/T_{J,O}$ = 1.0 (for the system studied) then a Ct of 0.673 corresponds with an Φ' of 3.0, while Φ' = 1.0 would correspond with Ct = 0.230.

A.2 Relationship between Φ' and β_{tn}, β_{TN}

Beér and Chigier give a definition of the Thring-Newby criterion that can be expressed as:

$$\beta_{tn} = \frac{1}{\bar{C}_f'} D \left(\frac{\rho_{J,O}}{\rho_{s,O}}\right)^{1/2} \left[1 + \bar{U}\left(\frac{1}{\bar{C}_f'} - 1\right)\right]^{1/2} \qquad (A.5)$$

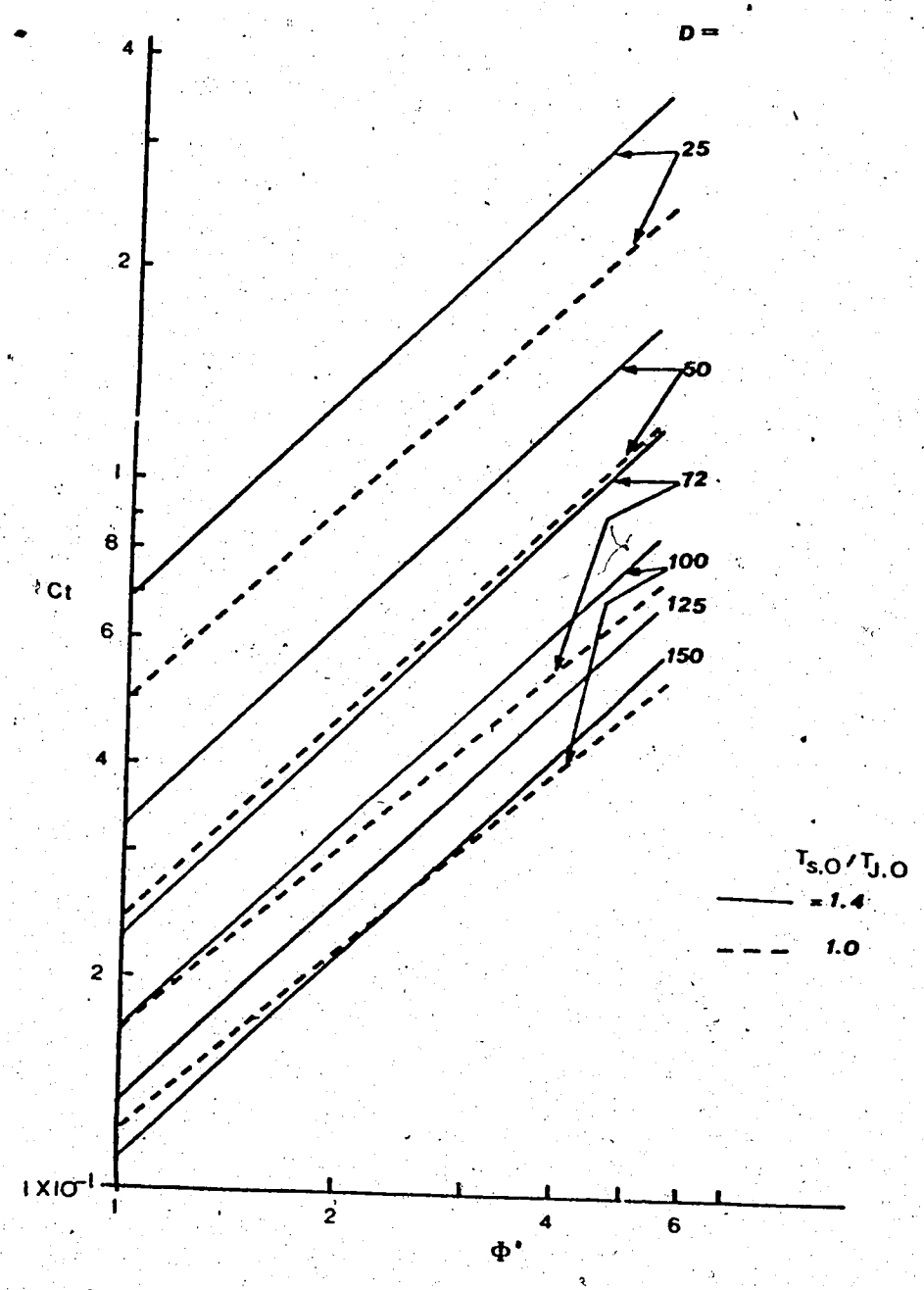

Figure A.1. Ct vs Φ' for $T_{S,O}/T_{J,O}$ = 1.0, 1.4 at Various Values of D.

The modified Thring-Newby criterion is defined [6] as;

$$\beta_{TN} = \frac{1}{\bar{C}'_f D} \left(\frac{\rho_{J,O}}{\rho_{s,O}}\right)^{1/2} \qquad (A.6)$$

Hence

$$\beta_{tn} = \beta_{TN} \; / \; [1 + \bar{U}(\frac{1}{\bar{C}'_f} - 1)]^{1/2} \qquad (A.7)$$

Equations (A.3) to (A.7) inclusive embody the relationship between β_{tn} or β_{TN} and Φ'. Similar considerations apply to this relationship as were discussed in connection with the Craya-Curtet Number (section A.1).

APPENDIX B

TRANSFORMING THE EQUILIBRIUM COMPUTATION EQUATIONS

B.1 The Equations

Equations (13), (17), (18) constitute a set of $i^O + 1$ equations in as many variables:

$$\bar{\mu}_i - \sum_{k=1}^{k^O} \nu'_{ki} \bar{\mu}_k = 0 \qquad (18)$$

$$k^O < i \leq i^O$$

$$\sum_{i=1}^{i^O} (\nu'_{ki} n_i) + b_k^O = 0 \qquad (17)$$

$$1 \leq k \leq k^O$$

and

$$n - \sum_{i=1}^{i^O} n_i = 0 \qquad (13)$$

As commented on in Chapter III, these equations are non-linear and as such can only be solved iteratively. A recommended line of approach is the Newton-Raphson method [36]. Furthermore, the risk of obtaining negative mole numbers necessitates the adoption of some artifice to ensure the avoidance of that potential difficulty. This is by way of replacing the mole numbers with their

logarithms as the new variables.

In applying the Newton-Raphson functional iteration (equation (21)) to the set of equations, use would be made of the following;

$$\bar{\mu}_i = \bar{\mu}_i^* + \ln n_i - \ln n$$

from which follow

$$\partial\bar{\mu}_i/\partial (\ln n_j) = n_j (\partial\bar{\mu}_i/\partial n_j) = \delta_{ij}$$

and

$$\partial\bar{\mu}_i/\partial (\ln n) = n (\partial\bar{\mu}_i/\partial n) = -1$$

One then obtains the following set of equations:

$$(1 - \sum_{k'=1}^{k^o} \nu'_{k'i}) \Delta\ln n_i - (1 - \sum_{k'=1}^{k^o} \nu'_{k'i}) \Delta\ln n$$

$$= -(\bar{\mu}_i - \sum_{k'=1}^{k^o} \nu'_{ki}\bar{\mu}_{k'}) \qquad \text{(B.1a)}$$

$$k^o < i \leq i^o$$

$$\sum_{i=1}^{i^O} \nu'_{ki} n_i \Delta \ln n_i = \varepsilon'_{b,k} \qquad \text{(B.1b)}$$

$$1 \leq k \leq k^O$$

$$n \Delta \ln n - \sum_{i=1}^{i^O} n_i \Delta \ln n_i = -\varepsilon_n \qquad \text{(B.1c)}$$

where the ε's are as defined in Chapter III following equation (23). Upon inspection, equation (B.1a) would seem to indicate the need to define a new variable;

$$u_i = \bar{\mu}_i + \Delta \ln n_i - \Delta \ln n$$

By making that substitution, equations (22) and (23) of Chapter III are obtained, the solution of which constitutes the object of the computer program, EQUICALX, listed in this Appendix. At each iteration the corrected mole numbers are computed using the $\Delta \ln n_i$ in the format of equation (24c) (Chapter III). These $\Delta \ln n_i$ are in turn computed from the u_i thus;

$$\Delta \ln n_i = u_i - \bar{\mu}_i + \Delta \ln n$$

B.2 The Computer Program, EQUICALX

A listing of this program follows. The program, written in FORTRAN IV, was run on an IBM System 360/67 machine at the University of Alberta Computing Services installation.

```
C  EQUICALX
C  COMPUTES EQUIL COMPOSITIONS IN COMBUSTION PROCESSES
C  METHOD OF COMPUTATION  - NEWTON-RAPHSON FUNCTIONAL
C                           ITERATION AS DEVELOPED BY
C                           ZELEZNIK AND GORDON
      DIMENSION  STDMU(30,20),CHEMU(30),
     .  TMP(20),SPECS(30),VNU(30,5),QKZ(5),
     .  BNJ(30,3),BNJG(30,3),NBNJG(30),BNL(3),BNLG(3),BNS(3),
     .  RMEX(8,8),UVEC(8),CVEC(8),ARR(99),DLNJ(30,3),
     .  ERRPSI(1500)
C
C  STDMU        STD-STATE CHEMICAL POTS OF SPECIES
C  CHEMU        CURRENT CHEMICAL POTS OF SPECIES
C  TMP          TEMPS OF AVAILABLE STD-STATE CHEMICAL POTS
C  SPECS        SPECIES LIST
C  VNU          STOICH COEFFICIENTS
C  QKZ          TOTAL # OF COMPONENT MOLECULES PRESENT
C  BNJ          # OF MOLECULES OF EACH SPECIES
C  BNJG         INITIAL GUESSES AT MOLE NOS
C  NBNJG        SERIAL # OF SPECIES
C  BNL          CURRENT TOTAL MOLE NOS
C  BNS          SUM OF CURRENT SPECIES MOLE NOS
C  BNLG         GUESSED TOTAL MOLE NOS
C  RMEX         JACOBIAN MATRIX
C  UVEC,CVEC    VECTORS
C  ARR          INPUT ARRAY FOR IBM SSP ROUTINE 'GELG'
C  DLNJ         INCREMENTAL LOGS OF SPECIES MOLE NOS
C  ERRPSI       ERROR FUNCTION ARRAY
C
C  DATA INPUT
      READ 251, MSPEC, LCOMP,NPH,NGES, NTEMP,NTMP,KDT
      READ 251, ITA, ITZ, NITER
      READ 252, (SPECS(I),I=1,MSPEC)
      READ 253, ((VNU(I,J),J=1,LCOMP),I=1,MSPEC)
      READ 255,((NBNJG(N),(BNJG(N,L),L=1,NPH)),N=1,NGES)
      READ 270, (BNLG(LFA), LFA=1,NPH)
      READ 256, (QKZ(I),I=1,LCOMP)
      READ 257, (TEMP(I),I=1,NTEMP)
      READ 257, (TMP(I),I=1,NTMP)
      READ  58, R,PRES
      READ 259, TOL,ERFLIM,XJLIM
      READ 261, (STDMU(I,J),J=1,NTEMP),I=1,MSPEC)
C
C  MSPEC        # OF SPECIES
C  LCOMP        # OF COMPONENTS
C  NPH          # OF PHASES (MAX=3)
C  NGES         # OF GUESSED SPECIES MOLE NOS
C  NTEMP        # OF TEMPS OF INTEREST
C  NTMP         # OF TEMPS OF AVAILABLE STD-STATE CHEM POTS
C  KDT          CODE FOR IDENTITY OR OTHERWISE OF 'TEMP', 'TMP'
C  ITA,ITZ      FIRST AND LAST TEMPS OF INTEREST
C  NITER        MAX NO OF ITERATIONS SPECIFIED (< 1500)
C  TOL          ERROR TOLERANCE FOR 'GELG'
C  ERFLIM       MINIMUM VALUE FOR ERROR PARAMETER
C  XJLIM        MINIMUM ALLOWABLE MOLE FRACTION
C  R            UNIVERSAL GAS CONSTANT
C  PRES         PRESSURE
C
      DO  2 N=1,NGES
      DO 1  LFA=1,NPH
```

```
      NN=NBNJG(N)
      BNJ (NN,LFA)     =    BNJG(N,LFA)
    1 CONTINUE
    2 CONTINUE
      DO 3  LFA=1,NPH
    3 BNL(LFA)=BNLG(LFA)
      DO 5 LFA =1,NPH
      BNS(LFA) = 0
      DO 4 J =1,MSPEC
    4 BNS(LFA) = BNS(LFA) + BNJ(J,LFA)
    5 CONTINUE
      LNP=LCOMP+NPH
      PRLOG = ALOG(PRES)
      DO 240 ITEMP = ITA,ITZ
      GOTO (10,6), KDT
    6  IF(TEMP(ITEMP) .GE. TMP(1) .AND.
     .   TEMP(ITEMP) .LE. TMP(NTMP))  GOTO  7
      PRINT 322, ITEMP,TEMP(ITEMP)
      GOTO  250
    7 DO 8  IB=1,NTMP
      IF (TMP(IB) .GT. TEMP(ITEMP))  GOTO  9
    8 CONTINUE
    9  FR = (TEMP(ITEMP)-TMP(IB-1))/(TMP(IB)-TMP(IB-1))
   10 CONTINUE
      IHOLD = 0
      DO 195 ITER = 1,NITER
C
C  COMPUTE THE CHEMICAL POTENTIALS
   14    CONTINUE
      DO 35 LFA=1,NPH
      DO 30 J=1,MSPEC
      XJ = ABS(BNJ(J,LFA) / BNS(LFA))
      XLOG = ALOG(XJLIM)
      IF (XJ .GE. XJLIM)  XLOG = ALOG(XJ)
      GOTO  (25,20),KDT
   20 USTD = FR*STDMU(J,IB)+(1-FR)*STDMU(J,IB-1)
      GOTO  29
   25 USTD = STDMU(J,ITEMP)
   29 CHEMU(J) = USTD + PRLOG + XLOG
   30 CONTINUE
   35 CONTINUE
C
C  TEST FOR CONVERGENCE
C  (A) EVALUATE ERROR PARAMETER
   40 SUMQ=0.
      ERF = 3*MSPEC*ERFLIM
      DO 43 K=1,LCOMP
      SUMB=0.
      DO 42 LFA=1,NPH
      SUMA=0.
      DO 41 J=1,MSPEC
   41 SUMA=SUMA+VNU(J,K) *BNJ(J,LFA)
   42 SUMB=SUMB+SUMA
   43 SUMQ=SUMQ + (QKZ(K) - SUMB)**2
      SUMN=0.
      DO 45 LFA=1,NPH
   45 SUMN=SUMN+(BNL(LFA) - BNS(LFA)) **2
      SUMG=0.
      DO 47 J=1,MSPEC
      SUMB=0.
```

```
      DO 46 K=1,LCOMP
   46 SUMB=SUMB + VNU(J,K)  *CHEMU (K)
   47 SUMG = SUMG + (CHEMU(J) - SUMB)**2
      ERRPSI(ITER) = .5* (SUMQ + SUMN + SUMG)
      IF (ERRPSI(ITER) .GE. ERF) GOTO  54
C
C  (B) EVALUATE MOLE FRACTION CORRECTIONS .
      IF (ITER .EQ. 1)  GO TO 54
      DO 49 LFA =1,NPH
      JCOUNT = 0
      DO 48 J =1,MSPEC
      XJ = BNJ(J,LFA) / BNS(LFA)
      DXJ = XJ * DLNJ(J,LFA)
      IF (ABS(DXJ) .GE. 0.5E-05)  GO TO 48
      JCOUNT = JCOUNT + 1
   48 CONTINUE
      IF (JCOUNT .LT. MSPEC)  GO TO 54
   49 CONTINUE
   50 PRINT 300, TEMP(ITEMP)
      PRINT 259,SUMQ,SUMN,SUMG
      PRINT 311
      DO 53 NR =1,LNP
   53 PRINT 321, (RMEX(NR,NC),NC =1,LNP), CVEC(NR)
      PRINT 311
      PRINT 271, (CHEMU(J),J =1,MSPEC)
      PRINT 310
      PRINT 270, (BNS(LFA),LFA =1,NPH)
      GO TO 196
C
C  SET UP MATRIX 'RMEX'
   54 DO 70 K=1,LCOMP
      DO 65 I=1,LCOMP
      BKT =0.
      DO 60 LFA=1,NPH
      SUM=0.
      DO 55 J=1,MSPEC
      ADD=VNU(J,I) *VNU(J,K) * BNJ(J,LFA)
      SUM=SUM+ADD
   55 CONTINUE
   60 BKT=BKT + SUM
   65 RMEX(K,I)=BKT
   70 CONTINUE
      DO 90 LFA=1,NPH
      LCF = LCOMP+LFA
      DO 85 K=1,LCOMP
      SUM=0.
      DO 80 J=1,MSPEC
      ADD=VNU(J,K) * BNJ(J,LFA)
   80 SUM=SUM + ADD
      RMEX(K,LCF) = SUM
      RMEX(LCF,K) = SUM
   85 CONTINUE
      RMEX(LCF,LCF) = BNS(LFA) - BNL(LFA)
   90 CONTINUE
C
C  FILL UP 'CVEC'
  100 DO 140 K=1,LCOMP
      SUM=0.
      DO 135 LFA=1,NPH
      SUMA=0.
```

```
      SUMB=0.
      DO 130 J=1,MSPEC
      ADD=VNU(J,K)*BNJ(J,LFA)
      SUMA=SUMA+ADD
      SUMB=SUMB+CHEMU(J) * ADD
  130 CONTINUE
  135 SUM=SUM + SUMB - SUMA
      CVEC(K) = SUM + QKZ(K)
  140 CONTINUE
      DO 150 LFA=1,NPH
      GBFN=0.
      DO 145 J=1,MSPEC
      GBFN=GBFN + BNJ(J,LFA) *CHEMU(J)
  145 CONTINUE
      CVEC(LCOMP+LFA)  = GBFN  - BNS(LFA) +  NL(LFA)
  150 CONTINUE
C
C  SOLVE FOR UVEC
C  REARRANGE DATA FOR 'GELG'
  154 DO 160 J=1,LNP
      JJ=(J-1) * LNP
      DO 155 I=1,LNP
      ARR(JJ+I) = RMEX(I,J)
      UVEC(I) = CVEC(I)
  155 CONTINUE
  160 CONTINUE
      IER = 0
      CALL GELG (UVEC,ARR,LNP,1,TOL,IER)
      IF (IER .EQ. 0) GOTO  161
      PRINT 251, IER
      GOTO  250
C
C    COMPUTE CORRECTED SPECIES MOLE NOS AND TOTAL MOLE NOS
      LCF=LCOMP+LFA
  161 DO 180 LFA=1,NPH
      FACT = 1.
C
C  (A) DETERMINE OPTIMUM STEPSIZE FACTOR
      UI=UVEC(LCF)
      UAB=ABS(UI)
      IF(UAB .LE. 2.0) GO TO 162
      FACT = 2.0 / UAB
  162 UZ = 2. + UI
      DO 175 J=1,MSPEC
      SUMA=0.
      XJ = BNJ(J,LFA) / BNS(LFA)
      IF(ABS(XJ) .GE. XJLIM) GO TO 166
      XJ = XJLIM
      BNJ(J,LFA) = XJLIM * BNS(LFA)
  166 XJL=ALOG(XJ)
      UX = - 11.212 - XJL
      IF (XJL .LT. - 18.5)  UZ = UZ + UX
      DO 170 I=1,LCOMP
  170 SUMA=SUMA+VNU(J,I)*UVEC(I)
      DLJ =   UI + SUMA - CHEMU(J)
      DLNJ(J,LFA) = DLJ
      IF (DLJ .LE. 0.)  GO TO 175
      IF (DLJ .LE. UZ)  GO TO 175
      RATIO = ABS(UZ / DLJ)
      IF (RATIO .LT. FACT) FACT = RATIO
```

```
  175 CONTINUE
C
C   (B) APPLY COMPUTED CORRECTIONS
  177 BNS(LFA) = 0.
      DO  179 J=1,MSPEC
      ADD = FACT * DLNJ(J,LFA) * BNJ(J,LFA)
      BNJ(J,LFA) =      BNJ(J,LFA) + ADD
      IF (BNJ(J,LFA) .LT. 0.)  BNJ(J,LFA) = 0.
  178 BNS(LFA) = BNS(LFA) + BNJ(J,LFA)
  179 CONTINUE
      ADD = FACT * UI * BNL(LFA)
      BNL(LFA) = BNL(LFA) + ADD
      IF (BNL(LFA) .LT. 0.)  BNL(LFA) = BNS(LFA)
  180 CONTINUE
      PRINT 311
  195 CONTINUE
      GO TO 50
C
C  OUTPUT
  196    CONTINUE
      PRINT 320
      PRINT 311
      DO 198 I=1,ITER,5
      IA = I-1
      IB = IA + 4
      IC = I + 4
  198 PRINT 301, IA,((ERRPSI(J),J),J=I,IB),ERRPSI(IC)
      PRINT 312
      IF (ITEMP .EQ. ITA)  PRINT 309
      PRINT 313,(L,L=1,NPH)
      PRINT 311
      PRINT 302,((SPECS(J),(BNJ(J,LFA),LFA=1,NPH)),
     .           J=1,MSPEC)
      PRINT 310
      PRINT 303,(BNL(LFA),LFA=1,NPH)
      PRINT 324
      PRINT 311
      DO 230 L=1,NPH
      PRINT 323,L
      PRINT 310
      DO 225 J=1,MSPEC
      XJL = BNJ(J,L)/BNL(L)
  225 PRINT 302, SPECS(J),XJL
  230 CONTINUE
  240 CONTINUE
  250 STOP
C
  251 FORMAT(10I5)
  252 FORMAT(10(1X,A4))
  253 FORMAT(4F5.2)
  255 FORMAT (8(I5,F5.1))
  256 FORMAT(4F10.3)
  257 FORMAT(5F10.1)
  258 FORMAT(2F10.3)
  259 FORMAT(8E10.3)
  261 FORMAT(5F15.3)
  270 FORMAT(3F10.3)
  271 FORMAT(5F10.3)
  300 FORMAT ('1',1X,//T50,'TEMP = ',F6.1,2X,'DEG R')
  301 FORMAT( I10,4(E15.3,I10),E15.3)
```

```
  302 FORMAT(40X,A4, F20.5)
  303 FORMAT(T36,'TOTAL NO. MOLES =',F10.5)
  305 FORMAT(1X,I5,F20.5)
  309 FORMAT  (//T60,'RESULTS')
  310 FORMAT('-',1X)
  311 FORMAT(' ',1X)
  312 FORMAT ('1',1X)
  313 FORMAT(///T41,'SPECIES',T57,'MOLE NOS',
     .          //T49,'PHASE',I10,2I20)
  320 FORMAT(//T50,'ERROR PARAMETER TRACE')
  321 FORMAT (' ',8F10.3,F10.3)
  322 FORMAT ('1',1X,///T55,'TEMP(',I2,') = ',F8.1,5X,
     .  'OUTSIDE RANGE OF TMP)
  323 FORMAT ('-',T51,'PHASE',I5)
  324 FORMAT (///T44,'MOLE FRACTIONS')
C
      END
```

APPENDIX C

GRAY GAS APPROXIMATIONS TO REAL GASES

C.1 Termination of the Gray Gas Computations

The computation of a mixed gray+1-clear-gas approximation to a real gas is, in essence, approached through the progressive 'extraction' of the contributions of successive gray gases to the radiative properties of the real gas. This is effected by performing the computations within the beam length ranges in which the different gray gases effectively control all variation of the radiative properties of the overall gas mass.

As suggested by the discussion in Chapter IV, the order of 'extraction' of the gray gases is that of increasing absorption coefficients, K_i. Successive K_i are at least an order of magnitude different from one another, and so are the $a_{G,i}$.

The computation of the component gray gases is to be terminated if the estimated maximum contribution of any as yet uncomputed gray gases (i.e., its weighting factor) is judged insignificant. Thus the specification of this discriminatory level of significant contribution annihilates

any need for an a priori statement of m, the total number of gray gases required.

The extraction of each gray gas is carried out within the range of beam lengths in which the variation of its contribution determines the variation of the overall gas property. The upper limit of this range of beam lengths can be estimated for each gray gas except the very first to be computed. At this upper limit, the contribution of the gray gas is just beginning to be insignificant, for example, at 5 per cent. of its maximum value;

i.e., $$1 - e^{-K_i L_{max,i}} \approx 5\ (10^{-2})$$

i.e., $$L_{max,i} \approx 5(10^{-2})/K_i$$

But $$K_i \approx 10\ K_{i-1}$$

therefore $$L_{max,i} \approx 5(10^{-3})/\ K_{i-1}$$

As a check on the decision to terminate the computation of the gray gases, it may be worthwhile determining the beam length $L'_{max,i}$ at which the contribution of the uncomputed (ith) gray gas is at the minimum allowable level (0.0005, say)

i.e., $a_{G,i}\ (1 - e^{-K_i L'_{max,i}}) \approx 5(10^{-4})$

i.e., $L'_{max,i} \approx 5(10^{-4})/(a_{G,i} K_i)$

i.e., $L'_{max,i} \approx 5(10^{-4})/(a_{G,i-1} K_{i-1})$

Thus the decision to terminate would be vindicated if

$$L'_{max,i} > L_{max,i}$$

C.2 The Listing of GRAYGAS

The graygas approximation program, GRAYGAS, employing the technique set out in Chapter IV and this Appendix, is listed in this section. It is a FORTRAN IV program that was successfully run on an IBM System 360/67 computer installed at the Computing Services of the University of Alberta.

```
C
C   GRAYGAS
C   -COMPUTES A MULTIPLE-GRAY-PLUS-CLEAR-GAS APPROXIMATION
C    TO BURNED GASES IN A COMBUSTION CHAMBER OF GIVEN
C    GEOM USING AS MANY GRAY GASES AS REQD
C    (MAXIMUM 5)
C   -FITS A TEMPERATURE POLYNOMIAL TO EACH GRAY GAS WT-ING
C    FACTOR OVER A GIVEN TEMPERATURE RANGE
C
C
      DIMENSION  EC(30,20),EW(30,20),EG(5,30),AGI(5,30),
     .     GAM(5,5),GMA(5,5),DELTA(30,20),DELTB(30,20),
     .     PLC(30),PLW(30),PWR(10),PCWL(15),
     .     TGP(20),TG(30),TD(5),
     .     BML(20),SIGMA(20),SLK(5),EGAS(20),VGI(20),
     .     AGZ(30),AGR(200),GAR(30),
     .     NPVT(5),FLU(5),RCF(5),VEC(5),VECS(5)
C
C
      COMMON    /XFE/IB,JB,EA,EB
     .          /POL/NTG,NGRAY,MP
C
C   EC,EW          EMISSIVITY (EM) TABLES FOR CO2,H2O
C   EG             GAS  EM  VS BEAM LENGTH (B-L) VS TEMPERATURE (TEMP
C   AGI,AGZ        EM WT-ING FACTORS
C   GAM,GMA        MATRICES
C   DELTA,DELTB    EM DATA CORRECTION TABLES
C   PLC,PLW        PL-VALUES FOR CO2,H2O EM'S
C   PWR            PRESS-RATIOS FOR AVAILABLE H2O
C                  PRESSURE-BROADENING CORRECTIONS
C   PCWL           PL-VALUES FOR EM CORRECTIONS
C   TGP            TEMPS FOR AVAILABLE EM DATA
C   TG             GAS TEMPS OF INTEREST
C   TD             TEMPS  OF AVAILABLE EM CORRECTION DATA
C   BML            BEAM LENGTHS (B-L)
C   SIGMA          B-L/MEAN B-L RATIOS
C   SLK            GRAY GAS EXTNCTN COEFS
C   EGAS           GAS EM VS B-L TABLE AT MID-RANGE TEMP
C   VGI            VARIABLES
C   AGR,GAR,NPVT,
C   VEC,VECS       VARIABLES
C   FLU,RCF        WORKSPACE (FOR CSLNIL)
C
```

```
C DATA INPUT
      KE = 1
C
    1 FORMAT (5I5)
    2 FORMAT (F10.3,9F5.3)
    4 FORMAT (5E15.6)
    5 FORMAT (2F10.3)
    6 FORMAT (5F10.3)
    7 FORMAT (6F10.5)
C
      READ(5,1) NTG,NGR,NSSG,NQ
      READ(5,1)  NTGP,NPC,NPW,MP
      READ(5,1) NF,NL
      READ(5,6)  DIAM,AXIS,DND,XND
      READ(5,6)  PDB,PERM,PLI
      READ(5,4) EGMIN
      READ(5,4) EMIN,DTMIN
      READ(5,4) (SIGMA(ISIG),ISIG=1,NSSG)
      READ(5,2) (PLC(IPC),(EC(IPC,ITGP),ITGP=1,NTGP),IPC=1,NPC)
      READ(5,6)  (TGP(ITGP),ITGP =1,NTGP)
      READ(5,6)  (TG(ITG),ITG=1,NTG)
      READ(5,5)  CCFAC,CWFAC
      READ(5,5)   PHI
      READ(5,6)  (ZET(IZ),IZ=1,NZET)
      READ(5,2)  (PLW(IPW), (EW(IPW,ITGP),ITGP=1,NTGP),IPW=1,NPW)
      READ(5,6)  (TD(I),I=1,2)
      READ(5,6) (PWR(I),I=1,6)
      READ(5,6) (PCWL(I),I=1,10)
      READ(5,7) ((DELTA(I,J), J=1,6),I=1,10)
      READ(5,7) ((DELTB(I,J), J=1,6),I=1,10)
C
C  NTG              # OF GAS TEMPS OF INTEREST
C  NGR              MAX # OF GRAY GASES
C  NSSG             # OF B-L/MEAN B-L RATIOS CONSIDERED
C  NQ               MIN # OF TERMS IN STR-LINE-FIT
C  NTGP             # OF TEMPS FOR GIVEN CO2, H2O EM'S
C  NPC,NPW          # OF PL-VALUES FOR CO2,H2O EM DATA
C  MP               MAX DEGREE OF TEMP POLYNOMIAL
C                   APPROX TO THE WT-ING FACTORS
C  NF,NL            ENTRY # OF MIN,MAX TG OF INTEREST
C  DIAM,AXIS,
C  DND,XND          DIMENSIONS OF COMB CHAMBER
C  PDB,PERM,
C  PLI              MIN FRACNL AGREEMENT BETWEEN:
C                  -PREDICTED & ACTUAL VALUES AT MAX B-L OF
C                   LHS OF EQN (    ),
C                  -ACTUAL & ALLOWABLE MEAN-SQ-ERROR
C                   FOR STR-LINE-PLOT
C                  -(L-MAX) & (L'-MAX)  - APPENDIX C
C  CCFAC,CWFAC      CORRECTION FACTORS FOR  CO2,H2O EM'S
C  PHI              INVERSE OF EQUIVALENCE RATIO
C
C  GET MIDDLE RANGE TEMP  (TG-MIDRANGE)
      RANGE = (NF + NL) / 2
      MIDR = RANGE
      TGMR = TG(MIDR)
      FR = (TGMR-TD(1))/(TD(2)-TD(1))
      IF (FR .LT. 0)  FR = 0
      DEN = 1 + 23.8*PHI
      ZETA = 1.0
```

```
      FZ    = ZETA /(DEN + ZETA)
      PRC = 3*FZ
      PRW = 4*FZ
      PTOT = PRC + PRW
      PR = PRW/PTOT
      PRF = 0
      CALL     FIND (PWR,6,PR,PRF,0,1)
      JBS = IB
C
C  GET THE MEAN B-L
      XLM = BEAM(AXIS,DIAM,XND,DND)
      PRINT 325, XLM
      PRINT 360, TGMR
C
C  CONSTRUCT THE GAS EM VS. B-L TABLE
C  AT TG-MIDRANGE
      TFR = 0.
      KODE = 0
      CALL FIND (TGP,NTGP,TGMR,TFR,KODE,1)
      IF (KODE .NE. 9)  GO TO 15
      PRINT 305
      PRINT 276, TGMR
      GO TO 200
   15 JBX = IB
      DO 45 ISIG=1,NSSG
      JB = JBX
      BM = SIGMA(ISIG) * XLM
      BML(ISIG) = BM
      PC = PRC * BM
      PW = PRW * BM
      PL = PC + PW
      EGX = 0.
      KD = 1
      KE = 1
      PFR = 0.
      KODE = 0
      CALL FIND (PLC,NPC,PC,PFR,KODE,1)
      IF (KODE .NE. 9)  GO TO 20
      PRINT 295
      XP = PC
      UP = PLC(1)
      GOTO  27
   20 CALL EINT (EC,TFR,KE)
      FAC = CCFAC
      GOTO  35
   25 KD = 2
      PFR = 0.
      KODE = 0
      CALL FIND (PLW,NPW,PW,PFR,KODE,1)
      IF (KODE .NE. 9)  GO TO 30
      PRINT 300
      XP = PW
      UP = PLW(1)
   27 PRINT 276, XP
      PFR = XP/UP
      KE = 2
      GOTO (20,30), KD
   30 CALL EINT (EW,TFR,KE)
      FAC = CWFAC
   35 ADD = 0.
```

```
      IF (EA .NE. 0.)  ADD = FAC*(EB*PFR+EA*(1-PFR))
   40 EGX = EGX + ADD
      IF (KD .EQ. 1)  GO TO 25
      PLF = 0
      KODE = 0
      CALL    FIND(PCWL,10,PL,PLF,KODE,1)
      IF (KODE .NE. 99)  GOTO  42
      IB = 10
      PLF = 1.0
   42 JB = JBS
   43 CALL    EINT(DELTA,PRF,01)
      DELA = PLF*EB+(1-PLF)*EA
      CALL    EINT(DELTB,PRF,01)
      DELB = PLF*EB+(1-PLF)*EA
      DEL = DELB*FR+(1-FR)*DELA
      IF (EGX .LT. DEL)  DEL = 0.5*(EGX-DEL)
      EGAS(ISIG) = EGX-DEL
      IF (PL .LT. PCWL(2))  DEL = 0.
   45 CONTINUE
      PRINT 320
      PRINT 220,(BML(I),I=1,NSSG)
      PRINT 220, (EGAS(I),I=1,NSSG)
C
C  CALCULATE THE EXTNCTN COEFS
      NS = 11
      MU = 1
      NU = 2
      AGSUM = EGAS(NSSG/3)
      AGSTP = 0.20*(EGAS(NSSG)-AGSUM)
      PER = PERM
      PEL = ALOG10(PER)
      PDL = ALOG10(PDB)
      PLLN = ALOG(PLI)
   50 AGO = 1.0
      NGRAY = NGR
      SMX = 0.9
      DO 70 IGRAY =1,NGRAY
      IF (IGRAY .GT. 1)  GOTO 51
      F = 0
      KS = 0
      CALL    FIND (EGAS,NSSG,AGSUM,F,KS,2)
      PRINT 240
      PRINT 216, AGSUM
      PRINT 241
      IF (KS.EQ.9 .OR. IB.LT.2)  GOTO  80
      IF (SIGMA(IB) .LT. SMX)  GOTO  80
      SD = 10**0.2
   51 SREF = 0.01*SMX/SD
      DO 53 I=1,NS
      SREF = SREF*SD
      S = SREF
      IF (I .EQ. 1)  S = 0
      BML(I) = S*XLM
      FR = 0.
      KS = 0
      EGX = 0.
      CALL    FIND(SIGMA,NSSG,S,FR,KS,2)
      IF (IB .GT. 1) EGX = EGAS(IB-1)*(EGAS(IB)
     ./EGAS(IB-1))**FR
      IF (KS .EQ. 9)EGX = S*EGAS(1)/SIGMA(1)
```

```
      GAR(I) = EGX
   53 CONTINUE
      IF (BML(NS) .GT. BML(2))  GOTO  54
      DO 58 I=2,NS
      J = NS-I+2
      HB = BML(I)
      BML(I) = BML(J)
      BML(J) = HB
      HG = GAR(I)
      GAR(I) = GAR(J)
      GAR(J) = HG
   58 CONTINUE
   54 DO 60 I=1,NS
      ARG = AGSUM - GAR(I)
      IF (IGRAY .EQ. 1)  GOTO 56
      IGRA = IGRAY - 1
      DO 55 JG=1,IGRA
   55 ARG = ARG - AGI(JG,1)*EXP(-SLK(JG)*BML(I))
   56 CONTINUE
      IF (ARG)  52,52, 59
   52 IF (IGRAY .EQ. 1)  GOTO 80
      FI2 = I/2
      IF ((FI2+BML(I-1)/XLJ) .LE. 2)  GOTO  57
      SMX = BML(I-1)/XLM
      GOTO  51
   57 NGRAY = IGRA
      GOTO  71
   59 VGI(I) = ALOG10(ARG)
      AGR(I) = ARG
   60 CONTINUE
      SK=(VGI(NS-1)-VGI(NS-2))/(BML(NS-1)-BML(NS-2))
      VGQ = VGI(NS-1)+SK*(BML(NS)-BML(NS-1))
      DB = VGQ-VGI(NS)
      IF ((IGRAY/NU) .GE. 1)  GOTO 65
      IF (-ABS(DB)/PDL-1)65,72,72
   65 CONTINUE
      NSQ = NS-NQ+1
      DO 68 L=1,NSQ
      A = 0.
      B = 0.
      C = 0.
      D = 0.
      DO 66 I=L,NS
      BL = BML(I)
      VG = VGI(I)
      A = A + BL
      B = B + BL*BL
      C = C + VG
      D = D + BL*VG
   66 CONTINUE
      ZL = NS-L+1
      BOT = A*A-B*ZL
      SLN = (A*C-D*ZL)/BOT
      AGL = (A*D-B*C)/BOT
      ERR = 0.
      DO 67 J=L,NS
   67 ERR = ERR+(AGL+SLN*BML(J)-VGI(J))**2
      ERR = SQRT(ERR/ZL)
      IF (-ERR/PEL-1)69,68,68
   68 CONTINUE
```

```
      NQZ=ZL
   69 SLK(IGRAY) = ABS(SLN)*ALOG(10.0)
      AGI(IGRAY,1) = 10**AGL
      IF (IGRAY .EQ. 1)  PRINT 340
      IF(IGRAY.EQ.1) PRINT 220, DB,ERR,PDB,PER,PLI
      PRINT 306, IGRAY
      PRINT 220, (BML(I),I=1,NS)
      PRINT 220, (AGR(I), I=1,NS)
      PRINT 308, L, BML(L)
      PRINT 307,SLK(IGRAY),AGI(IGRAY,1)
      AGO = AGO-AGI(IGRAY,1)
      XLI = -PLLN/SLK(IGRAY)
      XLJ = EMIN/AGI(IGRAY,1)/SLK(IGRAY)
      IF (XLI .LE. XLJ)  NGRAY = IGRAY
      SMX = XLI/XLM
      PRINT 230, XLI
   70 CONTINUE
   71 CONTINUE
      PRINT 225, NGRAY
      NGC = 0
      GO TO 85
   72 GOTO (79,78,76), MU
   73 AGSUM = AGSUM-DB*AGSTP/(DB-DA)
      GOTO  77
   76 IF ((DA-DZ)*(DB-DA) .GT. 0)  GOTO  78
      XA = .5*(DB-DZ)/(-DZ+2*DA-DB)
      XB = (DB-DA)*(DA-DZ)
      XC = (AGSTP+XB/AGSTP)*XA
      AGSUM = AGSUM-AGSTP+XC
   77 NU = 1
      GOTO  81
   78 IF (DA*DB .LT. 0)  GOTO  73
      DZ = DA
   79 DA = DB
      IF (MU .LT. 3)  MU = MU+1
   80 AGSUM = AGSUM + AGSTP
   81 CONTINUE
      IF (LAB .EQ. 50)  GOTO 82
      PRINT 335, DB
      IF (LAB .EQ. 562)  GOTO  82
      PRINT 330
      PRINT 215, (BML(I),I=1,NS)
      PRINT 220, (AGR(I), I=1,NS)
   82 IF (AGSUM .LE. 1.) GO TO 50
      GO TO 200
C
C  CHECK
   85 PRINT 240
      PRINT 310
      PRINT 311
      ES = 0.
      DO 90 I=1,NSSG
      BML(I) = SIGMA(I)*XLM
      EGC = 0.
      DO 89 J=1,NGRAY
      PJI = SLK(J)*BML(I)
      AD = AGI(J,1)
      SU = 0.
      IF (PJI .LE. 175.0)  SU = AD*EXP(-PJI)
      EGC = EGC+AD-SU
```

```
   89 CONTINUE
      PRINT 315,BML(I),EGAS(I),EGC
      E = 100*(EGC/EGAS(I)-1)
      PRINT 312, E
   90 CONTINUE
      PRINT 245
      IF (NGC .EQ. 1)  GOTO 134
C
C  CONSTRUCT A TABLE OF GAS  EMISSIVITIES
C  GAS EM'S VS B-L VS TEMP
      DO 130 ITG=1,NTG
      FR = (TG(ITG)-TD(1))/(TD(2)-TD(1))
      IF (FR .LT. 0)  FR=0.
      TFR = 0
      KODE = 0
      CALL FIND (TGP,NTGP,TG(ITG),TFR,KODE,1)
      IF (KODE .NE. 9)  GO TO 94
      PRINT 305
      PRINT 276, TG(ITG)
      GO TO 200
   94 JBX = IB
      BMX = SIGMA(NSSG)*XLM
      DO 125 I=1,NGRAY
      BMN = -ALOG(PLI)/SLK(I)
      BML(I) = 0.5*(BMX+BMN)
      BMX = BMN
      IF (NGRAY .EQ. 1) BML(I) = XLM
      JB = JBX
      PCL = PRC*BML(I)
      PWL = PRW*BML(I)
      PL = PWL+PCL
      EGX = 0.
      KD = 1
      PFR = 0.
      KODE = 0
      CALL FIND (PLC,NPC, CL,PFR,KODE,1)
      IF (KODE .NE. 9)  GO TO 100
      PRINT 295
      XP = PCL
      UP = PLC(1)
      GO TO 115
  100 CALL EINT (EC,TFR,KE)
      FAC = CCFAC
      GO TO 121
  110 KD = 2
      PFR = 0.
      KODE = 0
      CALL FIND (PLW,NPW,PWL,PFR,KODE, )
      IF (KODE .NE. 9)  GO TO 120
      PRINT 300
      XP = PWL
      UP = PLW(1)
  115 PRINT 276, XP
      PFR = XP/UP
      KE = 2
      GO TO (100,120), KD
  120 CALL EINT (EW,TFR,KE)
      FAC = CWFAC
  121 ADD = 0.
      IF (EA .NE. 0.) ADD = FAC*(EB*PFR+EA*(1-PFR))
```

```
  122 EGX = EGX + ADD
      IF (KD .EQ. 1) GO TO 110
      PLF = 0
      KODE = 0
      CALL     FIND(PCWL,10,PL,PLF,KODE,1)
      IF (KODE .NE. 99)  GOTO  123
      IB = 10
      PLF = 1.0
  123 JB = JBS
  124 CALL     EINT(DELTA,PRF,01)
      DELA = PLF*EB+(1-PLF)*EA
      CALL     EINT(DELTB,PRF,01)
      DELB = PLF*EB+(1-PLF)*EA
      DEL = DELB*FR+(1-FR)*DELA
      IF (PL .LT. PCWL(2))  DEL = 0.
      IF (EGX .LT. DEL)  DEL = 0.5*(EGX-DEL)
      EG (I,ITG) = EGX-DEL
  125 CONTINUE
  130 CONTINUE
         DO 131 I=1,NTG
      PRINT 285, TG(I),
     .           (EG(J,I), J=1,NGRAY)
  131 CONTINUE
      DO 133 I=1,NGRAY
      DO 132 J=1,NTG
      IF (EG(I,J) .GE. EGMIN)  GOTO 132
      NGRAY = I-1
      PRINT 225, NGRAY
      NGC = 1
      GOTO 85
  132 CONTINUE
  133 CONTINUE
C  CALCULATE THE WT-ING FACTORS
C  FOR ALL TEMPS
C  WITH CONST EXTNCTN COEF
  134 DO 140 I=1,NGRAY
      DO 135 J=1,NGRAY
      PJI = SLK(J)*BML(I)
      SU = 0.
      IF (PJI .LE. 175.0)  SU = EXP(-PJI)
      GAM(I,J) = 1.0-SU
      GMA(I,J) = GAM(I,J)
  135 CONTINUE
  140 CONTINUE
      PRINT 240
      PRINT  345
      DO 141 I=1,NGRAY
  141 PRINT 215, (GAM(I,J), J=1,NGRAY)
      PRINT 241
      IF (NGRAY .EQ. 1)  GOTO  157
C  TEST FOR ILL-CONDITIONING
      DO 144 I=1,NGRAY
      SUM = 0.
      DO 142 J=1,NGRAY
  142 SUM = SUM+GMA(I,J)**2
      RMS = SQRT(SUM/NGRAY)
         DO 143 K=1,NGRAY
  143 GMA(I,K) = GMA(I,K)/RMS
  144 CONTINUE
      DT = 0.
```

```
      M = 0
      CALL    CSLND(GMA,5,NGRAY,DT,M,GMA)
      PRINT 309, DT,M
      PRINT 350
      IF (ABS(DT*10**M)-DTMIN) 146,146,155
C  USE APPROPRIATE CSLIB SUBRTNE FOR ILL-COND  EQNS
  146 DO 152 J=1,NTG
      DO 147 I=1,NGRAY
  147 VEC(I) = EG(I,J)
      IF (J .GT. 1)  GOTO  149
  148 CALL    CSLNIL(GAM,VEC,VECS,NGRAY,FLU,RCF,NPVT)
      GOTO  150
  149 CALL    CSLNIS(VEC,VECS,NGRAY)
  150 DO 151 K=1,NGRAY
  151 AGI(K,J) = VECS(K)
  152 CONTINUE
      GOTO  175
C  COMPUTE  INVERSE OF  MATRIX
  155 GOTO (157,158,173,173,173), NGRAY
  157 GMA(1,1) = 1./GAM(1,1)
      GOTO  159
  158 DT = 0.
      M = 0
      CALL    CSLNI(GAM,5,NGRAY,DT,M,GMA)
      PRINT 309, DT,M
      PRINT 355
  159 DO 162 J=1,NTG
      DO 161 I=1,NGRAY
      AGI(I,J) = 0.
      DO 160 K=1,NGRAY
  160 AGI(I,J) = AGI(I,J)+GMA(I,K)*EG(K,J)
  161 CONTINUE
  162 CONTINUE
      GOTO  175
C  USE APPROPRIATE SSPLIB SUBRTINE FOR WELL-COND EQNS
  173 CALL    XMOVE(GAM,GAR,NGRAY,NGRAY,5,1)
      CALL    XMOVE(EG,AGR,NGRAY,NTG,30,1)
      IER = 0
      CALL    GELG(AGR,GAR,NGRAY,NTG,0.5E-06,IER)
      IF (IER .EQ. 0)  GOTO 174
      PRINT 206, IER
         GOTO 200
  174 CALL    XMOVE(AGI,AGR,NGRAY,NTG,30,2)
  175 DO 177 ITG=1,NTG
      AGZ(ITG) = 1.0
      DO 176 J=1,NGRAY
  176 AGZ(ITG) = AGZ(ITG) - AGI(J,ITG)
  177 CONTINUE
C
C  RESULTS
C
      PRINT 245
      PRINT 255
      GOTO  178
      PRINT 265, DIAM , AXIS
  178 PRINT 256, PHI
      PRINT 240
      PRINT 270
      PRINT 275, (SLK(IGRAY),IGRAY =1,NGRAY)
      PRINT 280
```

```
      PRINT 281
      PRINT 282
      PRINT 284
      PRINT 283
      DO 179 ITG =1,NTG
      PRINT 285, TG(ITG),AGZ(ITG),
     •           (AGI(IGRAY,ITG),IGRAY=,,NGRAY)
  179 CONTINUE
      CALL    POLY(TG,AGI,NTG,NGRAY,MP)
  180 CONTINUE
  200 STOP
  206 FORMAT ( I10)
  210 FORMAT (F10.1)
  215 FORMAT (/10F13.5)
  216 FORMAT (//T55,'AGSUM = ',F10.5)
  220 FORMAT (/10E13.5)
  225 FORMAT (///T10,'TOTAL NO OF GRAY GASES = ',I2)
  230 FORMAT (///T2,'BEAM LENGTH FOR MIN GRAY GAS ',
     •        'EM CONTR =',E13.5)
  240 FORMAT ('-')
  241 FORMAT (//)
  245 FORMAT ('1')
  255 FORMAT(T53,11H**RESULTS**///)
  256 FORMAT (//T27,'PHI = ',F6.1)
  265 FORMAT (/26X,6HDIAM =,F5.2,10X,8HLENGTH =,F5.2)
  270 FORMAT ('-', 5X,'GRAY-GAS EXTNCTN COEFS')
  275 FORMAT (10X,5F20.6)
  276 FORMAT (10X,3F10.5)
  280 FORMAT (////45X, 'GRAY-GAS EM WT-ING FACTORS')
  281 FORMAT (/T20,'GAS TEMP')
  282 FORMAT ('+',T30,'A,I: I=')
  283 FORMAT (T22,'DEG R')
  284 FORMAT ('+',T41,'0',13X,'1',13X,'2',13X,'3',13X,
     •        '4',13X,'5')
  285 FORMAT (/F27.1,T30,6E14.5)
  295 FORMAT (10X,'**PLC TBL TOO NARROW**')
  300 FORMAT (10X,'**PLW TBL TOO NARROW**')
  305 FORMAT (10X,'** TG TOO LOW FOR TGP TBL *')
  306 FORMAT  (//T2,'GRAY GAS  #  ',I2)
  307 FORMAT (//T2,'EXTNCTN COEF =',F10.5,
     •        'EM WT-ING FACTOR =',E13.6)
  308 FORMAT (//T2,'STR LINE PLOT EFFECTIVELY STARTS ',
     •        'AT PT # ',I2,
     •         '     CORR BEAM LENGTH = ',E12.5)
  309 FORMAT (/'DETERMINANT: ',T25,'MATRIX : ',F10.5,
     •
  310 FORMAT (///T40,'CHECK EG-VALUES',
     •        //T35,'BEAM LENGTH',T50,'EG-OLD',T60,
     •        'EG-APPROX')
  311 FORMAT ('+',T76,'ERROR'//)
  312 FORMAT ('+',T70,F10.2)
  315 FORMAT (T32,E12.3,E12.3,E15.5)
  320 FORMAT (///T2,'A DISPLAY OF BEAM LENGTHS AND  ',
     •        'CORRESPONDING EMISSIVITIES FOLLOWS :'//)
  325 FORMAT ('1'///T20,'MEAN BEAM LENGTH =',E20.6///)
  330 FORMAT (///T2,'A BEAM LENGTH VERSUS VGI-VALUE ',
     •           'CHECK PRINTOUT FOLLOWS :'//)
  335 FORMAT (//T2,'INDICATED ERROR IN VGI-VALUE',
     •        'AT MAX BEAM LENGTH ;'
     •        /T25,'STR LINE PLOT ASSUMPTION :',E15.5)
```

```
  340 FORMAT (/T2,6X,'DB = ',8X,'ERR = ',7X,'PDB = ',
     .7X,'PER = ',7X,'PLI = ')
  345 FORMAT (/T2,'COEF MATRIX FOR EM-WTG FAC CALC :'/)
  350 FORMAT ('+',T15,'NORMALISED')
  355 FORMAT ('+',T17,'ACTUAL')
  360 FORMAT (//T20,'MID-RANGE TEMP :',F12.1,
     .        'DEGREES R'//)
      END
      SUBROUTINE      POLY(TG,AGI,NTG,NGRAY,M)
C  POLYNOMIAL-FITTING SUBROUTINE
C  TG              TEMPS
C  AGI             DISCREET FUNCN VALUES (WT-ING FACS)
C  NTG             # OF TEMPS
C  NGRAY           # OF SETS OF FUNCN VALS (E.G. GRAY GASES)
C  M               DEGREE OF APPROXIMATING POLYNOMIAL
      DIMENSION       TG(30),AGI(5,30),
     .                BCH(25),BN(10),DAT(25),WK(20)
C  BCH             TEMP COEFS FOR APPROX CHEBYSHEV POLY
C  BN              TEMP COEFS FOR EQUIVT ORDINARY POLY
C  DAT, WK         WORKSPACES FOR SSP SUBROUTINES
      PRINT 26, M
      DO 1 J=1,NTG
    1 DAT(J) = TG(J)
      DO 4 I=1,NGRAY
      PRINT 25, I
      DO 2 J=1,NTG
    2 DAT(NTG+J) = AGI(I,J)
      DAT(2*NTG+1) = -1
      TA = 0.
      TB = 0.
      IER = 0
      CALL      APCH(DAT,NTG,M,TA,TB,BCH,IER)
      PRINT 23, IER
      PRINT 22, TA,TB
      PRINT 28
      DO 14 MC =1,M
      M1 = MC*(MC-1)/2+1
      M2 = M1+MC-1
      PRINT 5, (BCH(IB),IB=M1,M2)
   14 CONTINUE
      IER = 0
      CALL      APFS(BCH,M,IR,.02,.5E-05,.5E-01,IER)
      PRINT 24, IER
      PRINT 27, IR
      DO 3 K=1,IR
      KB = K*(K-1)/2+1
      KE = KB+K-1
      PRINT 9, K
      PRINT 5, (BCH(IB),IB=KB,KE)
      DO 13 IB =1,K
   13 BN(IB) = BCH(KB+IB-1)
      CALL          TCNP(TA,TB,BN,K,BN,WK)
       PRINT 12
      PRINT 5, (BN(IB),IB=1,K)
      PRINT 21, K
      DO 11 JJ=1,NTG
      S = BN(1)
      T = 1.0
      IF (K .LT. 2)  GOTO 15
      DO 10 II=2,K
```

```
      T = T*TG(JJ)
   10 S = S+BN(II)*T
   15 ERR = (S/AGI(I,JJ)-1)*100.
      IF (I+K.EQ.2 .AND. JJ.EQ.1) PRINT 8
      PRINT 7, TG(JJ),AGI(I,JJ),S,ERR
   11 CONTINUE
    3 CONTINUE
    4 CONTINUE
    5 FORMAT (5E20.5)
    6 FORMAT (/5I10)
    7 FORMAT (F27.1,2E20.5,F20.2)
    8 FORMAT (/T22,'TEMP',T39,'AGI-OLD',T59,
     .        'AGI-NEW',T81,'ERROR'//)
    9 FORMAT (///T1,'DEG OF APPROX POL :',I5/T1,
     .        'CHEBYSHEV POL COEFS')
   12 FORMAT (/T1,'ORDINARY POL COEFS')
   21 FORMAT (/T40,I5,5X,'COMPUTED RESULTS'/)
   22 FORMAT (/T1,'CHEBYSHEV ARG. TRANSFMTN FACTRS: ',
     .        'XD = ',E14.5,'X0 = ',E14.5)
   23 FORMAT (/T1,'APCH SUBPTN RTRN CODE : ',I2)
   24 FORMAT (/T1,'APFS SUBRTN RTRN CODE : ',I2)
   25 FORMAT ('1',////T50,'GRAY GAS    # ',I2)
   26 FORMAT (//T1,'# FUNDMNTL CHEBYSHEV FNS USED : ' ,I2)
   27 FORMAT (T1,'DIMNSN OF LEAST-SQ FIT OBTAINED :',I2)
   28 FOFMAT (T1,'APCH SUBRTN RESULTS')
      RETURN
      END
      FUNCTION      BEAM(AXSS,DIA ,XNS,END)
C  GIVES THE MEAN BEAM LENGTH OF A CLOSED CYLINDER
      UA = DIA *DIA
      UB = END*END
      UC = (DIA  + END)**2
      UD = XNS / (DIA  - END)
      UE = SQRT(1 + 16*UD*UD)
      UTOP = 4*UA*AXSS + UC*XNS
      UBOT = 8*DIA *AXSS + UA*(2 + UE) + UB*(2 - UE)
      BEAM = 3.5*(UTOP/UBOT)/2.0
      RETURN
      END
      SUBROUTINE       FIND (RAY,N,Q,FR,KDR,KF)
C  AN INTERPOLATION ROUTINE: LOG OR LINEAR
C  DEPENDING ON KF,
C  IN A ONE DIMENSIONAL ARRAY.
      DIMENSION    RAY(30)
      COMMON  /XFE/IB
      IF (Q .LE. RAY(N))  GOTO  5
      KDR = 99
      IB = N
      GOTO  25
    5 DO 10 I=1,N
      IF (RAY(I) .GT. Q)  GO TO 15
   10 CONTINUE
   15 IB = I
      IF (IB .GT. 1) GO TO 20
      KDR = 9
      GO TO 25
   20 GOTO  (21,22), KF
   21 FR = (Q-RAY(IB-1))/(RAY(IB)-RAY(IB-1))
      GO TO 25
   22 IF (RAY(IB-1) .EQ. 0.)  GOTO 21
```

```
      FR = ALOG10(Q/RAY(IB-1))/ALOG10(RAY(IB)/RAY(IB-1))
   25 RETURN
      END
      SUBROUTINE      EINT(TABLE,FR,K)
C  LINEAR INTEPPOLATION
C  IN A 2-D TABLE
      DIMENSION     TABLE(30,20)
      COMMON        /XFE/IB,JB,EA,EB
      EA = 0.
      GOTO (1,2), K
    1 EA = TABLE(IB-1,JB-1)*(1-FR) + TAB_E(IB-1,JB)*FR
    2 EB = TABLE(IB,JB-1)*(1-FR) + TABLE(IB,JB)*FR
      K = 1
      RETURN
      END
      SUBROUTINE      XMOVE(A,B,N,M,NJ,KB)
C  AN ARRAY-MOVING ROUTINE:
C  BETWEEN 1D AND 2D ARRAYS
C  DEPENDING ON KB
      DIMENSION     A(5,NJ),B(200)
      DO 4   J=1,M
      K = (J-1)*N
         DO 3   I=1,N
      GOTO (1,2), KB
    1 B(K+I) = A(I ,J)
      GOTO 3
    2 A(I,J) = B(K+I)
    3 CONTINUE
    4 CONTINUE
      RETURN
      END
```

APPENDIX D

MEAN ABSORPTION COEFFICIENTS K'_R AND K'_S; AND FTFIELDX

D.1 The Rosseland-mean absorption Coefficient, K'_R

The definition of K'_R is given in different forms by Abu-Romia and Tien [1], Deissler [10] and Hottel and Sarofim [19]. Following Hottel and Sarofim, it may be written as follows:

$$1/K'_R = \int_0^\infty \frac{1}{K_\lambda} (\partial E_\lambda / \partial E)_\lambda \, d\lambda \qquad (37a)$$

Recognition of the fact that K_λ is not a continuous function of λ and that there are 'windows' (K_λ=0) in the spectrum suggests that equation (37a) be redefined thus [1,10,21]:

$$1/K'_R = \sum_{i=1}^{m} \int_{\Delta\lambda_i} \frac{1}{K_\lambda} (\partial E_\lambda / \partial E)_\lambda \, d\lambda \qquad (D.1)$$

in which the integral is conducted separately within each

of the m wavebands, $\Delta\lambda_i$. If a mean value, K_i, is used for K in each waveband equation (D.1) becomes,

$$1/K'_R = \sum_{i=1}^{m} \frac{\Delta f^*_i}{K_i} \qquad (D.2)$$

where the function f* is defined as

$f^* = \int_o^{\lambda} (\partial E_\lambda / \partial E)_\lambda \, d\lambda$ (19), so that $\Delta f^* = \int_{\Delta\lambda_i} df^*$

Equation (D.2) may alternatively be looked upon as the 'gray gas approximation' to equation (37a), in which case m is the number of gray gases involved.

Now the function f, related to f*, is defined by Hottel and Sarofim [19] as

$$f = \int_o^{\lambda} \frac{E_\lambda}{E} \, d\lambda$$

from which it can be easily deduced that

$$f^* = f + E \frac{df}{dE} \qquad (D.3)$$

Hence

$$\Delta f_i^* = \Delta f_i + E\, d(\Delta f_i)/dE$$

$$= a_{G,i} + \frac{1}{4} T\, da_{G,i}/dT \quad \text{(Chapters IV and V)}$$

so that

$$1/K_R' = \sum_{i=1}^{m} (a_{G,i} + \frac{1}{4} T\, da_{G,i}/dT)/K_i \qquad \text{(D.4)}$$

Upon using the polynomial expression for $a_{G,i}$ in terms of T (equation (34a)) one finds that

$$1/K_R' = \sum_{i=1}^{m} \left(\sum_{j=0}^{j_{max}} b'_{ij}\, T^j \right)/K_i \qquad \text{(D.5)}$$

where $b'_{ij} = (1 + j/4)\, b_{ij}$

D.2 The Rosseland-mean-related mean absorption coefficient, K_S'

Deissler [10] defines this quantity as

$$1/K_S' = \int_0^{\lambda} \frac{1}{K_\lambda^2} (\partial E_\lambda/\partial E)_\lambda \, d\lambda$$

which, by analogy with equations (D.1) and (D.2), readily leads to

$$1/K'_S = \sum_{i=1}^{m} (\Delta f_i^*/K_i^2) \qquad (D.6)$$

and then to

$$1/K'_S = \sum_{i=1}^{m} \left(\sum_{j=0}^{j_{max}} b'_{ij} T^j \right)/K_i^2 \qquad (D.7)$$

D.3 The Program, FTFIELDX

This program is listed below. It is a FORTRAN IV program successfully run on an IBM System 360/67 installation at the Computing Services of the University of Alberta.

```
C*
C*
C  FTFIELDX
C  CALCULATES THE TEMPERATURE AND HEAT FLUX
C  DISTRIBUTIONS IN A COMBUSTION CHAMBER USING THE  ZONE METHOD
C  SUPPORTED BY EIGHT  SUBROUTINES, NAMELY:
C  ZONIR1      -GENERATES ZONES AND THEIR COORDINATES
C  NEIBR2      -PICKS OUT NEIGHBOURING ZONES FOR
C               EACH ZONE
C  EXCH3       -CALCULATES EXCHANGE AREAS
C  EQNS4       -SETS UP  MATRIX OF ENERGY BALANCE EQNS
C  RHSP5       -CREATES RHS OF ENERGY BALANCE EQNS
C  SOLV6       -SOLVES  MATRIX EQUATION
C  QFLX7       -COMPUTES NET FLUX ON EACH SURFACE ZONE
C  EBLC8       -DOES AN ENERGY BALANCE FOR SYSTEM
C  FFSUB9      -A TEMP FUNCTION SUBROUTINE
C
C
C  ABOVE SUBROUTINES  USE FOLLOWING FUNCTIONS
C  CONVRT      -CONVERTS BETWEEN TEMP & EMISSIVE PWR
C  AKGR        -SUM OF (A*K) PRODUCTS FOR GRAY GAS MIX
C  HRADQ       -RAD EQUIVT OF CONV. OR BULK FLOW HT TRANS
C               COEF TIMES INTERFACE AREA
C  AREA        - FUNCTION TO COMPUTE AREAS OF
C               DISCS AND CYLINDERS
C  ROSK        -ROSSELAND. AND A RELATED MEAN ABSORPTION COEF
C               FUNCTION
C  AG0         -CLEAR GAS WT-ING FAC AT ANY  TEMP
C  DIRECT      -COMPUTES THE DIRECT EXCH AREA FOR COAXAL
```

```
C                CIRCULAR DISCS
C  OTHER SUBROUTINES ARE CALLED FROM *CSLIB AND *SSPLIB
C
      DIMENSION TZN(25),EZN(25),BN(5,10),SK(5),
     .  EAR(25,25),QFX(25),NABOR(25,5),XDI(6,6)
      COMMON  /A2/TZN /A3/BN,SK /A5/NABOR,EAR,XDI
     .  /A8/QFX /A9/EZN
     .  /B1/AX,DI,HTS /B3/NXG,NRG /B4/NZ,NES,NE,NS,NG
     .  /B5/NE1,NES1
     .  /C1/RM,HTC,ES,CP,FLO /C2/TSURR,TSUPP,CFU,QCO,FLM
     .  /C3/NGR,NB
C
C
C  TZN          - ZONE TEMPERARURES
C  EAR          - EXCHANGE AREAS
C  QFX          - ZONE FLUX DENSITIES
C  NABOR        -  NEIGHBOURING ZONES OF EACH ZONE
C
    2 FORMAT (5I10)
    3 FORMAT (5F10.3)
    4 FORMAT (5F15.6)
    5 FORMAT (8F10.6)
    6 FORMAT (6E13.5)
C
C  INPUT OF DATA
C
      PRINT 98
      READ (5,3) AX,DI,RM
      READ (5,3) FLO,CFU,FLM
      READ (5,3) CP,ES,QCO
      READ (5,3) HTC,HTS,TSURR,TSUPP
      READ (5,2) NGR,NB
      READ (5,2) NXG,NRG
      READ (5,3) TBS, TBG
C
C  AX, DI, RM - CHAMBER L, D AND EXIT-PORT R
C  FLO, CFU   - MASS FLOW RATES ( PRODUCT GASES , FUEL)
C  FLM        - FLAME LENGTH
C  CP         - MEAN 'CP' OF PRODUCT GASES
C  ES         - WALL (GRAY) SURFACE EMISSIVITY
C  QCO        - ENTHALPY OF COMB OF FUEL PER UNIT MASS
C  HTC, HTS   - CONV HT TRANS COEF (INSIDE , OUTSIDE CHAMBER)
C  TSURR      - AMBIENT TEMPERATURE
C  TSUPP      - INITIAL TEMPERATURE OF REACTANTS
C  NGR        - NO OF GRAY GASES IN COMB PRODUCT GASES
C  NB         - DEGREE OF APPROXIMATING POLYNOMIAL FOR
C               GRAY GAS WT-INGFACTORS
C  NXG, NRG   - NO OF GAS ZONES ON AXIS, RADIUS
C               S (SURFACE), G (GAS)
C  TBS, TBG   - STARTING TEMPS FOR ITERATIVE SOLUTION
C
      READ (5,2) ITN, ITERM
      READ (5,6) ((BN(I,J),J=1,NB),I=1,NGR)
      READ (5,4) (SK(I),I=1,NGR)
C
C  ITERM      - MAX NO OF ITERATIONS SPECIFIED
C  BN         - COEFS OF APPROXIMATING POLYNOMIAL OF
C               GRAY GAS WT-ING FACTORS
C  SK         - GRAY GAS ABSORPTION COEFICIENTS
C
```

```
      PRINT 98
C
C  GENERATE ZONES AND THEIR COORDS
      CALL          ZONIR1(KSUB)
      PRINT 55
      PRINT 60, KSUB
C  SELECT NEIGHBOURING ZONES OF EACH ZONE
      CALL          NEIBR2(KSUB)
      PRINT 65
      PRINT 60,KSUB
C  GENERATE INITIAL ZONE TEMPERATURES
      ITR = 1
      TB = TBS
      DO 10 I=1,NZ
      IF (I .GT. NES)  TB = TBG
      TZN(I) = TB
   10 CONTINUE
      PRINT 3, (TZN(I),I=1,NZ)
      PRINT 98
C  COMPUTE DIRECTED-FLUX AREAS
   15 CALL          EXCH3 (KSUB,ITR,ITN)
      PRINT70
      PRINT 60,KSUB
C  SET UP MATRIX OF ENERGY BALANCE EQNS
      CALL          EQNS4(KSUB)
      PRINT 75
      PRINT 60,KSUB
      IF (ITR .GT. 1) GOTO 20
C  FILL RHS VECTOR
      CALL          RHSP5 (KSUB)
      PRINT 80
      PRINT 60,KSUB
C  SOLVE MATRIX EQN
   20 CALL          SOLV6 (ITR,ERR,KSUB)
      PRINT 85
      PRINT 60, KSUB
      PRINT 86, ITR,ERR
      NU = 0
      DO  22  I=1,NZ
      IF  (EZN(I) .GT. 0.)  GOTO  22
      IF  (NU .NE. 0)  GOTO  21
      NU = 1
      PRINT 125
   21 PRINT 130, I
   22 CONTINUE
      IF (ERR .LT. 5.0) GOTO 25
      ITR = ITR+1
      IF (ITR .LT. ITERM)  GOTO 15
      PRINT 135
      PRINT 140
      PRINT 114, ((I,TZN(I)),I=1,NZ)
      PRINT 98
      PRINT 145
      DO 24 I=1,NZ
   24 PRINT 100, (EAR(I,J),J=1,NZ)
      GOTO  200
C  CALCULATE SURFACE FLUXES
   25 CALL          QFLX7 (KSUB)
      PRINT 90
      PRINT 60,KSUB
```

```
      PRINT 95
      PRINT 105
      DO 30 I=1,NE
      PRINT 99,I
   30 PRINT 100, (EAR(I,J),J=1,NZ)
      PRINT 106
      DO 35 I=NE1,NES
      PRINT 99,I
   35 PRINT 100, (EAR(I,J),J=1,NZ)
      PRINT 107
      DO 40 I= NES1,NZ
      PRINT 99, I
   40 PRINT 100, (EAR(I,J),J=1,NZ)
      PRINT 110
      PRINT 105
      PRINT 114, ((I,TZN(I)),I=1,NE)
      PRINT 106
      PRINT 114, ((I,TZN(I)),I=NE1,NES)
      PRINT 107
      PRINT 114, ((I,TZN(I)),I=NES1,NZ)
      PRINT 120
      PRINT 105
      PRINT 115, ((I,QFX(I)),I=1,NE)
      PRINT 106
      PRINT 115, ((I,QFX(I)),I=NE1,NES)
   45 CALL          EBLC8 (KSUB)
      PRINT 91
      PRINT  60, KSUB
   50 CONTINUE
   55 FORMAT (//T2,'ZONIR1 :')
   60 FORMAT ('+',T15,'SUBRTNE RC=',I2)
   65 FORMAT (//T2,'NEIBR2 :')
   70 FORMAT (//T2,'EXCH3 :')
   75 FORMAT (//T2,'EQNS4 :')
   80 FORMAT (//T2,'RHSP5 :')
   85 FORMAT (//T2,'SOLV6 :')
   86 FORMAT (//T10,'ITERATION #',I4,T35,'RMS ERROR =',
     .  E15.6)
   90 FORMAT (//T2,'QFLX7 :')
   91 FORMAT (//T2,'EBLC8 :')
   95 FORMAT ('1',///T55,'***RESULTS***'//T46,
     .  '(1):EXCHANGE AREAS'/)
   98 FORMAT ('1',1X)
   99 FORMAT (T2,I2)
  100 FORMAT (/T2,10E13.4)
  105 FORMAT(/T1,'END ZONES')
  106 FORMAT(/T1,'WALL ZONES')
  107 FORMAT(/T1,'GAS ZONES')
  110 FORMAT ('1',///T50,'(2) :  ZONE TEMPERATURES'//
     .  T45,'ZONE NO.',T70,'ZONE TEMP.'/T70,11H(DEGREES R))
  114 FORMAT (T45,I5,T70,F9.2)
  115 FORMAT (T45,I5,T60,E20.5)
  120 FORMAT ('1',///T53,'(3) :  ZONE FLUXES'//
     .  T45,'ZONE NO.',T70,'ZONE FLUX DENSITY'/T70,5H(BTU/,
     2              9HSQ FT-HR))
  125 FORMAT (///T2,'INVALID ZONE TEMPERATURES'/T2,
     .  'AT ZONE NOS :')
  130 FORMAT (/T2,I10)
  135 FORMAT (///T2,35HSPECIFIED NO OF ITERATIONS EXCEEDED
     .26H...EXECUTICNTERMINATING  )
```

```
  140 FORMAT (/T2,35HCURRENT TEMPS (DEG R) ARE AS FOLLOW/
     .  /T45,6HZONE #,T70,9HZONE TEMP)
  145 FORMAT (//T2,17HEXCH AREAS FOLLOW)
  200 STOP
      END
      SUBROUTINE ZONIR1 (KSUB)
      DIMENSION    XMN(25),RMN(25)
      COMMON      /A1/RMN,XMN
     .  /B1/AX,DI /B2/DX,DR /B3/NXG,NRG
     .  /B4/NZ,NES,NE,NS,NG /B5/NE1,NES1
     .  /C1/RM
C  CALCULATE TOTAL NO. OF ZONES
      NE = NRG+NRG
      NE1 = NE+1
      NS = NXG
      NES = NE+NS
      NES1 = NES+1
      NG = NXG*NRG
      NZ = NES+NG
C
C  GENERATE COORDS OF EACH ZONE
C
C  (A)    END ZONES
C
      RAD = DI/2
      DR = RAD/NRG
C  NOTE:  NRG IS TO BE SUCH THAT RM < DR
      DO 10 I=1,NE,2
      XI = I
      RMN(I) = (XI/2-0.5)*DR
   10 RMN(I+1) = RMN(I)
      DO 15 I=1,NE,2
      XMN(I) = 0.
   15 XMN(I+1) = AX
C  (B)    WALL ZONES
      DO 20 I=NE1,NES
   20 RMN(I) = RAD
      DX = AX/NXG
      A = -DX
      DO 25 I= NE1,NES
      A = A+DX
   25 XMN(I) = A
C  (C)    GAS ZONES
      DO 35 I=1,NRG
      R = (I-1)*DR
      A = -DX
      K = NES+(I-1)*NXG
      DO 30 J=1,NXG
      A = A+DX
      K = K+1
      RMN(K) = R
   30 XMN(K) = A
   35 CONTINUE
C  EXHIBIT THE RESULTS OF THIS SUBROUTINE
      PRINT 40, NZ,NE,NS,NG
      PRINT 45
      PRINT 50
      PRINT 55, ((I,XMN(I),RMN(I)),I=1,NE)
      PRINT 60
      PRINT 55, ((I,XMN(I),RMN(I)),I=NE1,NES)
```

```
      PRINT 65
      PRINT 55, ((I,XMN(I),RMN(I)),I=NES1,NZ)
      KSUB = 0
      RETURN
   40 FORMAT (///T2,'TOTAL NO. OF ZONES =', I3,//
     .   T1,'BREAKDOWN FOLLOWS :'/
     .   T20,'END ZONES :',I4/T19,'WALL ZONES :',I4/
     .   T20,'GAS ZONES :',I4)
   45 FORMAT (//T23,'ZONE NO.',T62,'AXIAL COORD',T102,
     .     'RADIAL COORD'/)
   50 FORMAT (/T10,'END :')
   55 FORMAT (I28,2F41.3)
   60 FORMAT (/T10, 'WALL :')
   65 FORMAT (/T10,'GAS :')
      END
      SUBROUTINE NEIBR2 (KSUB)
      DIMENSION     RMN(25),XMN(25),NABOR(25,5)
      COMMON      /A1/RMN,XMN /A5/NABOR
     .  /B2/DX,DR   /B4/NZ,NES,NE /B5/NE1,NES1
C
C  INITIALISE NABOR
      DO 2 J=1,5
      DO 1 I=1,NZ
    1 NABOR(I,J) = 0
    2 CONTINUE
C
C  (A) END ZONES
      DO 15 I=1,NE
      K = 1
      GOTO  6
C  A.1, A.2  NEIGHBOURING SURFACE ZONES
    3 DO 5 J=1,NES
      IF (RMN(J)-DR .NE. RMN(I))  GOTO 5
      IF (XMN(J) .NE. XMN(I).AND.XMN(J)+DX .NE. XMN(I))  GOTO 5
      K = K+1
      NABOR(I,K) = J
    5 CONTINUE
C  A.3 NEIGHBOURING GAS ZONES
    6 DO 10 J=NES1,NZ
      IF (RMN(J) .NE. RMN(I)) GOTO 10
      IF (XMN(J) .NE. XMN(I).AND.XMN(J)+DX .NE. XMN(I))
     .GOTO 10
    9 K = K+1
      NABOR(I,K) = J
   10 CONTINUE
      NABOR(I,1) = K-1
   15 CONTINUE
C  (B)   WALL ZONES
      DO  35 I=NE1,NES
      K = 1
      GOTO  26
C  B.1, B.2  NEIGHBOURING SURFACE ZONES
   16 DO 20 J=1,NE
      IF(RMN(J)+DR .NE. RMN(I))  GOTO 20
      IF (XMN(J) .NE. XMN(I).AND.XMN(J)-DX .NE. XMN(I))  GOTO 20
      K = K+1
      NABOR(I,K) = J
   20 CONTINUE
      DO 25 J=NE1,NES
      IF (XMN(J)-DX .NE. XMN(I).AND.XMN(J)+DX .NE. XMN(I))  GOTO 25
```

```
      K = K+1
      NABOR(I,K) = J
   25 CONTINUE
C  B.3  NEIGHBOURING GAS ZONES
   26 DO 30 J=NES1,NZ
      IF (XMN(J) .NE. XMN(I)) GOTO 30
      IF (RMN(J)+DR .NE. RMN(I))  GOTO 30
      K = K+1
      NABOR(I,K) = J
   30 CONTINUE
      NABOR(I,1) = K-1
   35 CONTINUE
C  (C)   GAS ZONES
      DO 55 I=NES1,NZ
      K = 1
C C.1  NEIGHBOURING END-ZONES
      DO 40 J=1,NE
      IF (XMN(J) .NE. XMN(I).AND.XMN(J)-DX .NE. XMN(I))  GOTO 40
      IF (RMN(J) .NE. RMN(I)) GOTO 40
      K = K+1
      NABOR(I,K) = J
   40 CONTINUE
C C.2  NEIGHBOURING WALL ZONES
      DO 45 J=NE1,NES
      IF (XMN(J) .NE. XMN(I)) GOTO 45
      IF (RMN(J)-DR .NE. RMN(I)) GOTO 45
      K = K+1
      NABOR(I,K) = J
   45 CONTINUE
C C.3  NEIGHBOURING GAS ZONES
      DO 50 J=NES1,NZ
      IF (XMN(J) .EQ. XMN(I))  GOTO  46
      IF (XMN(J)-DX .NE. XMN(I).AND.XMN(J)+DX .NE. XMN(I))  GOTO 50
      IF (RMN(J) .NE. RMN(I))  GOTO  50
      GOTO  49
   46 IF (RMN(J)-DR .NE. RMN(I).AND.RMN(J)+DR .NE. RMN(I))  GOTO  5(
   49 K = K+1
      NABOR(I,K) = J
   50 CONTINUE
      NABOR(I,1) = K-1
   55 CONTINUE
C
C  PRINT  RESULTS OF THIS SUBROUTINE
C
      PRINT 70
      PRINT 75
      PRINT 80
      K = 0
      IL = 1
      IU = NE
   59 DO 60 I=IL,IU
      PRINT 85, I,NABOR(I,1)
      JM = NABOR(I,1)+1
      IF (JM .EQ. 1) GOTO 60
      PRINT 90, (NABOR(I,J),J=2,JM)
   60 CONTINUE
      K = K+1
      GOTO (61,62,63), K
   61 PRINT 95
      IL = NE1
```

```
      IU = NES
      GOTO 59
   62 PRINT 100
      IL = NES1
      IU = NZ
      GOTO 59
   63 KSUB = 0
      RETURN
   70 FORMAT('1',//T40,'ARRAY OF ZONES AND NEIGHBOURS FOLLOWS')
   75 FORMAT (/T14,'ZONE',T25,'NO. OF',T50,'NEIGHBOURING ZONES'/
     .  T14,'NO.',T25,'NEIGHBOURS'//)
   80 FORMAT (T1,'END ZONES :')
   85 FORMAT (T13,I2,T30,I2)
   90 FORMAT ('+',T40,5I10)
   95 FORMAT (T1,'WALL ZONES :')
  100 FORMAT (T1,'GAS ZONES :')
      END
      SUBROUTINE   EXCH3 (KSUB,ITR,ITN)
      COMMON      /A1/RMN,XMN /A2/TZN /A5/NABOR,EAR,XDI
     .  /B1/AX,DI /B2/DX,DR /B3/NXG,NRG /B4/NZ,NES,NE,NS,NG
     .  /B5/NE1,NES1
     .  /C1/RM,HTC,ES
      DIMENSION    RMN(25),XMN(25),TZN(25),
     .  EAR(25,25),NABOR(25,5),
     .  UAB(25,5),RSK(25,5),
     .  XDI(6,6),LW1(6),LW2(6),
C
C  INITIALIZE THE ARRAY 'EAR'
      DO 10 I=1,NZ
      DO 5 J=1,NZ
    5 EAR(I,J) = 0.
   10 CONTINUE
         V0 = AREA(DI,DI/4)
         V1 = AREA(DI,DX)
         V2 = 1/ES-0.5
         V3 = AREA(2*DR,DX)
         HOL = AREA(RM,RM)
      DO 57 I= 1,NZ
      R1 = RSK(TZN(I),1)
      R2 = RSK(TZN(I),2)
      RF = 0.75*R1
      M = NABOR(I,1)+1
      IF (M .GT. 1) GOTO 25
   15 PRINT 130, I
   20 KSUB = 1
      RETURN
C  (1)  GET A TWO-TERM REPRESENTATION OF
C  RECIPROCAL OF UNIT-AREA DIR-FLUX AREA:
   25 IF (I .GT. NES)  GOTO 50
      IF (I .GT. NE) GOTO 40
C  END ZONES
   30 B = DX/2
      DO 35 J=2,M
      K = NABOR(I,J)
      UAB(I,J-1) = V2
      RSK(I,J-1) = RF*B
   35 CONTINUE
      GOTO 57
C  WALL ZONES
   40 B = DR/2
```

```
      IF (NRG .EQ. 1)  B = DR
      DO 45 J=2,M
      K = NABOR(I,J)
   44 UAB(I,J-1) = -RF*B*B/DI+V2+RF*RF/(R2*R1*DI/2)
   45 RSK(I,J-1) = RF*B
      GOTO 57
C  GAS ZONES
   50 DO 55 J=2,M
      K = NABOR(I,J)
C  (1,1)  GAS-END
      B = DX/2
      C = V2
      IF (K .LE. NE)  GOTO 53
C  (1,2)  GAS-WALL
      B = DR/2
      IF (NRG .EQ. 1)  B = DR
      C = -RF*B*B/DI+V2+RF*RF/(R2*R1*DI/2)
      IF (K .LE. NES)  GOTO 53
C  (1,3)  GAS-GAS
      B = DX
      C = 0.
      IF (RMN(K) .EQ. RMN(I))  GOTO 53
      B = DR
   53 UAB(I,J-1) = C
   55 RSK(I,J-1) = RF*B
   57 CONTINUE
C  (2)  COMPUTE DIRECTED-FLUX AREAS
C  (GRAY GAS CONTRIBUTIONS)
      DO 70  I=1,NZ
      AN = AREA(2*RMN(I)+DR,DR)
      M = NABOR(I,1)
      IF (I .GT. NES)  GOTO  61
C  (2,1), (2,2)  GAS-SURFACE
      A = AN
      IF (I .GT. NE)A = V1
      DO 60 J=1,M
      K = NABOR(I,J+1)
   60 EAR (I,K) = A/(UAB(I,J)+RSK(I,J))
      GOTO  70
C  (2,3)  GAS-GAS
   61 DO 65 J=1,M
      K = NABOR(I,J+1)
      A = AN
      IF (K .GT. NES)  GOTO  62
      IF (K .GT. NE)A = V1
      GOTO  65
   62 L = K-I
      IF (L .LT. 0)L = -L
      IF (L .EQ. 1)  GOTO 65
      A = A*DX/DR+V3
      IF (K .LT. I)A = A-V3
   65 EAR(I,K) = A/(RSK(I,J)+UAB(I,J))
   70 CONTINUE
C
      IF (ITR .GT. 1)  GOTO 121
      PRINT 131, ITR
      DO 71 I=1,NZ
      M = NABOR(I,1)+1
      PRINT 132, I,(NABOR(I,J),J=2,M)
      M = M-1
```

```
      PRINT 133, (UAB(I,J),J=1,M)
      PRINT 133, (RSK(I,J),J=1,M)
      M = M+1
      PRINT 133, (EAR(I,NABOR(I,J)),J=2,M)
   71 CONTINUE
C
C  GET DIRECT EXCH AREAS FOR SURFACE-SURFACE EXCH
C   BY DIRECT COMPUTATION
C  THENCE TRANSFER MATRIX FOR TOT EXCH AREA CALCS
C
      DO 80 I=1,NES
      IF (I .EQ. NES)  GOTO 121
      A2 = RMN(I)
      A1 = A2
      IF (I .LE. NE)  A1 = A1+DR
      I1 = I+1
      DO 79 J=I1,NES
      B4 = RMN(J)
      B3 = B4
      IF (J .LE. NE)  B3 = B3+DR
      XJI = XMN(J)-XMN(I)
      XK = ABS(XJI)
      X13 = XK
      K = I
      IF (XJI .LT. 0.)  K = J
      IF (K .GT. NE)  X13 = X13-DX
      X14 = XK
      IF (XJI .LT. 0.)  GOTO 73
      IF (I .LE. NE.AND.J .GT. NE)  X14 = X14+DX
   73 X23 = XK
      IF (XJI .GT. 0.)  GOTO 74
      IF  (I .LE. NE.AND.J .GT. NE)  X23 = X23-DX
   74 X24 = XK
      K = J
      IF (XJI .LT. 0.)  K = I
      IF (K .GT. NE)  X24 = X24+DX
      EX = DIRECT(A1,B3,X13)+DIRECT(A2,B4,X24)
     .    -(DIRECT(A1,B4,X14)+DIRECT(A2,B3,X23))
      XDI(I,J) = EX
   79 XDI(J,I) = EX
   80 CONTINUE
C
C  CORRECT FOR END (EXIT) HOLE PRESENCE
  121 DO 125 I=2,NE,2
      IF (RMN(I) .GT. RM) GOTO 126
      F = HOL/AREA(2*RMN(I)+DR,DR)
      DO 124 J=1,NZ
      IF (J .EQ. I)  GOTO 124
      IF (ITR .GT. 1)  GOTO 122
      IF (J .GT. NES)  GOTO 122
      A3 = RMN(J)
      A2 = A3
      IF (J .LE. NE)  A2 = A2+DR
      XIJ = AX-XMN(J)
      X12 = XIJ
      IF (J .GT. NE)  X12 = X12-DX
      X13 = XIJ
      A = DIRECT(RM,A2,X12)-DIRECT(RM,A3,X13)
      XDI(I,J) = XDI(I,J)-A
      XDI(J,I)  = XDI(J,I)-A
```

```
      GOTO  124
  122 AI = EAR(I,J)*F
      AJ = EAR(J,I)*F
  123 EAR(I,J) = EAR(I,J)-AI
      EAR(J,I) = EAR(J,I)-AJ
  124 CONTINUE
  125 CONTINUE
C
  126 IF (ITR .GT. 1) GOTO  152
      DO 144 I=1,NES
      A = V1
      IF (I .GT. NE)  GOTO  142
      D1 = 2*RMN(I)+DR
      A = AREA(D1,DR)
      IF (XMN(I) .EQ. AX.AND.RMN(I) .LT. RM) A=A-HOL
  142 SU = -A*ES/(1-ES)
      DO 143 J=1,NES
  143 SU = SU-XDI(I,J)
  144 XDI(I,I) = SU
C
C  COMPUTE TOTAL EXCH AREAS
C   (CLEAR GAS CONTRIBUTIONS)
      PRINT 136
      DO 145 I=1,NES
  145 PRINT 134, (XDI(I,J),J=1,NES)
  151 CALL          MINV(XDI,NES,DD,LW1,LW2)
      PRINT 138, DD
      PRINT 137
      DO 146 I=1,NES
  146 PRINT 134, (XDI(I,J),J=1,NES)
  152 DO 150 I=1,NES
      A = V1
      IF (I .GT. NE) GOTO 147
      D1 = 2*RMN(I)+DR
      A = AREA(D1,DR)
      IF (I .EQ. 2)  A = A-HOL
  147 AE = A*ES/(1-ES)
      AGI = AGO(TZN(I))
      IF (I .EQ. NES)  GOTO 150
      J1 = I+1
      DO 149 J=J1,NES
      A = V1
      IF (J .LE. NE)  A = AREA(2*RMN(J)+DR,DR)
      IF (J .EQ. 2)  A = A-HOL
      AF = A*ES/(1-ES)
      WE = -XDI(I,J)*AF*AE
      EAR(I,J) =   AGI*WE
      EAR(J,I) = AGO(TZN(J))*WE
  149 CONTINUE
  150 EAR(I,I) = -AGI*(XDI(I,I)*AE+ES)*AE
C* *
C  SELF EXCH AREAS:SURFACE ZONES
C  END ZONES
      DO 155 I=1,NE
      A = AREA(2*RMN(I)+DR,DR)
      IF (XMN(I) .EQ. AX.AND.RMN(I) .LT. RM) A=A-HOL
      ESF = ES*A
      DO 154 J=1,NZ
      IF (J .EQ. I)  GOTO 154
      ESF = ESF-EAR(I,J)
```

```
  154 CONTINUE
      IF (ESF .GE. 0.)  EAR(I,I) = ESF
  155 CONTINUE
C   WALL ZONES
      DO 160 I= NE1,NES
      A = V1
      ESF = A*ES
      DO 159 J=1,NZ
      IF (J .EQ. I)  GOTO  159
      ESF = ESF-EAR(I,J)
  159 CONTINUE
      IF (ESF .GE. 0.)  EAR(I,I) = ESF
  160 CONTINUE
C SELF EXCH AREAS:GAS ZONES
  165 DO 170 I=NES1,NZ
      VK = 4*ROSK(TZN(I),1)*DX*AREA(2*RMN(I)+DR,DR)
      DO 169 J=1,NZ
      IF (J .EQ. I)  GOTO  169
      VK = VK-EAR(I,J)
  169 CONTINUE
  170 EAR(I,I) = VK
C* *
  130 FORMAT (///T40,'** EXCH3 ERROR : ISOLATED ZONE, NO.',
     .   I3,' **')
  131 FORMAT ('1',T45,'EXCH3 : CHECK PRINTOUT'/T3,
     .   'ITERATION #',I3/)
  132 FORMAT (/I10,I21,4I13)
  133 FORMAT (/T25,5E13.4)
  134 FORMAT (/T2,10E13.4)
  135 FORMAT (//T2,'CLEAR GAS CONTRIBUTIONS :')
  136 FORMAT ('1',T25,'TRANSFER MATRIX FOR TOT EXCH AREA CALCS'//)
     .   'AREA CALCS'//)
  137 FORMAT (///T25,'INVERSE OF TRANSFER MATRIX'//)
  138 FORMAT (///T2,'DETERMINANT OF TRANSFER MATRIX = ',
     .   E13.4///)
  200 KSUB = 0
      RETURN
      END
      SUBROUTINE EQNS4 (KSUB)
      DIMENSION    RMN(25),XMN(25),EAR(25,25),NABOR(25,5),
     .  AMX(25,25),TZN(25)
      COMMON      /A1/RMN,XMN /A2/TZN,AMX /A5/NABOR,EAR
     .   /B1/AX,DI,HTS /B2/DX,DR /B3/NXG,NRG /B4/NZ,NES,NE
     .   /B5/NE1,NES1
     .  /C1/RM,HTC,ES,CP,FLO
C
C   INITIALISE THE MATRIX
      DO 2 I=1,NZ
      DO 1 J=1,NZ
    1 AMX(I,J) = EAR(J,I)
    2 CONTINUE
      A0 = AREA (DI,DI/4)
C  ADD THE CONVECTION TERMS (RAD. EQUIVT.)
C  (A)    GAS ZONES
C A.1, A.2  GAS-SURFACE
      AW = A0*4*DX/DI
      DO 10 I=NES1,NZ
      HCR = HRADQ(HTC,TZN(I))
      M = NABOR(I,1)+1
      DO 5 J=2,M
```

```
      K = NABOR(I,J)
      IF (K .GT. NES)  GOTO 5
      A = AW
      IF (K .LE. NE) A = AREA(2*RMN(K)+DR,DR)
      CALL          FFSUB9  (K,I,FF,1)
      HC = HCR*FF*A
      AMX(I,K) = AMX(I,K)+HC
      AMX(I,I) = AMX(I,I)-HC
    5 CONTINUE
   10 CONTINUE
C  A.3  GAS-GAS  (BULK FLOW)
      HB = FLO*CP/A0
      DO 20 I=NES1,NZ
      HBR = HRADQ(HB,TZN(I))
      M = NABOR(I,1)+1
      A = AREA(2*RMN(I)+DR, DR)
      DO 15 J= 2,M
      K = NABOR(I,J)
      IF (K .LT. NES1)  GOTO 15
      IF (RMN(K) .NE. RMN(I))  GOTO 15
      IF (XMN(K) .GT. XMN(I))  GOTO 15
      CALL          FFSUB9  (I,K,FF,2)
      HBB = HBR*FF*A
      AMX(I,K) = AMX(I,K)+HBB
   14 AMX(I,I) = AMX(I,I)-HBB
   15 CONTINUE
      V = DX*A
   20 AMX(I,I) = AMX(I,I)-4*ROSK(TZN(I),1)*V
C  A.4  INLET-PLANE GAS ZONES
      I = NES1-NXG
      DO 22 K=1,NRG
      I = I+NXG
      A = AREA(2*RMN(I)+DR, DR)
   22 AMX(I,I) = AMX(I,I)-HRADQ(HB,TZN(I))*A
C  (B),(C)  WALL- AND END- -ZONES
      DO 40 I=1,NES
      A = AW
      IF (I .GT. NE)  GOTO 26
   25 A = AREA(2*RMN(I)+DR,DR)
   26 AMX(I,I) = AMX(I,I)-(ES+HRADQ(HTS,TZN(I)))*A
      HCR = HRADQ(HTC,TZN(I))
      M = NABOR(I,1)+1
      DO 35 J=2,M
      K = NABOR(I,J)
      IF (K .LT. NES1)      GO TO 35
      CALL          FFSUB9  (I,K,FF,2)
      HC = HCR*FF*A
      AMX(I,K) = AMX(I,K)+HC
      AMX(I,I) = AMX(I,I)-HC
   35 CONTINUE
   40 CONTINUE
      KSUB = 0
      RETURN
      END
      SUBROUTINE RHSP5 (KSUB)
      DIMENSION     RHS(25),RMN(25)
      COMMON      /A1/RMN /A4/RHS
     .  /B1/AX,DI,HTS /B2/DX,DR /B3/NXG,NRG /B4/NZ,NES,NE
     .  /B5/NE1,NES1
     .  /C1/RM,HTC,ES,CP,FLO /C2/TSURR,TSUPP,CFU,QCO,FLM
```

```
C   (A),(B)  END- AND WALL- -ZONES
      A1 = AREA(RM,RM)
      DO 10 I=1,NES
      D = DI
      DL = DX
      IF (I .GT. NE)  GOTO 5
      D = 2*RMN(I)+DR
      DL = DR
    5 A = AREA(D,DL)
   10 RHS(I) = -HTS*A*TSURR
C   CORRECT FOR END (EXIT) HOLE PRESENCE
      DO 15 I=2,NE,2
      RI = RMN(I)
      IF (RI .GE. RM)  GOTO 15
      F = A1/AREA(2*RI+DR,DR)
      RHS(I) = (1-F)*RHS(I)
   15 CONTINUE
C   (C)  GAS ZONES
      DO 16 I=NES1,NZ
   16 RHS(I) = 0.
      NOG = FLM/DX
      MCO = NES+NOG
      QGN = QCO*CFU*DX/FLM
      DO 20 I=NES1,MCO
   20 RHS (I) = -QGN
      F = FLM/DX
      DO 21 J=1,NOG
   21 F = F-1.0
      IF (F .GT. 0. ) RHS(MCO+1) = -F*QGN
C   INLET-PLANE GAS ZONES
      I = NES1-NXG
      A0 = AREA(DI,DI/4)
      HB = FLO*CP/A0
      DO 23 K=1,NRG
      I = I+NXG
      A = AREA(2*RMN(I)+DR,DR)
   23 RHS(I) = RHS(I)-HB*TSUPP*A
      PRINT 25
      PRINT 30, (RHS(I),I=1,NZ)
   25 FORMAT (///T2,'RHSP5 OUTPUT :'/T2,'RHS OF THE EQNS :'/)
   30 FORMAT (10E13.4)
      KSUB = 0
      RETURN
      END
      SUBROUTINE SOLV6 (ITR,ERF,KSUB)
      COMMON        /A2/TZN,AMX /A4/RHS /A9/EZN
     1              /B4/NZ,NES,NE /B5/NE1,NES1
      DIMENSION     AMX(25,25),RHS(25),TZN(25),EZN(25),CFA(25),
     .  MAJOR(25),KRO(25),
     .  AMXV(10,10),
     .  AMT(25,25),FLU(25,2 ),RCF(25),NPV(25)
      PRINT 3
      PRINT 5
      DO 14 I=1,NZ
      IF (I .EQ. NE1.OR.I .EQ. NES1)  PRINT 4
      PRINT 2, (AMX(I,J),J=1,NZ)
   14 CONTINUE
C   TEST FOR ILL-CONDITIONING OF THE MATRIX 'AMX'
C   (1)  MOVE MATRIX INTO WORKING SPACE 'AMT'
      DO 20 I=1,NZ
```

```
      DO 15 J=1,NZ
   15 AMT(I,J) = AMX(I,J)
   20 CONTINUE
C  (2)  NORMALISE
      DO 30 I=1,NZ
      RMS = 0.
      DO 25 J=1,NZ
   25 RMS = RMS+AMT(I,J)**2
      RMS = SQRT(RMS/NZ)
      DO 29 J=1,NZ
   29 AMT(I,J) = AMT(I,J)/RMS
   30 CONTINUE
C  (3)  FIND DETERMINANT OF NORMALISED MATRIX
      D = 0.
      M = 0
      CALL          CSLND(AMT,25,NZ,D,M,AMT)
      PRINT 1, D,M
C        (4)  TEST THE MAGNITUDE OF THE DETERMINANT
      IF (ABS(D*10**M) .GE. 0.5)  GOTO 33
C  IF ILL-CONDITIONED USE THE *CSLIB SUBROUTINE CSLNIL
      PRINT 4
      PRINT 6
      DO 32  I=1,NES
      DO 31 J=1,NES
   31 AMXV(I,J) = AMX(I,J)
   32 CONTINUE
      CALL     CSLNIL(AMXV, RHS, EZN, NZ, FLU, RCF, NPV)
      GOTO 83
C  IF NOT ILL-CONDITIONED TEST FOR DIAGONAL DOMINANCE
   33  MU = 0
      DO 35  I=1,NZ
      AI = ABS(AMX(I,I))
      HU = AI
      M = I
      SU = 0.
      DO 34  J=1,NZ
      IF (J .EQ. I)  GOTO 34
      AJ = ABS(AMX(I,J))
      SU = SU+AJ
      IF (AJ .LE. HU)  GOTO  34
      HU = AJ
      M = J
   34 CONTINUE
      MAJOR (I) = M
      IF (AI .LE. SU)  MU = MU+1
   35 CONTINUE
      IF (MU .EQ. 0)  GOTO  36
      PRINT 4
      PRINT 7
      PRINT 8
      PRINT 11, ((I,MAJOR(I)), I=1,NZ)
      GOTO  40
C  IF SATISFIED, USE *CSLIB SUBROUTINE  CSLNS
   36 D = 0.
      M = 0
      CALL          CSLNS(AMX,25,NZ,RHS,EZN,D,M,AMT)
      GOTO  83
C  IF NOT, USE THE GAUSS-SEIDEL ITERATION
C   (1)  COMPUTE THE ORDER OF SOLUTION
   40 HU = 0.
```

```
      DO 38  J=1,NZ
      AJ = ABS(AMX(NZ,J))
      IF (AJ .LE. HU)  GOTO 38
      HU = AJ
      M = J
   38 CONTINUE
      MAJOR(NZ) = M
      I = NZ
      DO 60  II=2,NZ
      IA = II-1
      I = I-1
      DO 45 K=1,NZ
   45 KRO(K) = 1
      K = NZ+1
      DO 50 KK=1,IA
      K = K-1
   50 KRO(MAJOR(K)) = 0
      HU = 0.
      DO 59 J=1,NZ
      AJ = KRO(J)*ABS(AMX(I,J))
      IF (AJ .LE. HU)  GOTO  59
      HU = AJ
      M = J
   59 CONTINUE
   60 MAJOR(I) = M
      DO 61 I=1,NZ
   61 NPV(I) = MAJOR(NZ-I+1)
      PRINT 9
      PRINT 10, (NPV(I), I=1,NZ)
C    (2)  SOLVE EQNS IN THE PRE-DETERMINED ORDER
      IF (ITR .GT. 1)  GOTO  66
      DO  65 I=1,NZ
   65 EZN(I) = CONVRT(TZN(I),1)
   66 I = NZ+1
      DO 80 II=1,NZ
      I = I-1
      DO 70 K=1,NZ
   70 KRO(K) = 1
      DO 75 K=1,I
   75 KRO(MAJOR(K)) = 0
      SU = RHS(I)
      DO 79 J=1,NZ
   79 SU = SU-KRO(J)*AMX(I,J)*EZN(J)
   80 EZN(MAJOR(I)) = SU/AMX(I,MAJOR(I))
C  COMPUTE NEW TEMPS AND ERROR PARAMETER
   83 CF = 1.0
      MU = 1
      DO 85 I=1,NZ
      IF (EZN(I) .LE. 1714. )  MU = MU+1
   85 CONTINUE
      IF (MU .EQ. 1)  GOTO 121
      MU = 1
      DO 110 I=1,NZ
      EO = CONVRT(TZN(I),1)
  110 CFA(I) = ABS(EZN(I)/EO-1.0)
      CF = CFA(1)
      DO 115 I=2,NZ
      CI = CFA(I)
      IF (CI .EQ. 0. )  GOTO  115
      IF (CI .GT. CF)  CF = CI
```

```
  115 CONTINUE
      NU = 1
  117 IF (NU .NE. 1)  CF = 0.5*CF
      DO 120 I=1,NZ
      EO = CONVRT(TZN(I),1)
      EN = CF*EZN(I)+(1-CF)*EO
      IF (EN .GE. 1714. )  GOTO  120
      NU = 0
      MU = MU+1
      GOTO 117
  120 CONTINUE
  121 ERF = 0.
      DO 125 I=1,NZ
      EN = CF*EZN(I)+(1-CF)*CONVRT(TZN(I),1)
  123 T = CONVRT(EN,2)
      ERF = ERF+(T-TZN(I))**2
      TZN(I) = T
  125 CONTINUE
      PRINT 13, MU
      PRINT 12, CF
      ERF = SQRT(ERF/NZ)
    1 FORMAT (///T2,'DETERMINANT OF NORMALISED MATRIX =',
     .    F10.5,'E',I3)
    2 FORMAT (/10E13.4)
    3 FORMAT ('1')
    4 FORMAT (//1X)
    5 FORMAT (//T40,'COEF MATRIX OF THE ENERGY BALANCE EQNS'//)
    6 FORMAT (//T2,'COEF MATRIX ILL-CONDITIONED   USE CSLNIL')
    7 FORMAT (//T2,'COEF MATRIX NOT DIAG-DOMINANT'/T2,
     .   'PROCEED WITH GAUSS-SEIDEL ITERATION'/)
    8 FORMAT (/T2,'THE DOMINANT TERMS ARE :'/)
    9 FORMAT (//T2,'THE ORDER OF SOLUTION IS :'/)
   10 FORMAT (/T20, 5I5)
   11 FORMAT (/T2,5(2I4,3X))
   12 FORMAT (//T2,'MAX CORRECTION FACTOR = ',E11.4/)
   13 FORMAT (///T2,'# OF TRIAL CF-VALUES =',I10)
      KSUB = 0
      RETURN
      END
      SUBROUTINE QFLX7 (KSUB)
      DIMENSION    TZN(25),QFX(25)
      COMMON       /A2/TZN /A8/QFX
     1             /B1/HTS /B4/NZ,NES
     2             /C1/RM, HTC /C2/TSURR
      DO 10 I=1,NES
   10 QFX(I) = HTS*(TZN(I)-TSURR)
   20 KSUB = 0
      RETURN
      END
      SUBROUTINE   EBLC8 (KSUB)
C  ENERGY BALANCE FOR ENTIRE SYSTEM AS A CHECK ON CALCS
      COMMON     /A1/RMN  /A2/TZN  /A8/QFX /A9/EZN
     .  /B1/AX,DI  /B2/DX,DR  /B3/NXG,NRG
     .  /B4/NZ,NES,NE,NS,NG  /B5/NE1,NES1
     .  /C1/RM,HTC,ES,CP,FLO  /C2/TSURR,TSUPP,CFU,QCO,FLM
      DIMENSION    TZN(25),QFX(25),RMN(25),
     1             EZN(25)
C
C  NET ENERGY GENERATION RATE
      QGEN = QCO*CFU-CP*FLO*(TZN(NES+NXG)-TSUPP)
```

```
C  TOTAL NET HEAT FLUX (SURFACE ZONES)
      QFLUX = 0.
      DO 5 I=1,NE,2
      A = AREA(2*RMN(I)+DR,DR)
    5 QFLUX = QFLUX+A*QFX(I)
      A1 = AREA(RM,RM)
      DO 10  I=2,NE,2
      RI = RMN(I)
      A = AREA(2*RI+DR,DR)
      IF (RI .LT. RM)  A = A-A1
      QFLUX = QFLUX+A*QFX(I)
   10 CONTINUE
      A = AREA(DI,DX)
      DO 15 I=NE1,NES
   15 QFLUX = QFLUX+A*QFX(I)
C  COMPARE
      PC = QFLUX/QGEN*100.
C  OUTPUT
      PRINT 50, QFLUX,PC,QGEN
   50 FORMAT (///T2,'EBLC8 OUTPUT :'//T2,'TOTAL NET FLUX =',
     . E15.6,5X'BTU/HR'//T2,'WHICH IS',F8.2,2X,'% OF'//T2,
     . 'THE NET ENERGY GEN RATE OF',E15.6,5X,'BTU/HR')
      KSUB = 0
      RETURN
      END
      SUBROUTINE   FFSUB9  (I,J,FF,K)
      DIMENSION    TZN(25)
      COMMON       /A2/TZN
      T1 = TZN(I)/TZN(J)
      T2 = T1*T1
      FF = 1/((1+T1)*(1+T2))
      IF  (K .EQ. 2)  FF = T2*T1*FF
      RETURN
      END
      FUNCTION CONVRT(Q,K)
C  CONVERTS BETWEEN TEMP AND EMISSIVE PWR
C  --DEPENDING ON  K
      CO = 1,714.0
      D = 1000.0
      P = 4.0
      IF (K .EQ. 1)  GOTO 5
      H = CO
      CO = D
      D = H
      P = 0.25
    5 CONVRT = CO*(Q/D)**P
      RETURN
      END
      FUNCTION AKGR(TEMP)
C  COMPUTES SUM OF WT-ING FACTOR-ABSORPTION COEF PRODUCTS
      DIMENSION BN(5,10),SK(5)
      COMMON /A3/BN,SK /C3/NGRAY,NB
      AKGR = 0.
      DO 10 I=1,NGRAY
      T = 1.0
      AG = BN(I,1)
      DO 5 J=2,NB
      T = T*TEMP
    5 AG = AG+BN(I,J)*T
   10 AKGR = AKGR+AG*SK(I)
```

```
      RETURN
      END
      FUNCTION HRADQ (H,T)
C  COMPUTES AT TEMP T PRODUCT OF AREA AND RADIATIVE EQUIVT
C  OF CONV HT TRANSFER COEF
      HRADQ = H*T/CONVRT(T,1)
      RETURN
      END
      FUNCTION AREA (DIA,DEL)
C  COMPUTES AREAS OF CIRCLES, CIRCULAR ANNULI AND CYLINDERS
      PI = 0.31415926E 01
      AREA = PI*DEL*DIA
      RETURN
      END
      FUNCTION ROSK (TEMP,KRO)
C  GIVES THE ROSSELAND MEAN ABSORPTION COEF
C  OR A RELATED MEAN ABSORPTION COEF
C  (DEPENDING ON KRO)
C  FOR THE GRAY GAS MIXTURE
      DIMENSION BN(5,10),SK(5)
      COMMON /A3/BN,SK /C3/NGRAY,NB
      ROSK = 0.
      DO 10 I=1,NGRAY
      T = 1.0
      SU =  BN(I,1)
      DO 5 J=2,NB
      T = T*TEMP
      FJ = J+3
      FJ = 0.25*FJ
    5 SU = SU+FJ*BN(I,J)*T
   10 ROSK = ROSK+SU/(SK(I)**KRO)
      ROSK = 1/ROSK
      RETURN
      END
      FUNCTION AG0 (TEMP)
C  CALCULATES AT TEMP T CLEAR GAS WT-ING FAC
      DIMENSION BN(5,10)
      COMMON /A3/BN /C3/NGRAY,NB
      AG0 = 1.0
      DO 10 I=1,NGRAY
      T = 1.0
      AG0 = AG0-BN(I,1)
      DO 5 J=2,NB
      T = T*TEMP
    5 AG0 = AG0-BN(I,J)*T
   10 CONTINUE
      RETURN
      END
      FUNCTION     DIRECT(A,B,C)
C  COMPUTES DIRECT EXCH AREAS BETWEEN
C  ANY PAIR OF COAXAL CIRCULAR SURFACES
      PI = 0.31415926E 01
      ABC = A*A+B*B+C*C
      AB = A*B
      SUBT = SQRT(AEC*ABC-4*AB*AB)
      DIRECT = 0.5*PI*(ABC-SUBT)
      RETURN
      END
```